Award Number: W81XWH-11-1-0357

TITLE: ***New Treatments for Drug-Resistant Epilepsy that Target Presynaptic Transmitter Release***

PRINCIPAL INVESTIGATOR: Patric K. Stanton, Ph.D.

CONTRACTING ORGANIZATION: New York Medical College, Valhalla, NY 10595

REPORT DATE: July 2015

TYPE OF REPORT: Final Addendum

PREPARED FOR: U.S. Army Medical Research and Materiel Command
Fort Detrick, Maryland 21702-5012

REPORT DOCUMENTATION PAGE

Form Approved
OMB No. 0704-0188

1. REPORT DATE	2. REPORT TYPE	3. DATES COVERED
July 2015	Final Addendum	5/15/2012 – 5/31/2015

4. TITLE AND SUBTITLE
New Treatments for Drug-Resistant Epilepsy that Target Presynaptic Transmitter Release

5a. CONTRACT NUMBER

5b. GRANT NUMBER
W81XWH-11-1-0357

5c. PROGRAM ELEMENT NUMBER

6. AUTHOR(S)
Patric K. Stanton, Ph.D.

E-Mail: patric_stanton@nymc.edu

5d. PROJECT NUMBER

5e. TASK NUMBER

5f. WORK UNIT NUMBER

7. PERFORMING ORGANIZATION NAME(S) AND ADDRESS(ES)

New York Medical College
40 Sunshine Cottage Road
Valhalla, NY 10595

8. PERFORMING ORGANIZATION REPORT NUMBER

9. SPONSORING / MONITORING AGENCY NAME(S) AND ADDRESS(ES)
U.S. Army Medical Research and Materiel Command
Fort Detrick, Maryland 21702-5012

10. SPONSOR/MONITOR'S ACRONYM(S)

11. SPONSOR/MONITOR'S REPORT NUMBER(S)

12. DISTRIBUTION / AVAILABILITY STATEMENT
Approved for Public Release; Distribution Unlimited

13. SUPPLEMENTARY NOTES

14. ABSTRACT

We developed electrophysiological, two-photon laser scanning microscopic imaging and pharmacological tools to investigate the effects of levetiracetam, topiramate and carbamazepine on excitatory (glutamatergic) synaptic transmission and vesicular transmitter release at multiple synapses in *in vitro* brain slices from control and pilocarpine-treated epileptic rats and mice. We discovered that levetiracetam was more effective in reducing the frequency of excitatory synaptic transmission onto dentate granule cells in slices from chronically epileptic rats, while no significant effect was detected in the amplitude of mEPSCs, indicating a presynaptic site of action without postsynaptic effects on AMPA glutamate receptors. These data correlated well with findings in imaging experiments that LEV was more effective in suppressing the enhanced vesicular release of glutamate from mossy fiber terminals in field CA3 of epileptic mice, compared to non-epileptic control animals. These data indicate that presynaptically acting drugs such as levetiracetam may become a key piece in the arsenal of antiepileptic drugs in mesial temporal lobe epilepsy, and highlight the need for preventing the downregulation of sensitivity to levetiracetam observed with chronic administration in some patients. Thus, screening for a presynaptic site of action and assessment of chronic tachyphylaxis of presynaptic actions will be important to the discovery of novel and effective antiepileptic drugs.

15. SUBJECT TERMS
Epilepsy, presynaptic, antiepileptic drugs, levetiracetam, topiramate, carbamazepine, synaptic vesicle, seizures, synaptic vesicle proteins

16. SECURITY CLASSIFICATION OF:			17. LIMITATION OF ABSTRACT	18. NUMBER OF PAGES	19a. NAME OF RESPONSIBLE PERSON
a. REPORT	b. ABSTRACT	c. THIS PAGE			USAMRMC
U	U	U	UU	70	19b. TELEPHONE NUMBER *(include area code)*

Table of Contents

2012-15 FINAL ADDENDUM REPORT: DoD Grant - PR100534P1

Title: *New Treatments for Drug-Resistant Epilepsy that Target Presynaptic Transmitter Release*

Principal Investigator: Patric K. Stanton, PhD
Department of Cell Biology & Anatomy, New York Medical College (NYMC), Valhalla, NY

INTRODUCTION

Posttraumatic epilepsy is a major long-term complication of traumatic brain injury (TBI), that usually develops within 5 years of head injury [1], and is often expressed as medically intractable hippocampal epilepsy [2,3]. Posttraumatic epilepsy can develop after penetrating or severe non-penetrating brain injury. Although there are a variety of causes of traumatic epilepsy, the resulting chronic neurological condition is characterized by common features, including recurrent spontaneous seizures, neuronal damage, and, in ~30% of mesial temporal lobe epileptic (MTLE) patients, resistance to all available anticonvulsant drugs [4,5]. ***Therefore, it is of critical importance to develop novel models to study post-traumatic epilepsy, to facilitate discovery of new treatments.*** During epileptogenesis, seizure-related functional and structural reorganization of neuronal circuits leads to both hyperexcitability of glutamatergic neurons and defective inhibition [6,7]. While many postsynaptic alterations have been demonstrated, there is surprisingly little known concerning dysfunction of presynaptic transmitter release machinery in epilepsy. The recent successful introduction of the antiepileptic drug levetiracetam (LEV; 8), which acts on presynaptic molecular targets, suggests that controlling dysregulation of presynaptic function could be a promising new therapeutic target for treatment of unresponsive epilepsies. While LEV binds to both the synaptic vesicle protein SV2a and N-type Ca^{2+} channels [9,10,11] its precise mechanisms of action are not understood.

BODY

HYPOTHESIS AND OBJECTIVES:

During periods of intense neuronal activity such as seizures, a larger pool of vesicles could result in more glutamate being released and long-lasting aberrant excitation. We propose to explore the effects of seizures on transmitter release and the presynaptic action of AEDs on these changes. We will use electrophysiology and multiphoton confocal microscopy. Preliminary data indicate that SE induces long-lasting potentiation of synaptic vesicle release in epileptic rats. We hypothesize that successful AED treatment might prevent or reverse these seizure-induced molecular deficiencies (reduction of N-type VGCC, mGluR II and SV2a expression), and be antiepileptogenic as well. Our **central hypothesis** is that pharmacological regulation of glutamate transmitter release at presynaptic sites will be an effective, novel therapeutic strategy to ameliorate epileptogenesis and excessive synaptic excitation in epilepsy. The **long-term objectives** of this collaborative proposal are to: (1) identify the most effective AEDs which modulate presynaptic glutamate release, and (2) determine the presynaptic mechanism of action of the new AED LEV to modulate vesicular release properties. *Our central hypothesis is that pharmacological regulation of glutamate transmitter release at presynaptic sites will be an effective, novel therapeutic strategy to treat many cases of drug-resistant epilepsy, especially epileptogenesis following traumatic brain injury.* The **long-term goals** of this collaborative project are to: (1) identify the most effective antiepileptic drugs amongst compounds that modulate presynaptic glutamate release and (2) determine the presynaptic mechanism of action of the new antiepileptic drug **levetiracetam** (LEV). ***Over the grant period, we made ground-breaking observations showing that a single, severe seizure induced by pilocarpine results in long-lasting alterations in the ultrastructural anatomy of presynaptic mossy fiber excitatory terminals in the hippocampus, that these alterations are associated with appearance of an abnormal population of "high release" terminals, and that the anticonvulsant drug leviteracetam may have potential to treat, or even prevent, the development of pilocarpine-induced seizures.***

Specific Aim 1: *Determine which antiepileptic drugs are most effective at reducing glutamate release from mossy fiber presynaptic boutons (MFBs) in the pilocarpine model of mesial temporal lobe epilepsy (MTLE)* (months 1-12).

Working hypothesis: Drugs acting on presynaptic Ca^{2+} channels, autoreceptors, and SV2a will be more effective in reducing vesicular glutamate release at excitatory presynaptic terminals in the hippocampus.

Research Accomplishments:

Task 1. Evaluate the effects of different concentrations of "classical" (*e.g*. carbamazepine, lamotrigine, and topiramate, and "new generation" antiepileptic drugs (*e.g.* LEV) on presynaptic glutamate release by using two-photon imaging of vesicular release of the fluorescent dye FM1-43 from individual mossy fiber terminals in *in vitro* hippocampal slices.

Development of the pilocarpine model of epilepsy in mice and rats at both institutions. (Subtask 1a) single injection of pilocarpine in rats and in the transgenic Sp21 mice expressing the fluorescent reporter of synaptic vesicle release and presynaptic function synaptophlourin (SpH).

YEAR 01

- **Subtask 1a.** Develop chronic epileptic rats with a single injection of pilocarpine (Dr. Garrido, Dr. Pacheco, Dr. Stanton and Dr. Upreti; months 1-12).
- **Subtask 1b.** Prepare hippocampal slices from control and epileptic rats (Dr. Stanton, Dr. Upreti; months 1-12).
- **Subtask 1c.** Image presynaptic transmitter release from individual mossy fiber terminals using two-photon confocal laser scanning microscopy of the fluorescent dye FM1-43 (Dr. Stanton, Dr. Zhang and Dr. Upreti; months 1-12).
- **Subtask 1d.** Test whether antiepileptic drugs modify kinetics of transmitter release in control versus epileptic rats (Dr. Stanton, Dr. Zhang and Dr. Upreti; months 1-12).
- **Subtask 1e.** Statistical analysis of the experimental data (Dr. Stanton, Dr. Zhang and Dr. Upreti, months 9-12).

1.a and 1.b. Developed the pilocarpine model of epilepsy in mice and rats at NYMC and UTB:

Colonies of chronically epileptic Sprague Dawley rats and SynaptopHlourin (SpH) mice were established at both New York Medical College (NYMC) and the University of Texas at Brownsville (UTB), using protocols validated in Dr. Garrido's laboratory (**Subtask 1a)**. In addition, the pilocarpine model of mesial temporal lobe epilepsy (MTLE) was also developed in the SV2A/SV2B knockout mice in the laboratory of Dr. Garrido. Hippocampal slices for multiphoton laser scanning confocal imaging analysis of presynaptic release (Dr. Stanton, NYMC) and *in vitro* electrophysiology (Dr. Garrido, UTB) were obtained from control and epileptic rats and transgenic mice (**Subtask 1b**), levitiracetam was shown to depress presynaptic release from the readily-releasable vesicle pool that was detected by this method (**Subtask 1d**), and two-photon imaging of transmitter release from individual mossy fiber terminals using two-photon laser scanning microscopy of the fluorescent dye FM1-43 was completed, data analyzed, and published (**Subtask 1c and 1e**).

Development of the pilocarpine model in SpH and SV2A knockout mice: Previous studies have reported differential susceptibility of mouse strain to pilocarpine-induced *status epilepticus* and seizure-induced excitotoxic cell death [1]. Therefore, in close collaboration with the laboratory of Dr. Garrido-Sanabria at UTB, we optimized and fully characterized the pilocarpine model in SpH-expressing mice (Sp21 variant), which express a fusion protein of vesicle-associated membrane protein 2 (*Vamp2*) and a pH-sensitive green fluorescence protein under the control of the mouse thymus cell antigen 1 (*Thy1*) promoter, which drives expression of SpH in granule cells of dentate gyrus and their mossy fiber axons and presynaptic boutons in *stratum lucidum* of the hippocampus. Breeders were obtained from Jackson Laboratories *i.e.* B6.CBA-Tg(Thy1-spH)21Vnmu/J, C57BL/6J (Stock Number: 014651) to establish the

colony Dr. Garrido's laboratory, while this same strain was already available at Dr. Stanton's Laboratory (kind gift of Dr. Venkatesh Murthy, Harvard University). For the

induction of *status epilepticus* animals received methylscopolamine nitrate (0.1 mg/kg in saline, s.c.) thirty minutes before pilocarpine to minimize peripheral effects of cholinergic stimulation [2]. Thereafter, pilocarpine hydrochloride (350mg/kg) was intraperitoneally injected using different doses (300, 320, 350 and 380 mg/kg of body weight, 5 animals per group). The dose used was most efficient, yielding 90% of animals entering *status epilepticus* and 80% survival rate. After animals entered *status epilepticus*, a second dose of methylscopolamine was subcutaneously injected and animals were allowed to seize for 1 hour, after which motor seizures were terminated with injection of diazepam (10 mg/kg in saline *i.p.*). Only animals experiencing continuous SE during these periods were studied. Control animals received methylscopolamine and saline instead of pilocarpine. This pilocarpine model of mesial temporal lobe epilepsy was also optimized in wild type, heterozygous and knockout SV2A mice obtained from Jackson Laboratories (Stock number: 006383, B6; 129P2-*Sv2a*^{tm1Sud} *Sv2b*^{tm1Sud}/J). These animals were developed with the same genetic background (C57BL/6J) of the SpH21 mice. Accordingly, the same concentrations of methylscopolamine and pilocarpine were used following the same protocol as for SpH mice. *We extended the pilocarpine model to SV2A knockout mice, and these animals were employed in the the Garrido-Sanabria laboratory to examine its importance to excitatory activation of dentate granule cells using whole-cell recordings (Task 2).*

1.c.1 Two-photon laser scanning microscopy imaging of vesicular transmitter release from large mossy fiber boutons of epileptic rats and synaptopHluorin (SpH)-expressing mice.

Two-photon laser scanning microscopy imaging of large mossy fiber boutons of synaptopHluorin expressing transgenic mice in acute hippocampal slices – a new model to directly image presynaptic transmitter release during epilepsy

SynaptopHluorin (SpH) is a fusion protein that consists of a pH sensitive eGFP (pHluorin) fused to the C-terminus luminal domain of the vesicle SNARE protein synaptobrevin [24]. Under resting conditions, the luminal pH of the synaptic vesicle is acidic (pH~5.5), resulting in proton dependent quenching of SpH fluorescence. When vesicle exocytosis is triggered and glutamate released, the lumen of the vesicle is exposed to the more alkaline pH of the extracellular space (pH~7.2), resulting in a 20-fold increase in SpH fluorescence. When the vesicle membrane is retrieved by endocytosis and the vesicle reformed, it undergoes rapid reacidification by the vesicular ATPase, which returns SpH to its quenched state. The SpH21 transgenic mice line we used in this study, expresses SpH preferentially at glutamatergic synapses [4,5,25]. Representative two photon laser scanning image of the CA3 region of an acute hippocampal slice from this mouse (Figure. 1A) contains bright GFP positive boutons >2 μm in diameter, proximal to CA3 pyramidal cell bodies in the region innervated by mossy fiber axons of dentate granule cells [22,23]. Associational-commissural CA3 synapses are significantly smaller (<1 μm in diameter) and more distal to our region of interest (rectangular box, Figure 1A).

To confirm that large SpH expressing boutons were mossy fiber terminals, we used anterograde, bulk labeling of mossy fibers with Alexa Fluor 594 dextran introduced into the granule cell layer of the dentate gyrus (Figure 1B). During a 1.5-2 hour incubation, Alexa Fluor 594 dextran was taken up by granule cells and transported anterogradely to label mossy fiber axons and presynaptic boutons (Figure 1C). Figures 1E and 1F illustrate that some (solid arrows) but not all (broken arrows) SpH and Alexa Fluor 594-positive boutons were co-labeled confirming that, indeed, the large (>2μm in diameter) SpH fluorescent puncta within the proximal 60 μm of the CA3 cell body are the excitatory mossy fiber boutons (Figure. 1D). Associational-commissural CA3 synapses are significantly smaller (<1μm in diameter) and more distal to our region of interest (rectangular box, Fig. 1A). Incomplete co-localization is likely because Alexa Fluor 594-labeled a subset of mossy fiber axons in *stratum lucidum* in addition to sparse SpH expression in the excitatory terminals [4,5].

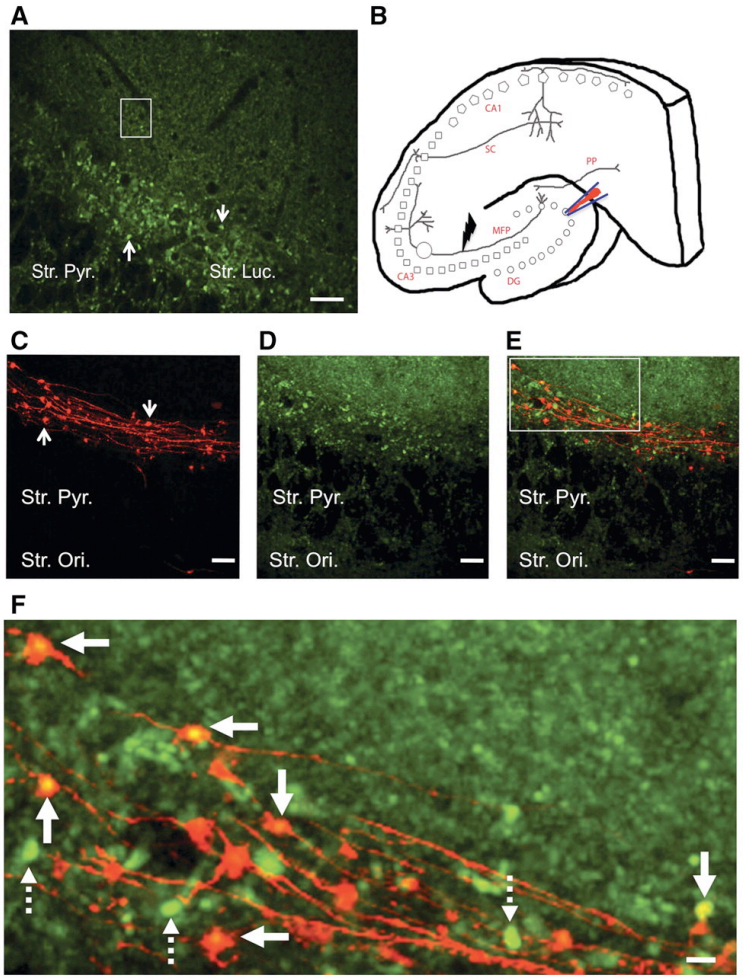

Figure 1: Visualizing mossy fiber boutons (MFBs) in acute hippocampal slices from SpH21 transgenic mice line. **(A)** Live cell two photon laser scanning image of field CA3 of SpH expressing glutamatergic terminals in a control hippocampal slice (postnatal 60 days). The arrows depict representative fluorescence puncta (about 4-5 µm in diameter) in the proximal (*stratum lucidum*) region of CA3 pyramidal cells (seen here as a ghost layer) that are likely to be giant MFBs. Distal puncta shown within the rectangular box are notably smaller in size and likely represent the associational-commissural synapses in the *stratum radiatum*. *Stratum pyramidale* (Str. Pyr.) and *Stratum Oriens* (Str. Ori.). Scale bar = 20 µm. **(B)** Cartoon representing the hippocampal circuitry with the circle in the mossy fiber pathway (MFP) depicting the area of imaging, depicts the area of local stimulation and the pipette in the dentate granule cell layer (DG) shows the area of Alexa Fluor 594 dextra containing pipette insertion. (PP: perforant path, SC: Schaffer collaterals, squares and pentagons depict CA3 and CA1 pyramidal cell layers respectively). **(C)** Alexa Fluor 594 dextran filled MF axons and giant MFB (arrows) showing characteristic en-passant arrangement along the axonal projections, visualized using 825nm excitation. **(D)** Same region as (**C**) but visualized with 890nm excitation to see SpH native fluorescence. CA3 pyramidal cell bodies can be seen as ghost cells in stratum pyramidal (Str. Pyr), and bright giant MFB in *stratum lucidum*. Scale bar = 20 µm (**C-E**). **(E-F)** Merged images of (**C**) and (**D**) show colocalization (f: arrows) between SpH and Alexa Fluor 594 dextran-labeled puncta. (**F**) Digital zoom of image from inset box in (**E**), scale bar = 4 µm. Not all SpH-positive puncta colocalized with Alexa Fluor 594 (F: broken arrows).

Pilocarpine-induced status epilepticus persistently increases size, vesicular release rate and endocytosis of mossy fiber boutons in SpH-expressing mice

Size: Live cell imaging of mossy fiber boutons in acute hippocampal slices was done by bulk loading a group of granule cells and their axons with Alexa Fluor 594-dextran. Dye-filled excrescences (Figure. 2A) were classified as the main body of giant mossy fiber boutons if they had at least a 4µm^2 cross-sectional area [23,95,100]. The mean area of mossy fiber boutons 1-2 months after pilocarpine induced-SE were significantly enhanced (~21.09%, Fig. 4C, P=0.008, Mann-Whitney U-test, n=7) when compared to aged matched controls (n=7). A frequency distribution histogram of individual mossy fiber boutons from epileptic animals revealed a significant rightward shift in the curves (Fig. 2B; P <0.05 Kolgomorov-Smirnov test) and an overall significant increase in mossy fiber bouton imaging area (Fig. 2C; P<0.05, Mann-Whitney U-test).

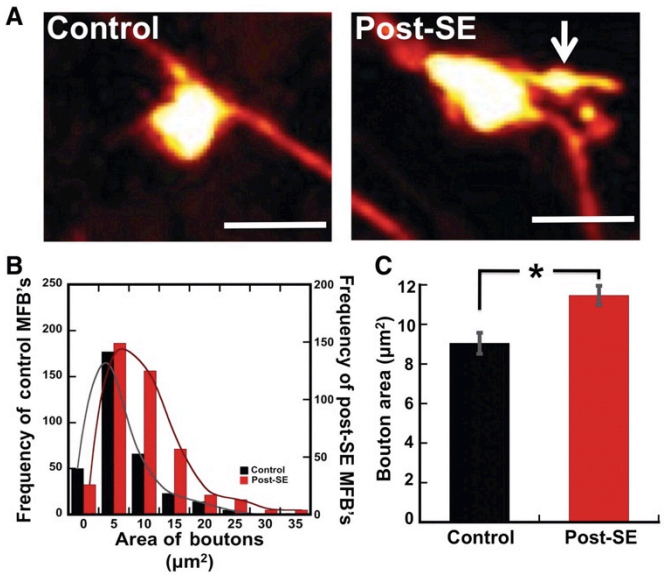

Figure 2: Pilocarpine-induced SE leads to persistent increase in dentate gyrus giant MFB area. (A) Live cell two-photon images of Alexa Fluor 594 dextran loaded giant mossy fiber terminals from field CA3 of acute hippocampal slices from control and post-SE mice. The arrow shows a filopodia-like projection arising from the giant MFB. Scale bar = 5 μm. **(B)** Frequency distribution histogram of individual MFBs area from control (black columns, total of 336 boutons, *n*=7) and 1-2 months post-SE mice (red columns, 394 boutons, *n*=7). (**C**) Mean MFB area for control (black column, 9.05 ± 0.52 μm^2) and epileptic (red column, 11.47 ± 0.48 μm^2) mice. Data plotted as mean ± SEM, * *P*<0.05, Mann-Whitney U-test.

Vesicular Exocytosis: To determine whether post-SE leads to functional differences in transmitter release from excitatory mossy fiber boutons we utilized two-photon live cell imaging in slices from SpH21 mice. To trigger vesicular release from mossy fiber boutons in CA3 *stratum lucidum* (Fig. 1B-F), slices from control and post-SE animals were stimulated with a single, continuous train of 600 stimuli at 20Hz (Fig. 2B), a paradigm that recruits both the RRP and rapidly recycling vesicle pools [5]. Representative time lapse images (Figure 3A) of control and post-SE SpH expressing mossy fiber boutons (solid arrows) showed robust, cumulative increases in SpH fluorescence intensity during the stimulus train, followed by return of fluorescence to baseline levels ~40 sec after stimulus termination (Figure 3B). Figure 3C plots the normalized mean SpH fluorescence responses in control versus post-SE animals, which showed significantly larger stimulus-evoked increases in SpH fluorescence (2.02 ± 0.15, red circles, *n*=8, *P*<0.05, Student's t-test) compared to controls (1.47 ± 0.03, black circles, *n*=10).

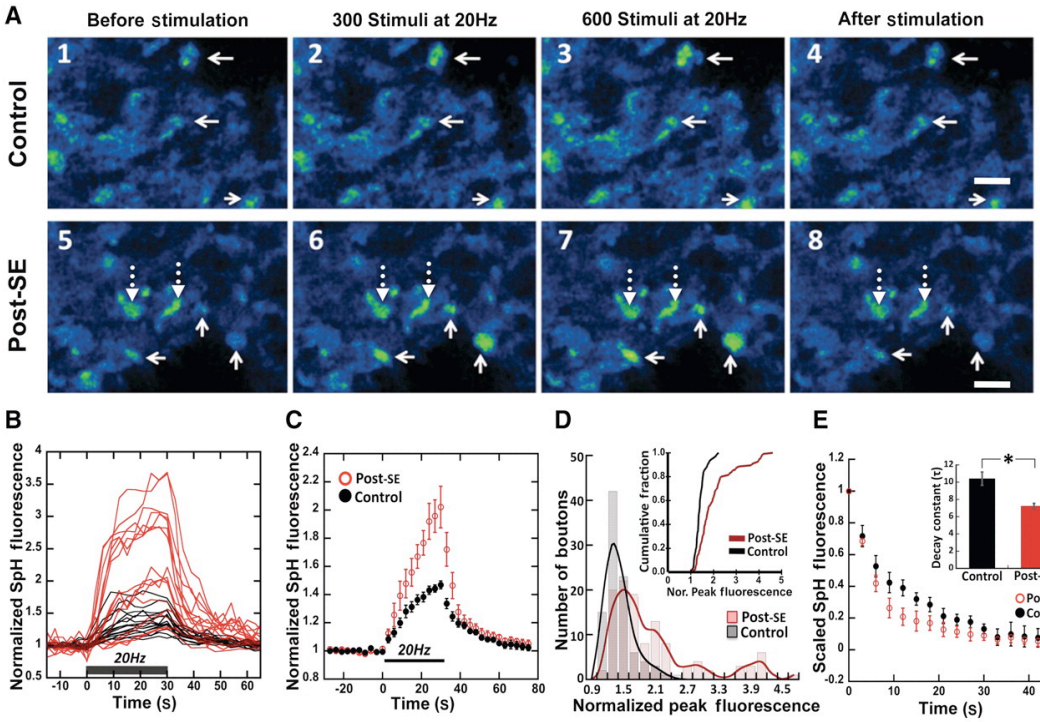

Figure 3: Pilocarpine-induced SE enhances vesicular release and endocytosis at mossy fiber terminals in CA3 *stratum lucidum*. (A) Two-photon images from control and post-SE SpH-expressing MFBs in proximal apical dendritic region of CA3 neurons. Solid arrows indicate puncta that showed activity-driven fluorescence changes during a 600 pulse 20 Hz stimulus train. The broken arrows in the lower panel show slowly fluorescing boutons in the epileptic slices. (Scale bar = 5 μm) **(B)** Representative time course of normalized fluorescence intensity of individual boutons from a control (black traces) and a post-SE (red traces) slice in response to the 600 pulse 20Hz MF stimulation (black bar shows duration of the train). **(C)** Normalized, evoked SpH fluorescence increases in response to a 600pulse 20Hz MF stimulus train, in MFBs from control (●, F_{peak} = 1.47 ± 0.03, *n*=10) and post-SE (○, F_{peak} = 2.02 ±0 .15, *n*=8) slices. F_{peak} was significantly increased in post-SE slices (*P*<0.05, Student's t-test; all values mean ± SEM). **(D)** Frequency distribution histogram of normalized peak SpH fluorescence for all MFB's in post-SE (F_{peak} = 1.76 ± 0.04, 100/115 puncta and 3.89 ± 0.10, 15/115 puncta) versus control (F_{peak} = 1.41 ± 0.025, 93 puncta). Inset is a cumulative

histogram of normalized peak SpH fluorescence, *P*<0.001 Kolgomorov-Smirnov test. **(E)** Mean fluorescence values of scaled SpH fluorescence decay (data normalized to respective peak fluorescence values from 4C) after cessation of stimulation, ● control and ⭘ Post-SE. Inset represents mean ± SEM of individual decay constants derived by a single exponential fit to the SpH fluorescence decay curve. Control (black bar), τ = 10.4 ± 0.77 s, *n*=67 and post-SE (red bar), τ =7.23 ± 0.32 s, *n*=133 (*, *P*<0.05, Student's t-test).

As shown in figure 4 below, we did not see any global change in VAMP-2 expression after the induction of SE. This result could be due to either a general increase in release probability of existing mossy fiber boutons or appearance of a distinct sub-population of terminals with higher release probabilities. To resolve this distinction, we plotted a distribution histogram (Figure 3D) of the normalized peak SpH fluorescence values, which are a function of the total number of vesicles released during the stimulus train. Control and post-SE distributions of peak SpH fluorescence for all individual mossy fiber boutons, indicate the appearance of a new sub-population of about 3-fold higher release rate MFBs in the post-SE animals. The cumulative probability distribution (Figure 3D inset) showed a significant increase in peak SpH fluorescence attained for the post-SE when compared to controls, *P*<0.001 Kolgomorov-Smirnov test).

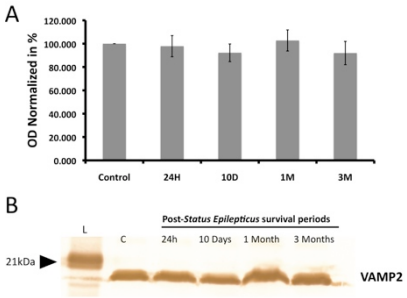

Figure 4: Western blot analysis of Synaptobrevin/VAMP2 expression after pilocarpine-induced *status epilepticus* (SE). **(A)** Graph representing semi-quantitative analysis of optical density (OD) for the synaptobrevin/VAMP2-positive bands revealed no significant differences among experimental groups (animals sacrificed at 24h, 10 days, 1 month and 3 months after SE) and control samples (data was normalized to control values and represented as bars=means ± SE, P>0.05, ANOVA n=3). **(B)** Representative Western blot experiment showing no apparent changes in the intensity of VAMP2-positive immunobands around 10-13kD for the different samples. C= Control. Ladder (L) indicates the molecular weight of 21 KDa.

Vesicular Endocytosis: To determine whether there are also changes in rate of vesicle *endocytosis* (recovery of vesicles for reuse after release) in mossy fiber boutons, we used the decay kinetics of SpH fluorescence after the end of the stimulus train. Since vesicle endocytosis is the rate-limiting step for decay in vesicle fluorescence determining the decay constant (τ) of this fluorescence gives an estimate of the rate of vesicle endocytosis. We first normalized the mean peak stimulus-evoked SpH fluorescence increases to 1.0 for control and post-SE slices, to compare directly the time courses of decay. As shown in figure 3E, the mean rate of decay of SpH fluorescence from peak to baseline for epileptic slices was significantly faster (red circles) when compared to control (black circles, *P*<0.05, Student's t-test), indicating an enhanced speed of endocytosis. We also fit single exponential decay functions to curves for individual mossy fiber boutons to determine the decay time constants in post-SE and control mossy fiber boutons. As shown in figure 3E inset above, chronic post-SE led to a significant decrease in decay time constants (red bar, τ =7.23 ± 0.32 s vs. control slices (black bar), τ =10.4 ± 0.77 s, *P*<0.05; Student's t-test) also consistent with acceleration in the rate of vesicle retrieval.

FM1-43 measurement of changes in vesicular release from the rat mossy fiber bouton readily releasable pool at early and late time points post-status epilepticus

As a second, independent measure of vesicular release, we estimated the time course of neurotransmitter release in slices from post-SE Sprague-Dawley rats using two-photon imaging of stimulus-evoked release of the styryl dye FM1-43 as described previously [97,107,108,110,111]. We loaded FM1-43 selectively into vesicles of the RRP with a 30 sec hypertonic shock and similar to SpH fluorescence, we visualized bright puncta in the proximal region of field CA3 >2 μm in diameter (Fig. 5A, solid arrows), presumably mossy fiber boutons [102]. It is postulated hypertonic solution produces $Ca2^{+}$ independent, asynchronous release of synaptic vesicles likely due to perturbations in the tension of the interacting membranes (synaptic vesicle membrane and the plasma membrane) that leads to a decrease energy barrier for membrane fusion (Stevens and Williams, 2000). More distal puncta (Fig. 5A, white rectangular box) that took up FM1-43 were much smaller in size and likely the associational-commissural synaptic terminals. Dye release was triggered by repetitive bursts of 50 mossy fiber stimuli at a frequency of 20Hz, spaced 30 sec apart (Fig. 5B), to allow binding and clearance by the scavenger ADVASEP-7 [100 μM; 111] and minimize potential movement artifacts.

Figure 5C shows mean time courses of RRP loaded stimulus-evoked FM1-43 destaining from mossy fiber boutons in slices up to 2 months (filled circles) post-SE was associated with a significantly enhanced release of

FM1-43 (~64% from prestimulus baseline, filled red circles, when compared to age matched controls (~51% from prestimulus baseline, filled black circles, *P*<0.05, Student's t-test). Interestingly, 11 months post-SE showed a substantial slowing in MFB release rate in the epileptic group (~21% from prestimulus baseline, open red circles) versus aged matched controls (~37% of baseline, open black circles, *P*<0.05, Student's t-test).

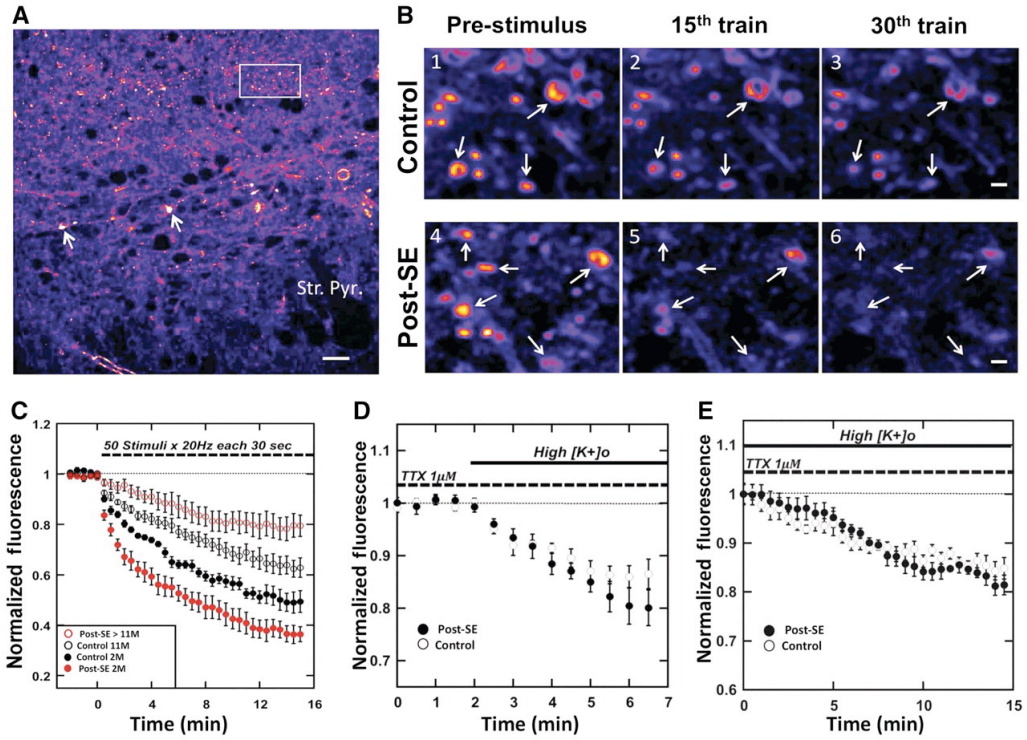

Figure 5: Pilocarpine-induced SE enhances evoked, but not action potential independent, presynaptic vesicular release of FM1-43 from the RRP in MFBs. **(A)** Two-photon image of a control field CA3 showing FM1-43 loaded RRP of MFBs. The solid arrows show staining of giant mossy fiber terminals, in the proximal region of CA3 stratum lucidum. The rectangular box outlines FM1-43 staining of puncta distal to the CA3 pyramidal cell bodies and much smaller in size, likely to be the associational-commissural synapses. Scale bar = 20 μm. **(B)** Representative time-lapse images of FM1-43 decay from the RRP using repetitive mossy fiber stimulus bursts (50 stimuli/20Hz each 30s) to evoke release from MFB in control and 2 month post-SE slices, respectively. Panels 1 and 4 illustrate pre-stimulus baseline fluorescence, panels 2 and 5 fluorescence intensity after 15 trains, and panels 3 and 6 fluorescence intensity after 30 trains of mossy fiber stimulation. Solid arrows indicate ROI's >2 μm in diameter that showed robust stimulus dependent FM1-43 destaining. Scale bar = 10 μm **(C)** Time course of FM1-43 destaining 1-2months (2M) post-SE slices (●, 0.36 ± 0.03, *n*=6), aged matched controls (●, 0.49 ± 0.04, *n*=5), >11 month (11M) post-SE slices (○, 0.79 ± 0.04, *n*=5) and aged matched controls (○, 0.62 ± 0.04, *n*=6). (All points are mean ± SEM of normalized fluorescence decay at 30th stimulus burst). *P*<0.05, Student's t-test. **(D)** Time course of first 4.5 minutes of action potential independent FM1-43 destaining in presence of TTX (1 μM) and 15 mM [K+]o from the RRP in MFBs of 2M post-SE (filled circles, *n*=4) and aged matched control (open circles, *n*=5) slices (All points are mean ± SEM). Decay after 4.5 minutes in high [K+]o: Control = 0.86 ± 0.028 (~14% of prestimulus baseline) and post-SE = 0.80 ± 0.034 (~20% of prestimulus baseline; *P*>0.20, Student's t-test) **(E)** Late phase of spontaneous release: Time course of renormalized spontaneous FM1-43 destaining after 10-25 minutes in *High[K+]o.* Control decay = 0.85 ± 0.02,post-SE decay = 0.81 ± 0.02 (*P*>0.20, Student's t-test, points mean ± SEM).

Action potential-independent release of FM1-43 is <u>not</u> altered by pilocarpine induced status epilepticus in rats

The above data suggests that changes in stimulus-evoked, but not necessarily spontaneous, release rate in the post-SE state. To measure presynaptic spontaneous release from the RRP, we loaded FM1-43 by hypertonic shock (800 mOsm/20 s), followed by bath application of tetrodotoxin (TTX 1 μM), and elevating to 15 mM extracellular [K^+]o (*High [K+]o)* to facilitate action potential-independent release (Axmacher *et al.*, 2004). To mark the early phase of AP-independent release, we monitored magnitude of FM1-43 destaining within the first 4.5 minutes of *High [K+]o* (Fig. 5D), which showed no significant difference between control (~15%) and post-SE (~20%) mossy fiber boutons *(P*>0.20, Student's t-test). To determine whether steady-state spontaneous release was altered, we examined the late phase of spontaneous release 10-25 minutes after application of *High [K+]o* (Figure 5E). As in early phase, there was no significant difference between the two groups after 25 min of *High [K+]o,* indicating AP-dependent and independent RRP vesicular release are differentially regulated post-SE.

Vesicle endocytosis becomes dynamin-independent after pilocarpine induced status epilepticus

Clathrin mediated endocytosis is the dominant mode of vesicle retrieval after synaptic vesicle endocytosis. The adaptor protein AP2, initiates the clathrin coat formation and helps recruits clathrin and the accessory protein amphiphysin to the site of endocytosis. Amphiphysin then recruits dynamin, a guanosine triphosphatase that is required for mediating membrane scission via GTP hydrolysis [103]. It has been demonstrated that dynamin-1 (a neuron specific dynamin) is required during intense neuronal activity [101]. Interestingly, it was recently reported that mice with a homozygous missense mutation in dynamin-1 exhibit lethal seizures, ataxia and neurosensory deficits, while the heterozygous condition leads to the occurrence of spontaneous recurrent seizures [98]. To determine if pilocarpine treated post-SE animals show altered sensitivity to dynamin inhibition, we measured SpH responses from mossy fiber terminals from control and post-SE slices that were incubated with dynasore (150-200μM), a highly specific, cell-permeable inhibitor of dynamin GTPase capable of arresting clathrin-mediated endocytosis [99,104,105], while not affecting vesicle exocytosis [105]. As shown in Figure 6 below, SpH fluorescence decay after cessation of stimulation was inhibited by dynasore treatment in control slices, suggesting a block in vesicle endocytosis [105]. Interestingly there was a significant increase in the peak SpH fluorescence attained in the presence of dynasore. This is likely due to an unmasking of endocytosis that occurs during the stimulation train [99,105]. However dynasore treatment of post-SE slices showed no increase in the peak fluorescence during the stimulus train, although there was an inhibition in the decay of SpH fluorescence after the end of the stimulation train.

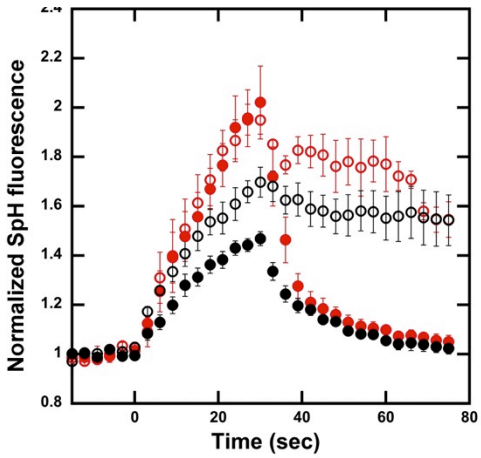

Figure 6: Differential effect of dynamin inhibition on vesicular recycling in control vs epileptic animals. Slices were pre-incubated with dynasore 150-200μM for 45minutes prior to and during image acquisition. Black filled circles represent control normalized SpH responses (with peak fluorescence at 1.4 ± 0.03 of baseline) to a 20Hz/600 stimulation train in the absence of dynasore, while the black empty circles represent a significant increase in the peak normalized SpH responses (1.7 ± 0.06, P<0.05) to 20Hz/600 stimulation in the presence of dynasore. Red filled circle represent control SpH responses to a 20Hz/600 stimulation train in the absence of dynasore leading to normalized peak fluorescence at 2.02 ± 0.15, while in the presence of dynasore (red empty circles) there was no significant increase in the normalized peak SpH fluorescence 1.95 ± 0.05) in response to a 20Hz/600 stimulation, P> 0.05.

Lack of boost in vesicle exocytosis during the stimulation train in epileptic tissue could be because of altered dynamin expression. To test this hypothesis, we immunoblotted extracts from hippocampal lysates with antibodies that recognize dynamin1,2,3 (pan dynamin) or individual isoforms of dynamin-1 or 2. As shown in figure 7A, a significant increase in pan dynamin expression was seen 24 hr, 10 days, 1 and 3 months post-SE, compared to age matched controls. There was, however, no difference detected in dynamin-1 or dynamin-2 expression alone. Additionally, there was an increase (~19.5%) in expression of phosphorylated Ser774 dynamin 1-3 (p-Dynamin) in 3-4 months epileptic rats vs controls (Figure 7C-D, Student's t-test, P<0.05). This could affect the interaction of dynamin with binding partners such as syndapin I and could alter synaptic vesicle endocytosis [96].

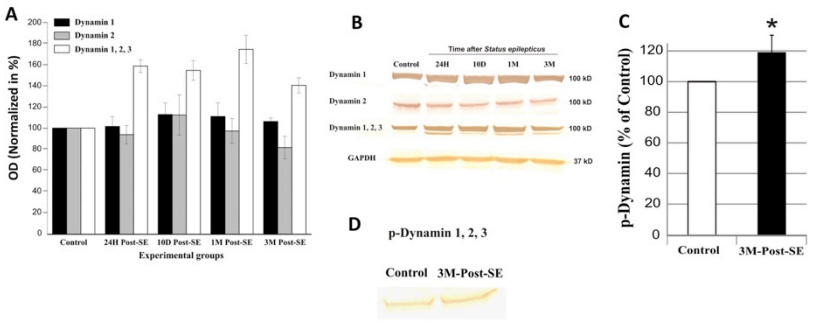

Figure 7: Western immunoblot analysis of dynamin in hippocampal lysates (A) from control rats and rats sacrificed at 24 hour, 10 days, 30–60 days (1 month) and 3 months post-SE. Bars represent mean optical density (OD) index normalized to control. Semi-quantitative OD analysis of bands revealed a significant increase in pan Dynamin expression (1-3) after SE (*one-way ANOVA, F =8.07, p < 0.0001* and HSD post-hoc *p<0.05*). **(B)** Immunoblots for Dynamin 1, 2 and pan Dynamin. GAPDH used as loading control. **(C)** Increased (~19.5%) expression of phosphorylated-Ser774 Dynamin 1-3 (p-Dynamin) in 3-4 mo epileptic rats vs controls (Student t-test, p <0.05). **(D)** Immunoblot of p-Dynamin.

Our results show that, in the first 1-2 months post-SE, morphological changes develop in the mossy fiber bouton cytoarchitecture, and are correlated with both an increase in vesiclular release rate of mossy fiber boutons and appearance of a high release rate sub-population. At late stages post-seizure (11 months), a time when substantial postsynaptic neuronal damage has occurred in hippocampal field CA3 (hippocampal sclerosis), transmitter release is markedly reduced, a potentially compensatory mechanism which, nevertheless, does not seem to prevent continued spontaneous seizures, and which will undoubtedly have important negative consequences for cognition and memory.

SE elicits long-term ultrastructural reorganization of active zones in MFBs

Previous literature has demonstrated clear correlations between release probability and synapse morphological parameters such as sizes of the RRP [26] and rapidly-recycling pools [27], active zone (AZ) [28,29] also known as 'release sites', postsynaptic density (PSD) [29] and presynaptic bouton [28]. Since we found increased release probability post-SE as measured by both SpH and FM1-43 destaining[7], we examined possible ultrastructural rearrangements in MFBs in CA3 *stratum lucidum* in post-SE and age-matched non-seizure Sprague-Dawley rats (Fig. 4a). Electron microscopy study was performed in collaboration with Dr. Dwight Romanovicz and Dr. Theresa Jones from University of Texas at Austin, Texas. Transmission electron microscopy (TEM) of large MFBs (2-5 μm in diameter) revealed multiple AZs facing PSDs, contained mitochondria of various sizes, and were filled with numerous small and large clear synaptic vesicles distributed throughout the terminal, as described previously [30-32]. Asymmetric AZs were distinguished in MFB synapses, by the dense accumulation of synaptic vesicles in close proximity to the presynaptic density and characteristic widening of the synaptic cleft[8]. There was a significant increase in number of AZ per MFB in post-SE rats (130 AZs in 6 control rats, 5.1 ± 1.36 AZs per MFB; 286 AZs in 7 post-SE rats, 7.7 ± 3.05 AZs per MFB, Student's t-test, $P<0.05$). The majority of EM variables failed to follow normal distributions, necessitating use of a nonparametric Kolgomorov-Smirnov two-sample test to assess between group differences in distributions. As reported previously[31,32] individual AZs varied substantially in shape and size; both very large and very small AZs were found in control (104-887nm) and post-SE (105-1837nm). Frequency distributions revealed the presence of a distinct group of synapses of larger length in epileptic animals that was not present in controls (Fig. 5b, panel a). A cumulative histogram indicated a significant leftward shift towards larger individual AZ lengths in MFBs post-SE (Fig. 5c), compared to controls (Table 1, Kolgomorov-Smirnov test, $P<0.005$). There was also a significant increase in mean PSD area in the post-SE group (Table 1) compared to controls (Table 1, Kolgomorov-Smirnov test $P<0.005$, an ~37% increase). In contrast, no significant changes were detected in average synaptic cleft width between control and post-SE AZs (Table 1).

***Table 1**. Summary of quantitative analysis of structural variables in AZs of MFBs.*

	Control	**Post-SE**		
AZ Ultrastructural Variables	Mean ± SD	Mean ± SD	% of Control	K-S *P*
Length of AZ (nm)	364.91 ± 44.81	485.27 ± 59.63	133.5	*P<0.005*
Length of synaptic cleft (nm)	26.93 ± 3.91	29.95 ± 2.46	107.4	*P=0.31*
PSD area (μm^2)	12.31 ± 3.03	16.90 ± 3.31	136.9	*P<0.005*
Number of SVs in RRP	7.43 ± 3.12	8.94 ± 1.78	120.3	*P<0.001*
Number of SVs in the RP	31.07 ± 6.05	33.44 ± 7.13	107.6	*P<0.05*
Number of docked SVs per AZ	1.96 ± 0.68	2.63 ± 0.56	134.2	*P<0.0005*
Docked SVs per AZ length (SV/μm)	5.48 ± 1.75	5.88 ± 0.90	108.9	*P<0.05*
% of Docked SVs of RRP	27.92 ± 6.45	29.56 ± 3.24	105.85	*P=0.59*

Measurements were obtained from analysis of active zone (AZ) variables in MFBs. Statistical comparisons were made by the Kolgomorov-Smirnov (K-S) two-sample test. Statistical significance was set at $P<0.05$. Values are presented as means ± SEM. PSD, postsynaptic density, SVs, synaptic vesicles, RRP, readily releasable pool.

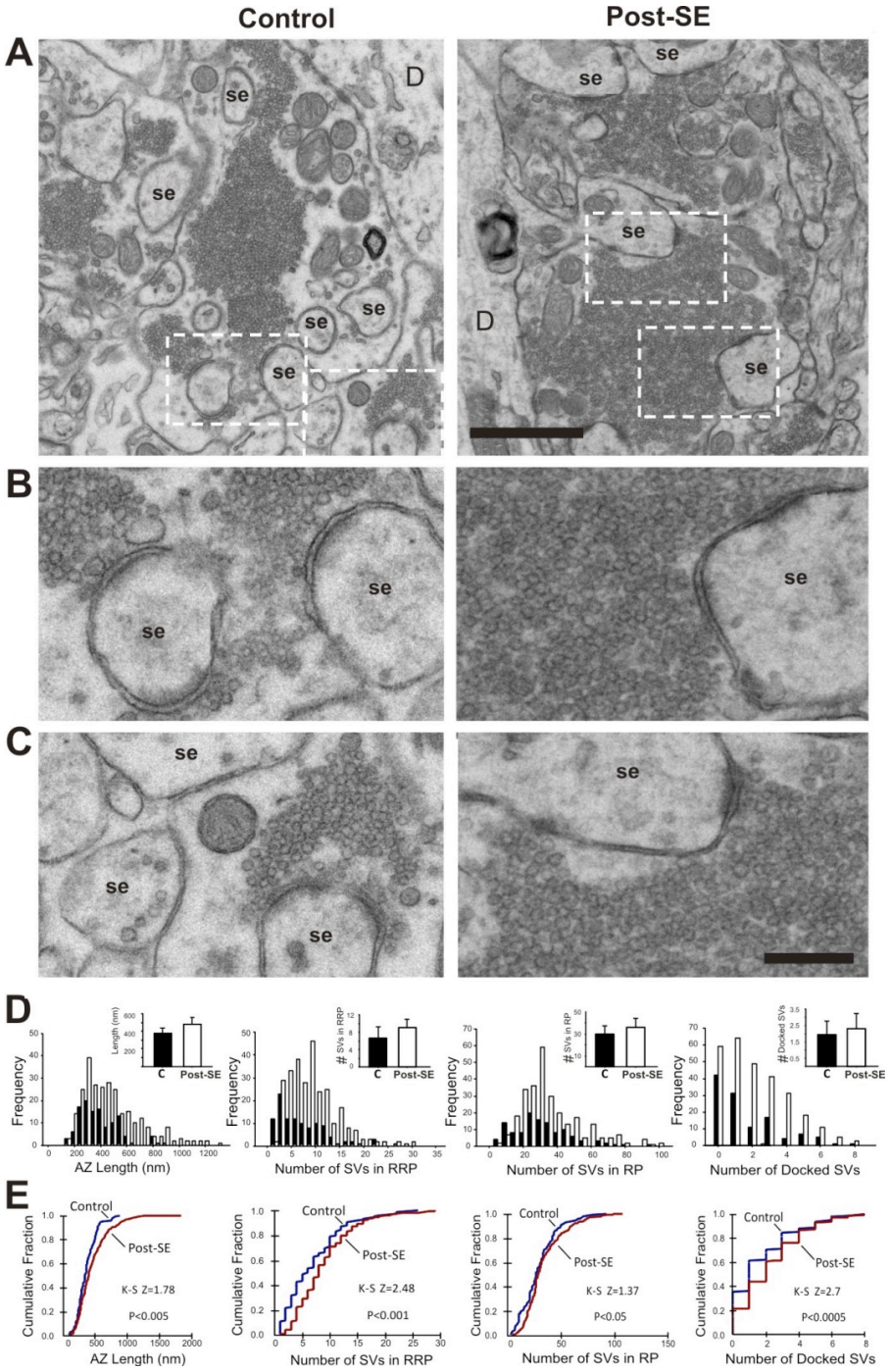

Fig. 8. Transmission electron microscopy (TEM) of active zones (AZs) in MFBs of control and post-SE rats. **(A)** Representative TEM images of control (Left column) and post-SE (right column) MFBs illustrating AZs on synaptic excrescences (se) showing an apparent increase in synaptic vesicle density in post-SE MFB. Boxed areas are depicted at higher magnification (x4) images **(B).(C)** showing arrangement of vesicles in the AZs of control and epileptic MFBs. Notice a larger density of vesicles and length of AZ in post-SE MFBs. Scale bar 2mm for a and 500 nm for all others, D=dendrite. **(D)** Frequency histograms and bar graph representation of data for AZ length, number of synaptic vesicles in RRP and RP, and number of docked synaptic vesicles. Notice appearance of increase number of AZs exhibiting larger lengths in post-SE (>800nm). **(E)** Cumulative histograms for these variables in control versus post-SE groups revealed significant rightward shifts toward the larger-size bins by Kolgomorov-Smirnov two-sample test (K-S).

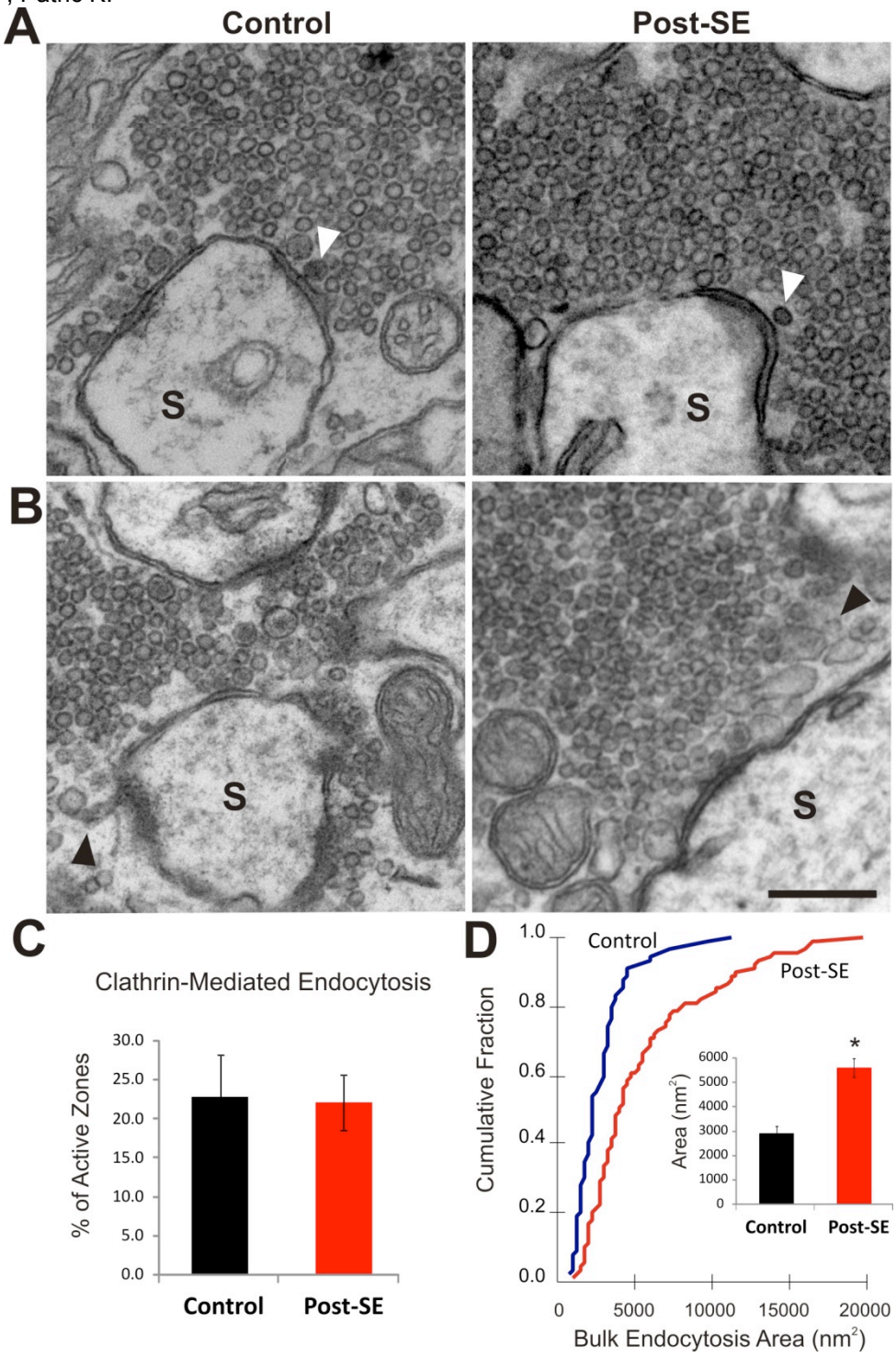

Fig. 9. Representative TEM images of active zones (AZs) in MFBs exhibiting structural signs of clathrin-mediated endocytosis and "bulk endocytosis" in control and epileptic rats. Putative clathrin-coated (dark) vesicles (white arrows) located proximal to presynaptic membrane AZs synapsing on spines (S) of Control **(A)** and post-SE **(B)** MFBs. Irregular membranous structures (black arrows) near AZs on spines (S) were observed in Control **(C)** and post-SE **(D)** MFBs. Note these structures were larger in post-SE rats. (Scale bar in **d** 500nm) **(E)** Mean ± SEM % AZs positive for clathrin-coated vesicles, showing no difference in control versus post-SE rats (P>0.20, Student's t-test). **(F)** Cumulative histogram plot of bulk endocytosis area showing a significant rightward shift on the size distribution towards larger values in post-SE MFBs (red) compared to Controls (blue, P<0.001, Kolgomorov-Smirnov test). (Inset: mean area of bulk endocytosis in Control (black) versus post-SE (red) rats (*, P<0.05, Student's t-test).

It has been previously suggested that a rapid refilling of the RRP from a larger releasable vesicle pool (RP) is a key mechanism in ensuring fidelity of mossy fiber-CA3 pyramidal cell neurotransmission[33]. To determine whether ultrastructural organization of synaptic vesicle pools is altered post-SE, we measured the number of vesicles docked, within 60nm of the AZ, 60-200nm from an AZ, and >200nm from an AZ, in MFBs of control versus epileptic animals. The RRP was defined as the sum of docked vesicles and those within 60 nm of the AZ, while the releasable pool (RP) was defined as vesicles 60 to 200 nm away from an AZ [33] (Fig. 5a, panel 2 and 6). Compared to controls, post-SE increased number of docked (+34.2%), RRP (+20.3%), and RP (+7.6%) synaptic vesicles (Table 1). A significant difference was detected in the analysis of the cumulative distributions of these variables by Kolmogorov-Smirnov test (Fig. 5c and Table 1). Although the percentage of docked vesicles relative to RRP size was not significantly different (Table 1), the average number of docked vesicles per length of AZs was significantly higher for post-SE (+8.9%, Table 1). Additionally, the number of synaptic vesicles in each of these pools was significantly correlated with the length of individual AZs in both control (RRP: r = 0.33, P<0.001 and RP: r =0.41, P<0.001) and post-SE MFB (RRP: r =0.57, P<0.001 and RP: r=0.55, P<0.001).

In order to assess endocytosis, we measured (a) the number and percent of clathrin-coated vesicles 0-200 nm from an AZ (Fig. 5a and b) and the area of membranous regions apparently internalized at the AZ, indicative of “bulk endocytosis” (Fig. 5c and d), in MFBs of control and post-SE. There were no statistical differences in percent of synapses exhibiting 1 or 2 putative clathrin-coated vesicles at AZ between control (22.7 ± 10.1%) and post-SE (22.0 ± 7.1%, Fig. 5e) animals, or percent synapses exhibiting bulk endocytosis (control: 48.7 ± 13.1%, epileptic: 40.7 ± 15.8%). In contrast, the area of large elliptical or irregular membranous structures at the AZ was significantly higher at MFB synapses post-SE (5662 ± 385 nm^2) compared to controls (2917 ± 287 nm^2, Kolmogorov-Smirnov test, P<0.001, Fig. 5f). Taken together, our EM data show pilocarpine-induced SE leads to profound and long-lasting rearrangement of MFB transmitter release sites, resulting in significant increases in number of release sites per MFB, length of individual release sites, and RRP and RP vesicle pools sizes that may underlie persistent increases in functional transmitter vesicular release rates, magnitude, and recycling properties. The pilocarpine model of epilepsy in the SpH21 transgenic mice is thereby an invaluable tool to investigate the presynaptic function using advanced imaging methods.

In a manuscript published in the high profile journal Brain (Upreti et al., 2012; 5-year Impact Factor 10.143, ranked 12th of 265 neuroscience journals), we described the epilepsy-associated long-term alterations in presynaptic morphology and synaptic vesicle recycling we discovered at mossy fiber-CA3 terminals of mice and rats subjected to pilocarpine-induced SE, a seizure model that produces a chronic epileptic state associated with spontaneous generalized seizures in 100% of animals [3]. We found increases in 1) mossy fiber bouton (MFB) size, 2) number of release sites per MFB, 3) number of RRP and RP vesicles, 4) active zone length, 5) action potential-driven vesicular release rate measured with either FM1-43 or SpH-expressing transgenic mice, and 6) vesicle endocytosis. These alterations persisted for 3 months following a single sustained SE, making it likely they are important contributors to development and maintenance of the epileptic state.

KEY RESEARCH ACCOMPLISHMENTS – YEAR 01:

- Established and optimized the pilocarpine model of chronic epilepsy in our laboratory for both rats and synaptopHluorin-expressing transgenic mice
- Comprehensive characterization of the baseline properties of presynaptic vesicular release from control mossy fiber terminals in hippocampal slices from both rats and synaptopHluorin-expressing transgenic mice
- Discovery that pilocarpine epilepsy is associated, 1-2 months post-seizures, with marked increases in the size of hippocampal mossy fiber terminals and the appearance of ectopic boutons that synapse in a layer of field CA3 where they do not normally synapse.

- Discovery that the appearance of these larger boutons correlates with marked increases in vesicular release from mossy fiber terminals and the appearance of a population of very high release rate boutons in both rats and SpH-expressing mice 1-2 months post-seizure.
- Discovery that, in addition to exocytosis, endocytotic vesicle recycling is also persistently enhanced 1-2 months following pilocarpine-induced seizures.
- Discovery that down-regulation of dynamin may be a key component in seizure-induced shifts in endocytotic recycling pathways and properties.
- Publication in the prestigious, high impact journal *Brain* of our study of pilocarpine-induced long-lasting morphological and functional alterations in mossy fiber terminals in both rats and SpH-expressing mice.
- Established the pilocarpine epilepsy model in SV2A knockout mice in the lab of Dr. Garrido-Sanabria at University of Texas Brownsville.
- Commenced studies using 2-photon laser scanning microscopy to evaluate the effects of levetiracetam, carbamezipine, lamotrigine and topiramate on presynaptic vesicular release in control versus pilocarpine-seized epileptic rats and SpH mice.

CONCLUSION

In year 01, we completed the majority of our studies in Aim 1 and a portion of Aim 2. We found that severe pilocarpine-induced seizures that result in long-term appearance of spontaneous epileptic seizures are associated with marked changes in the structure of hippocampal mossy fiber presynaptic terminals and functional hyperexcitability of presynaptic vesicular transmitter release. Mossy fiber terminals were greatly increased in size, as was the size of the transmitter release active zone and readily-releasable vesicle pool, and there was even sprouting of new mossy fiber terminals into the stratum oriens layer of field CA3 where such terminals do not normally synapse. Functionally, these presynaptic glutamatergic terminals showed greatly enhanced rate of vesicular release from the rapidly-recycling vesicle pool and accelerated endocytotic recycling of vesicles back into this vesicle pool. We showed these functional changes in both rats and mice, using two different fluorescent indicators to image, by 2-photon laser scanning microscopy, individual mossy fiber release sites in the hippocampal CA3 field. We commenced studies which will be completed in year 02 to test the ability of four antiepileptic drugs that act via differing mechanisms (levetiracetam, lamotrigine, carbamezipine and topiramate), to control presynaptic vesicular release two months after pilocarpine-induced seizures, when the brain has become spontaneously epileptic. We also discovered that the presynaptic vesicle protein dynamin, which is an essential component of one vesicle recycling pathway, is markedly down-regulated in expression and the dynamin pathway loses its ability to keep up with vesicular release in the epileptic brain.

Significance: While all but one antiepileptic drug acts by modifying postsynaptic neuronal excitability, our work indicates that extensive changes in presynaptic function are also associated with epilepsy. Increases in glutamate release, while certainly able to contribute to hyperexcitation in seizures, also have the potential to damage and even kill their postsynaptic target neurons. If we can find agents that can control presynaptic release, and do so even after development of epilepsy when release is enhanced, we would have a whole new class of treatments to help the 40% of epileptic patients who do not respond to any current therapeutics. Understanding the mechanisms by which seizures change presynaptic function is the essential first step towards this goal.

YEAR 02

HYPOTHESIS AND OBJECTIVES:

During periods of intense neuronal activity such as seizures, a larger pool of vesicles could result in more glutamate being released and long-lasting aberrant excitation. We propose to explore the effects of seizures on transmitter release and the presynaptic action of AEDs on these changes. We will use electrophysiology and multiphoton confocal microscopy. Preliminary data indicate that SE induces long-lasting potentiation of synaptic vesicle release in epileptic rats. We hypothesize that successful AED treatment might prevent or reverse these seizure-induced molecular deficiencies (reduction of N-type VGCC, mGluR II and SV2a expression), and be antiepileptogenic as well. Our **central hypothesis** is that pharmacological regulation of glutamate transmitter release at presynaptic sites will be an effective, novel therapeutic strategy to ameliorate epileptogenesis and excessive synaptic excitation in epilepsy. The **long-term objectives** of this collaborative proposal are to: (1) identify the most effective AEDs which modulate presynaptic glutamate release, and (2) determine the presynaptic mechanism of action of the new AED LEV to modulate vesicular release properties. *Our central hypothesis is that pharmacological regulation of glutamate transmitter release at presynaptic sites will be an effective, novel therapeutic strategy to treat many cases of drug-resistant epilepsy, especially epileptogenesis following traumatic brain injury.* The **long-term goals** of this collaborative project are to: (1) identify the most effective antiepileptic drugs amongst compounds that modulate presynaptic glutamate release and (2) determine the presynaptic mechanism of action of the new antiepileptic drug **levetiracetam** (LEV). ***In Year 2 of this proposal, we made substantial progress on experiments with specific anticonvulsant drugs in the remainder of specific Aims 1 and 2 tasks that form our portion of year 02 of the collaborative project, as outlined below.***

Specific Aim 1: *Determine which antiepileptic drugs are most effective at reducing glutamate release from mossy fiber presynaptic boutons (MFBs) in the pilocarpine model of mesial temporal lobe epilepsy (MTLE)* (months 1-12).

Working hypothesis: Drugs acting on presynaptic Ca^{2+} channels, autoreceptors, and SV2a will be more effective in reducing vesicular glutamate release at excitatory presynaptic terminals in the hippocampus.

Research Goals:

Task 1. Evaluate the effects of different concentrations of "classical" (*e.g*. carbamazepine, lamotrigine, and topiramate, and "new generation" antiepileptic drugs (*e.g.* LEV) on presynaptic glutamate release by using two-photon imaging of vesicular release of the fluorescent dye FM1-43 from individual mossy fiber terminals in *in vitro* hippocampal slices.

Development of the pilocarpine model of epilepsy in mice and rats at both institutions. (Subtask 1a) single injection of pilocarpine in rats and in the transgenic Sp21 mice expressing the fluorescent reporter of synaptic vesicle release and presynaptic function synaptophlourin (SpH).

- **Subtask 1c.** Test whether antiepileptic drugs modify kinetics of transmitter release in control versus epileptic rats (Dr. Stanton, Dr. Zhang; months 1-12).
- **Subtask 1d.** Statistical analysis of the experimental data (Dr. Stanton, Dr. Zhang;months 9-12).

Task 2. Evaluate the effects of different concentrations of "classical" (*e.g*. carbamazepine, lamotrigine, and topiramate, and "new generation" antiepileptic drugs (*e.g.* LEV) on patch-clamp electrophysiological recordings from dentate granule cells that give rise to mossy fibers to assess the effects of antiepileptic drugs on spontaneous miniature excitatory postsynaptic currents (mEPSC) in control versus pilocarpine-treated rats. Approximately 50 adult 150-250g Sprague Dawley rats will be used for these experiments.

Development of the pilocarpine model of epilepsy in mice and rats at both institutions. (Subtask 1a) single injection of pilocarpine in rats and in the transgenic Sp21 mice expressing the fluorescent reporter of synaptic vesicle release and presynaptic function synaptophlourin (SpH).

- **Subtask 2d.** Test whether antiepileptic drugs modify the frequency and amplitude of mEPSCs in granule cells in control versus epileptic rats (Dr. Stanton and Dr. Zhang; months 1-12).
- **Subtask 2e.** Statistical analysis of electrophysiology data (Dr. Stanton and Dr. Zhang, months 9-12).

1.c and 1.d. Test whether antiepileptic drugs modify kinetics of transmitter release in control versus epileptic rats

Experiments are nearing completion on the effects of acute administration of levetiracetam (LEV) on presynaptic vesicular transmitter release from excitatory Schaffer collateral terminals in hippocampal field CA1 using multiphoton laser scanning confocal imaging analysis of presynaptic release in both control and pilocarpine-induced epileptic transgenic SpH-expressing mice (**Subtask 1c and d)**. In addition, the pilocarpine model of mesial temporal lobe epilepsy (MTLE) has been optimized in SV2A/SV2B knockout mice in the laboratory of Dr. Garrido.

Pilocarpine-induced status epilepticus persistently increases size, vesicular release rate and endocytosis of mossy fiber boutons in SpH-expressing mice

Size: Live cell imaging of mossy fiber boutons in acute hippocampal slices was done by bulk loading a group of granule cells and their axons with Alexa Fluor 594-dextran. Dye-filled excrescences (Figure. 2A) were classified as the main body of giant mossy fiber boutons if they had at least a 4μm^2 cross-sectional area [23,95,100]. The mean area of mossy fiber boutons 1-2 months after pilocarpine induced-SE were significantly enhanced (~21.09%, Fig. 4C, *P*=0.008, Mann-Whitney U-test, *n*=7) when compared to aged matched controls (*n*=7). A frequency distribution histogram of individual mossy fiber boutons from epileptic animals revealed a significant rightward shift in the curves (Fig. 2B; *P* <0.05 Kolgomorov-Smirnov test) and an overall significant increase in mossy fiber bouton imaging area (Fig. 2C; *P*<0.05, Mann-Whitney U-test).

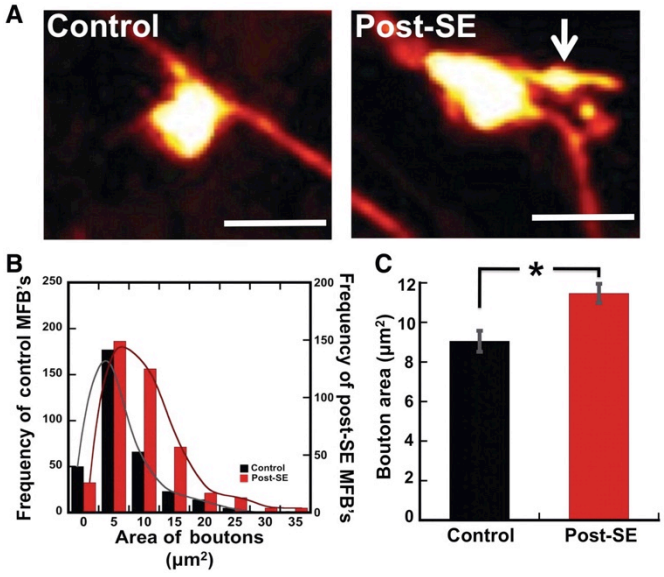

Figure 10: Pilocarpine-induced SE leads to persistent increase in dentate gyrus giant MFB area. (A) Live cell two-photon images of Alexa Fluor 594 dextran loaded giant mossy fiber terminals from field CA3 of acute hippocampal slices from control and post-SE mice. The arrow shows a filopodia-like projection arising from the giant MFB. Scale bar = 5 μm. **(B)** Frequency distribution histogram of individual MFBs area from control (black columns, total of 336 boutons, *n*=7) and 1-2 months post-SE mice (red columns, 394 boutons, *n*=7). (**C**) Mean MFB area for control (black column, 9.05 ± 0.52 μm^2) and epileptic (red column, 11.47 ± 0.48 μm^2) mice. Data plotted as mean ± SEM, * *P*<0.05, Mann-Whitney U-test.

Vesicular Exocytosis: To determine whether post-SE leads to functional differences in transmitter release from excitatory mossy fiber boutons we utilized two-photon live cell imaging in slices from SpH21 mice. To trigger vesicular release from mossy fiber boutons in CA3 *stratum lucidum* (Fig. 1B-F), slices from control and post-SE animals were stimulated with a single, continuous train of 600 stimuli at 20Hz (Fig. 2B), a paradigm that recruits both the RRP and rapidly recycling vesicle pools [5]. Representative time lapse images (Figure 3A) of control and post-SE SpH expressing mossy fiber boutons (solid arrows) showed robust, cumulative increases in SpH fluorescence intensity during the stimulus train, followed by return of fluorescence to baseline levels ~40 sec after stimulus termination (Figure 3B). Figure 3C plots the normalized mean SpH fluorescence responses in control versus post-SE animals, which showed significantly larger stimulus-evoked increases in SpH fluorescence (2.02 ± 0.15, red circles, *n*=8, *P*<0.05, Student's t-test) compared to controls (1.47 ± 0.03, black circles, *n*=10).

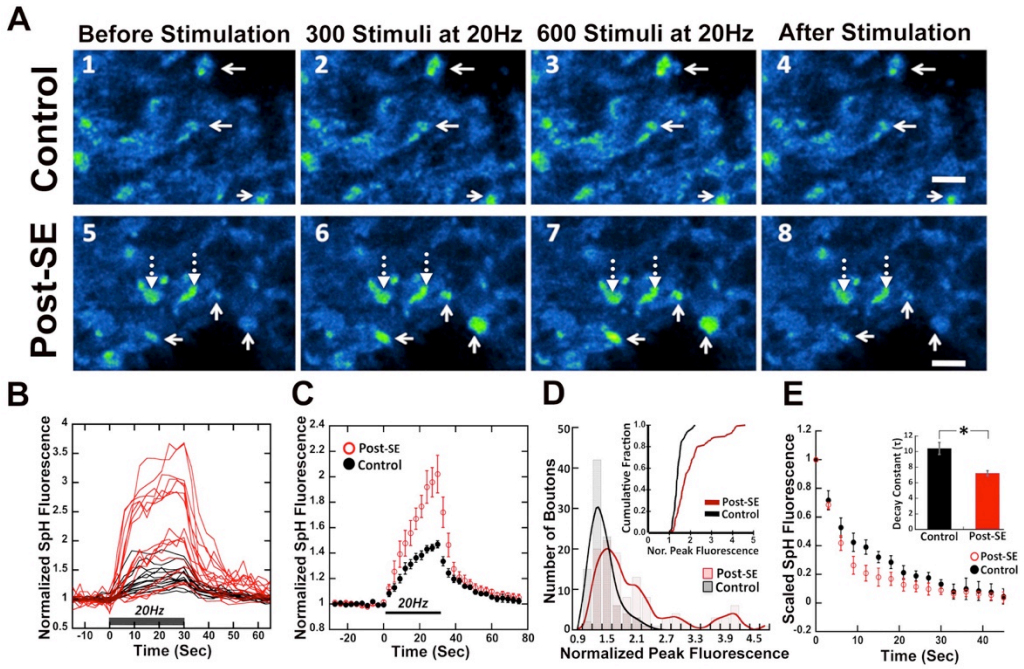

Figure 11: Pilocarpine-induced SE enhances vesicular release and endocytosis at mossy fiber terminals in CA3 *stratum lucidum*. (A) Two-photon images from control and post-SE SpH-expressing MFBs in proximal apical dendritic region of CA3 neurons. Solid arrows indicate puncta that showed activity-driven fluorescence changes during a 600 pulse 20 Hz stimulus train. The broken arrows in the lower panel show slowly fluorescing boutons in the epileptic slices. (Scale bar = 5 μm) **(B)** Representative time course of normalized fluorescence intensity of individual boutons from a control (black traces) and a post-SE (red traces) slice in response to the 600 pulse 20Hz MF stimulation (black bar shows duration of the train). **(C)** Normalized, evoked SpH fluorescence increases in response to a 600pulse 20Hz MF stimulus train, in MFBs from control (●, F_{peak} = 1.47 ± 0.03, *n*=10) and post-SE (○, F_{peak} = 2.02 ±0 .15, *n*=8) slices. F_{peak} was significantly increased in post-SE slices (*P*<0.05, Student's t-test; all values mean ± SEM). **(D)** Frequency distribution histogram of normalized peak SpH fluorescence for all MFB's in post-SE (F_{peak} = 1.76 ± 0.04, 100/115 puncta and 3.89 ± 0.10, 15/115 puncta) versus control (F_{peak} = 1.41 ± 0.025, 93 puncta). Inset is a cumulative histogram of normalized peak SpH fluorescence, *P*<0.001 Kolgomorov-Smirnov test. **(E)** Mean fluorescence values of scaled SpH fluorescence decay (data normalized to respective peak fluorescence values from 4C) after cessation of stimulation, ● control and ○ Post-SE. Inset represents mean ± SEM of individual decay constants derived by a single exponential fit to the SpH fluorescence decay curve. Control (black bar), τ = 10.4 ± 0.77 s, *n*=67 and post-SE (red bar), τ =7.23 ± 0.32 s, *n*=133 (*, *P*<0.05, Student's t-test).

Vesicular Endocytosis: To determine whether there are also changes in rate of vesicle *endocytosis* (recovery of vesicles for reuse after release) in mossy fiber boutons, we used the decay kinetics of SpH fluorescence after the end of the stimulus train. Since vesicle endocytosis is the rate-limiting step for decay in vesicle fluorescence [106], determining the decay constant (τ) of this fluorescence gives an estimate of the rate of vesicle endocytosis. We first normalized the mean peak stimulus-evoked SpH fluorescence increases to 1.0 for control and post-SE slices, to compare directly the time courses of decay. As shown in figure 3E, the mean rate of decay of SpH fluorescence from peak to baseline for epileptic slices was significantly faster (red circles) when compared to control (black circles, *P*<0.05, Student's t-test), indicating an enhanced speed of endocytosis. We also fit single exponential decay functions to curves for individual mossy fiber boutons to determine the decay time constants in post-SE and control mossy fiber boutons. As shown in figure 3E inset above, chronic post-SE led to a significant decrease in decay time constants (red bar, τ =7.23 ± 0.32 s vs. control slices (black bar), τ =10.4 ± 0.77 s, *P*<0.05; Student's t-test) also consistent with acceleration in the rate of vesicle retrieval.

LEV reduces enhanced vesicular release from mossy fiber boutons of chronically epileptic SpH-expressing transgenic mice expressing SpH at excitatory glutamatergic terminals

Levetiracetam (Keppra®, LEV) is a new class of antiepileptic drug exhibiting selective seizure protection in chronic animal models of epilepsy. Compelling experimental evidences indicate a presynaptic action site for LEV. For instance, LEV binds to the synaptic vesicle protein SV2A and LEV can modulate excitatory transmission by a mechanism depending on the inhibition of presynaptic Ca^{2+} channels. However, it is also known that LEV targets

SV2A undergo down-regulation during epileptogenesis in animal models and epileptic patients suffering mesial temporal lobe epilepsy (MTLE). Therefore, we evaluated the action of LEV on dentate gyrus excitatory circuits in MTLE. For this purpose, patch-clamp and field potential recordings were performed in hippocampal slices from control and epileptic rats obtained by the pilocarpine model of MTLE. In addition, the effect of LEV was was also assessed in mice with altered SV2A expression including hemizygous ($SV2A^{+/-}$) and knockout ($SV2A^{-/-}$) compared to wild-type controls and epileptic mice. By using 2-photon laser scanning confocal microscopy, we tested whether LEV was effective in reducing enhanced vesicle release in mossy fibers from control and epileptic transgenic SpH21 mice expressing synaptopHluorin (SpH) in mossy fiber boutons. Expression changes in SV2A, SV2B and SV2C were analyzed using immunofluorescence, western blotting and real-time quantitative PCR (qPCR). Action of LEV was occluded in animals lacking SV2A expression. Figure 4 (below) shows that, in four separate epileptic mice, LEV reduced excitatory (glutamatergic transmission) activity-dependent synaptic vesicle release from the sucrose-loaded readily releasable/recycling vesicle pool substantially more in chronically epileptic animals **(B)** compared to non-epileptic controls **(A)**, despite changes in SV2A expression and synaptic reorganization of excitatory terminals in MTLE.

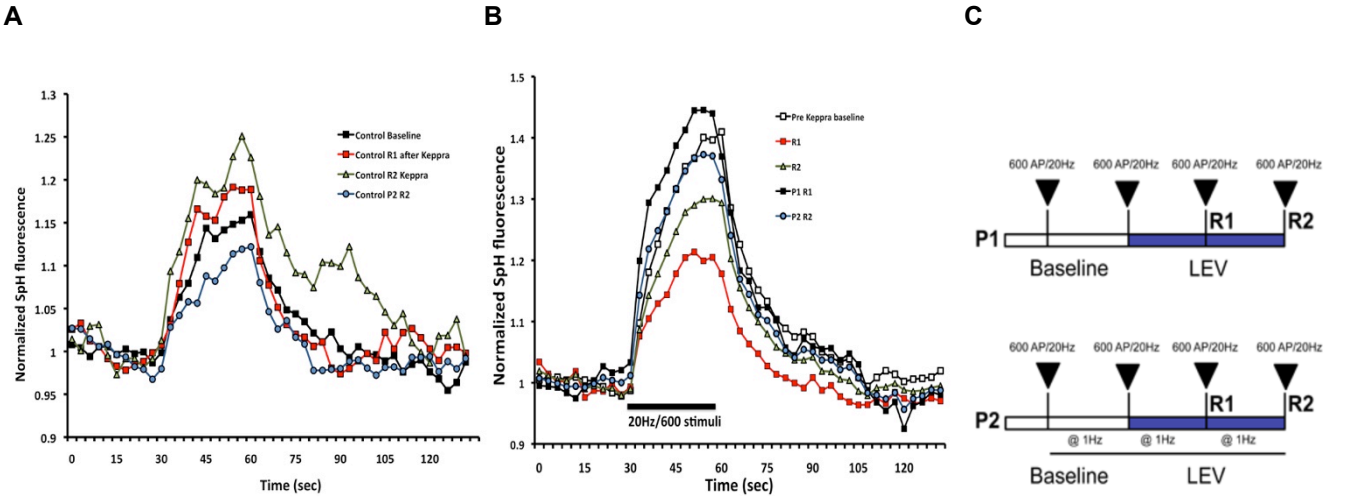

Figure 12: Normalized MFB fluorescence changes during 600 pulse 20 Hz train before **(A)** and after **(B)** incubation with LEV (Keppra™, 200 mM) in slices from control and epileptic SpH mice. Schematic representation **(C)** of stimulation paradigms for LEV incubation with and without 1 Hz stimulation (loading).

2.d and 2.e. Test whether antiepileptic drugs modify the frequency and amplitude of mEPSCs in granule cells in control versus epileptic rats

Levetiracetam (LEV) induces activity-dependent reduction of evoked fEPSP amplitude in dentate gyrus of pilocarpine-treated epileptic rats

In close collaboration with Drs. Garrido and Pacheco at the University of Texas Brownsville, experiments examining the acute effects of LEV on transmission at non-epileptic versus chronically epileptic perforant path-dentate granule cell synapses have been completed and are being prepared for publication. As shown if figure 5 below, LEV has no significant effects on synaptic transmission in non-epileptic tissue, but does show significant suppression of evoked synaptic responses in chronically epileptic animals treated with pilocarpine two months previously. These rats develop spontaneous partial and generalized seizures over this period.

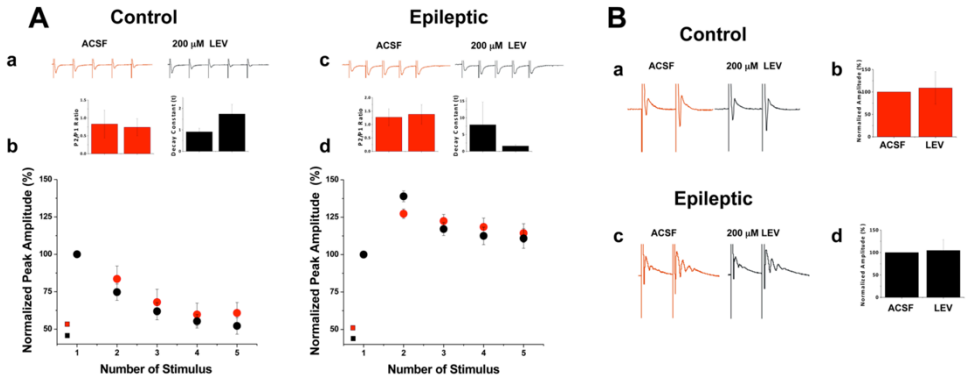

Figure 13. (A) Effect of LEV on evoked field excitatory postsynaptic potentials in dentate gyrus molecular layer upon perforant path sub-threshold burst stimulation (@10Hz, 5 stimuli) in slices from control and pilocarpine-treated epileptic rats. In control LEV did not reduce amplitude of fEPSP in the train **(a,b).** In contrast, in the epileptic group, LEV did not reduce amplitude of first fEPSPs, but did decrease amplitudes of second fEPSPs and showed a faster time constant to reduce amplitude of later fEPSPs in the train (c,d). **(B)** LEV incubation induced no significant changes in the amplitude or in the number of population spikes evoked at supra-threshold stimulation in CA1 area in either control or epileptic slices.

Levetiracetam reduces frequency of perforant path mEPSCs onto dentate granule cells in slices from both control and post-*status epilepticus* rats

We also examined the effects of LEV on miniature excitatory postsynaptic currents (mEPSCs) evoked by spontaneous release events from perforant path synapses on dentate granule neurons recorded using patch-clamp recording methods. As shown in figure 6 below, we found that LEV was able to significantly reduce spontaneous glutamate release-induced mEPSC frequency, indicative of a presynaptic action on perforant path terminals in slices from *both* non-epileptic (CONTROL) and pilocarpine-induced chronic epileptic (EPILEPTIC) rats, even though Dr. Garrido's laboratory has shown that SV2A expression is down-regulated in these epileptic rats (see Garrido progress report), and we have previously shown that pilocarpine epilepsy causes profound synaptic reorganization of excitatory terminals in the hippocampus (Upreti et al, *Brain,* **135**:869-885, 2012). These findings suggest that it is the chronic administration of LEV, rather than the chronic epileptic state *per se,* that may be responsible for the loss of efficacy of LEV that can be seen clinically. This hypothesis and regimens of chronic co-administration of multiple anticonvulsant therapies will be tested in year 03 for their ability to renormalize epileptic synaptic transmission and vesicular transmitter release, towards the goal of finding a treatment regimen that is not associated with desensitization to the anticonvulsant activity of LEV.

CONTROL **EPILEPTIC**

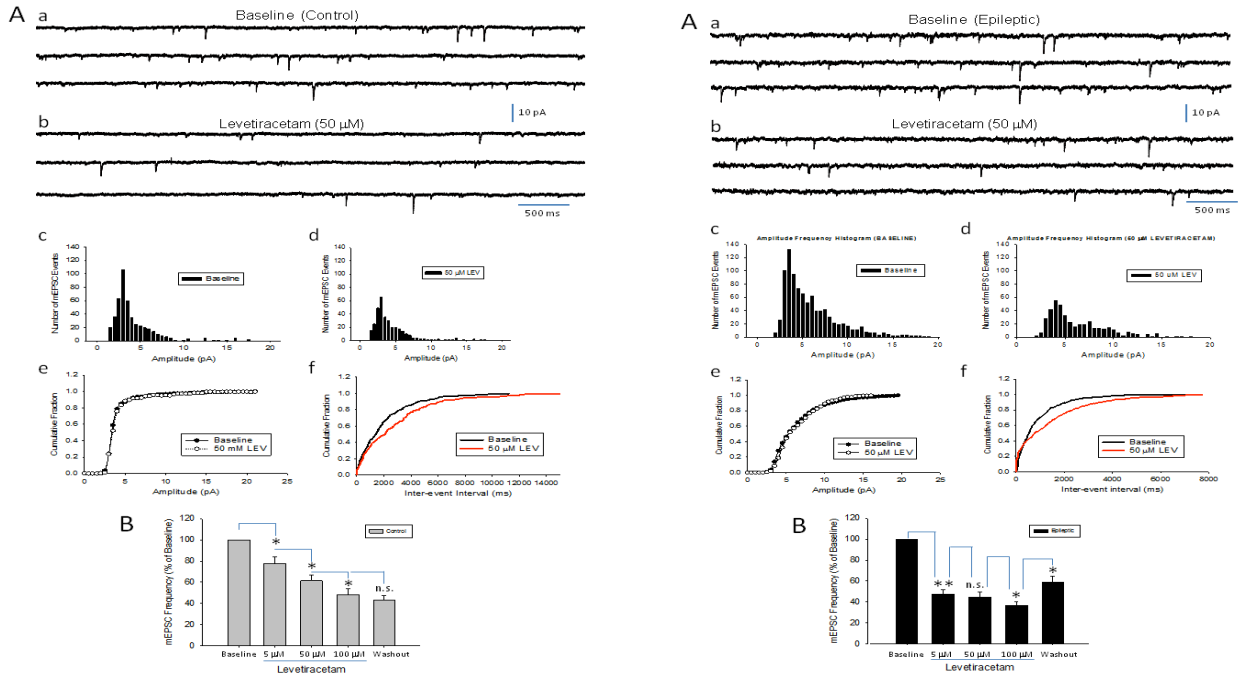

Fig. 14. LEV reduces frequency of spontaneous excitatory postsynaptic current onto dentate granule cells in slices from control (left panel) and pilocarpine-epileptic rat hippocampal slices (right panel) **(A) a.** Traces from a control (baseline) period of mEPSC recordings. **b.** traces from a period of incubation with 50mM LEV. **c,d.** Frequency histograms of mEPSC amplitude during baseline and LEV incubation respectively. **e.** Graph of cumulative fraction histograms shows no difference in cumulative fractions of amplitude in baseline compared to LEV (Kolgomorov-Smirnov test, $p>0.05$). **f.** Graph representing the analysis of cumulative histograms for inter-event of baseline period compared to LEV. Difference was significant by the Kolgomorov-Smirnov test). **(B)** Bar graph illustrating the percent changes in EPSC frequency relative to baseline period. * Statistical significance $p<0.05$, ** Statistical significance $p<0.05$, Paired student t-test compared to preceding concentration. One-way ANOVA statistical comparisons was significant, $p<0.01$ in both groups.

Specific Aim 2: *Assess whether antiepileptic drugs acting on presynaptic sites can reduce or prevent seizure-induced long-term enhancement of vesicular release from mossy fiber boutons in MTLE.*

Working hypothesis: Epileptic rats exhibit enhanced pool size and release probability from the rapidly-recycling vesicle pool, and SV2a down-regulation contributes to this enhanced release. Chronic treatment with LEV or other presynaptic antiepileptic drugs during epileptogenesis will protect presynaptic function and normal glutamate release, reducing or preventing seizures. (October 1, 2012–September 30, 2013 = 12 months).

This aim will consist of: (a) chronic treatment with antiepileptic drugs after pilocarpine injection (b) two-photon confocal imaging of FM1-43 release from readily-releasable and total vesicle pools, and (c) two-photon imaging of vesicle release, recycling, and exchange rates of vesicle pools in pilocarpine-treated epileptic mice expressing synaptopHfluorin (SpH), a genetically-encoded fusion protein of the vesicle protein Vesicular Associated Membrane Protein (VAMP2) and pH-sensitive Enhanced Green Fluorescent Protein (EGFP).

Research Goals:

The experiments in the tasks below are currently underway to assess the effects of *chronic*, as compared to acute, administration of LEV versus other anticonvulsant drugs on both excitatory synaptic transmission and presynaptic vesicular glutamate release in pilocarpine-induced epileptic rats and mice, and are expected to be completed within the next six months. Rats and SpH (Sp21 strain) expressing mice are now being chronically treated with therapeutic doses of LEV to examine release properties after 3-6 months of administration. In addition, we have now successfully established a colony of the Sp64 strain of SpH-expressing mice, which express the vesicular release indicator synaptopHluorin selectively in *GABAergic* inhibitory interneurons, which will allow us in year 03 to compare the effects of LEV on excitatatory and inhibitory presynaptic terminal release of glutamate versus GABA in control and epileptic mice.

Task 1. Assess the effect of chronic treatment with antiepileptic drugs acting on presynaptic glutamate release (LEV and other drugs characterized in Specific Aim 1) investigated by two-photon imaging of vesicular release of FM1-43 from individual mossy fiber terminals in hippocampal slices from non-epileptic and epileptic rats.

- **Subtask 1c.** Prepare hippocampal slices from control and epileptic rats chronically treated with antiepileptic drugs versus vehicle (Dr. Stanton and Dr. Zhang; months, 17-24).
- **Subtask 1d.** Image presynaptic release of FM1-43 from individual mossy fiber to test whether chronic treatment protects the kinetics of transmitter release in control versus epileptic rats (Dr. Stanton and Dr. Zhang; months 17-24).
- **Subtask 1e.** Statistical analysis of the experimental data (Dr. Stanton and Dr. Zhang, Months 17-24)

Task 2. Assess the effect of chronic treatment with different antiepileptic drugs (from Aim 1) acting on presynaptic glutamate release on presynaptic transmitter release investigated by two-photon imaging of vesicular release, recycling, and exchange rates between vesicle pools in control and pilocarpine-treated epileptic SpH mice treated with antiepileptic drugs.

- **Subtask 1b.** Systemic administration of antiepileptic drugs to different mice groups, versus vehicle controls, following pilocarpine administration. We will test chronic treatment with "non-classical" antiepileptic drugs versus LEV (Dr. Garrido and Dr. Pacheco; months 13-18).
- **Subtask 1c.** Prepare hippocampal slices from control and epileptic SpH mice chronically treated with antiepileptic drugs (Dr. Stanton and Dr. Zhang; months, 19-24).
- **Subtask 1d.** Image presynaptic release of FM1-43 from individual mossy fiber presynaptic terminals to test whether chronic treatment protects normal kinetics of transmitter release in epileptic SpH mice (Dr. Stanton and Dr. Zhang; months 19-24).
- **Subtask 1e.** Statistical analysis of the experimental data (Dr. Stanton and Dr. Zhang, Months 19-24)

Specific Aim 2: *Assess whether antiepileptic drugs acting on presynaptic sites can reduce or prevent seizure induced long-term potentiation of vesicular release from mossy fiber boutons in MTLE.* **Working hypothesis:** Epileptic rats exhibit enhanced pool size and release probability from the rapidly-recycling vesicle pool, and SV2a down-regulation contributes to this enhanced release. Chronic treatment with LEV or other presynaptic antiepileptic drugs during epileptogenesis will protect presynaptic function and normal glutamate release, reducing or preventing hyperexcitability and seizures (months 13-24).

2.3 Effect of LEV in network excitability and excitatory transmission in control and chronically epileptic rats.

We investigated whether acute or chronic treatment of slices with LEV will affect the excitability in hippocampal slices obtained from control and chronically epileptic rats. For this purpose, we performed extracellular recordings of population spikes in CA1 area of hippocampus and field excitatory postsynaptic potentials in dentate gyrus. In previous year, we demonstrated that LEV significantly reduced the frequency of excitatory postsynaptic currents onto granule cells of dentate gyrus in both mice and rats.

Brief description of methods for hippocampal slice preparation: Brains from >60 days of status epileptic or control Sprague Dawley rats were used for all experiments, and procedures were approved by The University of Texas at Brownsville Institutional Animal Care and Use Committee (Protocol 2011-001-IACU). After isoflurane anesthesia, rats were decapitated and their brains were quickly removed and submerged in 0 C artificial cerebral spinal fluid (ACSF) solution containing (in mM) 124 NaCl, 3 KCl, 2 $CaCl_2$, 1.3 $MgSO_4$, 1.25 NaH_2PO_4, 25 $NaHCO_3$ and 10 glucose. For preparation the hippocampal slices, the whole brain excluding the olfactory bulbs was rapidly removed after decapitation and immediately in cooled in oxygenated ice-cold ACSF. Horizontal hippocampal slices were cut at 350 μm using Leica Vibratome. The experiments were performed in slices from control and epileptic rats. To assess the effect of LEV in excitability and the antiepileptic action, slices were pre-incubated for 3 hours in ACSF solution containing 50μM AP5 to block NMDA receptors. A group of slices (Non-treatment) was incubated with this baseline sACSF solution while another group of slices from same animal was incubated with a treatment ACSF solution containing 300 μM LEV (Sigma Aldrich). After 3 h incubations slices were transferred to recording chamber (32^0C) and perfused at 2ml/min with oxygenated ACSF, or 300μM LEV (treatment).

2.3.1. Effects of LEV on population spikes evoked in CA1 area of hippocampal slices.

In these experiments LEV treatment resulted in a reduction of the amplitude of CA1 population spikes in both control and epileptics but this effect was not significant at least for our sample size. The effect of LEV in CA1 excitability of epileptic group was more pronounced (28.5% reduction, Fig. 17b2, Table 7.2) in contrast to effect on controls (20.7% reduction, Figure 17a2, Table 7.1). Population spikes in CA1 evoked for stimulation of the Shaffer collaterals were recoded and averaged in the Fig 17A and Fig 17B for the control and epileptic group respectively. The test stimulus intensity was adjusted to evoked 40% the maximal response of the input output (I/O). Levetiracetam did not have any significant effect on the mean population spike amplitude, slope and coastline in the control group (n=10) or in the chronic epileptic group (n=3). Synaptic responses in slices from the control and epileptic group were clearly altered after treatment with LEV (Figure 17A-a2 and 17B-b2) respectively. Although the inhibitory effect of LEV was very pronounced, analysis failed to reveal a statistical significance in neither of both groups. Paired t test analysis revealed, no significant effect were found in control group (n=10) in the amplitude (t=-09396, df=9, p= 0.37195), Coastline (t= 1.35339, df =9 p= 0.20894) and Slope (t=-100405, df=9 , p= 0.34159) before or after the application the 300μM the LEV. In addition, no significant effect in the effect of LEV treatment in slices from the epileptic group (SE-LEV) (n=3) was found in the analysis of the amplitude (t=-0.856, df=2, p=0.48868), coastline (t=0.24009, df=2, p=0.83262) or slope (t=-1.84803, df=3, p=0.20585) when compared with effect of LEV in slices of control group. These data indicate that potential antiepileptic action of LEV in chronically epileptic tissue is preserved despite seizure-mediated down-regulation of SV2A proteins as measured by immunohistochemistry, Western blotting and real-time quantitative PCR (see below). Understanding the antiepileptic effect of LEV despite down-regulation of pharmacological targets is important to design similarly effective drugs acting on presynaptic sites.

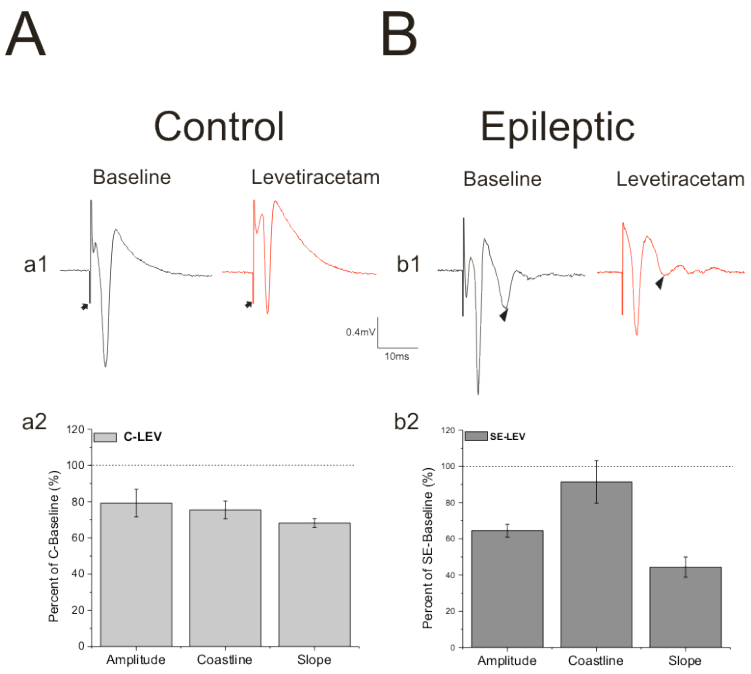

Figure 15. *LEV reduced amplitude of population spike responses evoked in the CA1 area of hippocampal slices.* (1A-1B). Representative recordings of population spikes show a reduction in amplitude after LEV treatment in control group (a1) control-baseline (black trace) compared to control-LEV (red trace) and (b1) epileptic(SE)-group where baseline (black trace) is compared to LEV treatment (SE-LEV, red trace). Graphs in a2 and b2 summarize percent changes of population spike amplitude, coastline and slope after LEV treatment in control and epileptic group respectively. Note reduction in the second population spike in chronic epileptic rat is observed (black triangle). Arrow shows stimuli artifacts.

Table 2.1 Paired samples *t*-test analysis for population spikes in CA1 area in control group

Population spikes Control (CA1)

		N	Mean	SD	SEM	t Stat	DF	Prob>|t|	% change
Amplitude	**C-Baseline**	10	-0.9877	0.48505	0.15339	-0.9396	9	0.37195	20.70%
	C-LEV	10	-0.7823	0.36989	0.11697				
	Difference		-0.2054						

		N	Mean	SD	SEM	t Stat	DF	Prob>|t|	% change
Coastline	**C-Baseline**	10	4.4394	2.17127	0.68662	1.35339	9	0.20894	24.55%
	C-LEV	10	3.3495	1.07123	0.33875				
	Difference		1.0899						

		N	Mean	SD	SEM	t Stat	DF	Prob>|t|	% change
Slope	**C-Baseline**	10	-1.4337	1.38163	0.43691	-1.00405	9	0.34159	31.17%
	C-LEV	10	-0.9779	0.33317	0.10536				
	Difference		-0.4558						

Table 2.2 Paired t-test analysis for population spikes in CA1 area in epileptic group

Population spikes Epileptic Group (CA1)

		N	Mean	SD	SEM	t Statistic	DF	Prob>|t|	% change
	SE-Baseline	3	-0.856	0.62521	0.36097	-0.84143	2	0.48868	28.5
Amplitude	**SE-LEV**	3	-0.612	0.19948	0.11517				
	Difference		-0.244						

		N	Mean	SD	SEM	t Statistic	DF	Prob>|t|	% change
	SE-Baseline	3	3.697	1.97978	1.14302	0.24009	2	0.83262	7.3
Coastline	**SE-LEV**	3	3.426	1.29803	0.74942				
	Difference		0.271						

		N	Mean	SD	SEM	t Statistic	DF	Prob>|t|	% change
	SE-Baseline	3	-1.083	0.97686	0.56399	-1.84803	2	0.20585	39.5
Slope	**SE-LEV**	3	-0.558	0.49915	0.28818				
	Difference		-0.525						

KEY RESEARCH ACCOMPLISHMENTS:

- Discovery that pilocarpine epilepsy, 3 months post-seizures, is associated with marked increases in size of hippocampal mossy fiber terminals, appearance of ectopic boutons that synapse in a layer of field CA3 where they are not normally present, marked increases in vesicular release from these terminals and the appearance of a population of very high release rate boutons in epileptic rats and SpH-expressing mice.
- Discovery that levetiracetam (LEV) elicits a potent suppression of vesicular glutamate release in chronically epileptic mice, but not in non-epileptic control mice.
- Discovery that LEV reduces the frequency of spontaneous miniature excitatory postsynaptic currents, indicative of spontaneous vesicular release events, in chronically epileptic, but not normal control, mice.
- Discovery that LEV is effective in inhibiting the excitability of neurons in field CA1 of the hippocampus, as measured by Schaffer collateral-evoked population spike amplitude in both control and epileptic rats.
- Commenced 2-photon imaging studies to evaluate effects of *chronic* repeat administration of anticonvulsant drugs on pathological up-regulation of vesicular release in pilocarpine epileptic SpH mice.

CONCLUSION

In year 02, we found that severe pilocarpine-induced seizures that result in long-term appearance of spontaneous epileptic seizures and enhanced presynaptic transmitter release upregulate the sensitivity of transmitter release to the anticonvulsant agent levetiracetam (LEV). Using two different fluorescent indicators to image, by 2-photon laser scanning microscopy, individual mossy fiber release sites in the hippocampal CA3 field, we found that vesicular glutamate release that is markedly enhanced in epileptic animals is significantly suppressed by acute administration of LEV. Studies are underway to test whether chronic administration of LEV, carbamezipine or topiramate) during the post-pilocarpine development of the epileptic brain, can retard or prevent epileptogenesis, and if LEV is anticonvulsant with prolonged administration.

Significance: While all but one antiepileptic drug acts by modifying postsynaptic neuronal excitability, our work indicates that extensive changes in presynaptic function are also associated with epilepsy. Increases in glutamate release, while certainly able to contribute to hyperexcitation in seizures, also have the potential to damage and even kill their postsynaptic target neurons. If we can find agents that can control presynaptic release, and do so even after development of epilepsy when release is enhanced, we would have a whole new class of treatments to help the 40% of epileptic patients who do not respond to any current therapeutics. Understanding the mechanisms by which seizures change presynaptic function is the essential first step towards this goal.

We obtained key data indicating that chronic slice treatment with LEV can reduce excitability and reduce excitatory synaptic transmission in hippocampal slices obtained from control and epileptic rats. These are significant findings because during the course of epilepsy LEV pharmacological target SV2A is down-regulated. Therefore, current data open two possibilities: (a) remaining SV2A receptors are still functional for LEV action and their activation is still effective in control presynaptic release of glutamate, overall excitability and ultimately seizures in epilepsy and/or (b) the action of LEV is independent of SV2A binding, but SV2A may act as a carrier/transport that mediates LEV molecules to enter the interior of the presynaptic boutons and act on secondary targets. Hence, even down-regulated, SV2A can bind and internalize enough LEV to act effectively in another intracellular targets or pathways. Although LEV has been shown to act on other targets like presynaptic Ca^{2+} channels[72,73], binding experiments only confirm SV2A as a sole molecular receptor. Additional studies are necessary to pin-point and differentiate the role of SV2A in mediating the antiepileptic effect of LEV as receptor-effector versus receptor-transporter molecular targets. Our data indicate that presynaptically acting drugs such as levetiracetam reduces hyperexcitability and inhibit presynaptic transmission in mesial temporal lobe epilepsy.

YEAR 03

HYPOTHESIS AND OBJECTIVES:

During periods of intense neuronal activity such as seizures, a larger pool of vesicles could result in more glutamate being released and long-lasting aberrant excitation. We propose to explore the effects of seizures on transmitter release and the presynaptic action of AEDs on these changes. We will use electrophysiology and multiphoton confocal microscopy. Preliminary data indicate that SE induces long-lasting potentiation of synaptic vesicle release in epileptic rats. We hypothesize that successful AED treatment might prevent or reverse these seizure-induced molecular deficiencies (reduction of N-type VGCC, mGluR II and SV2a expression), and be antiepileptogenic as well. Our **central hypothesis** is that pharmacological regulation of glutamate transmitter release at presynaptic sites will be an effective, novel therapeutic strategy to ameliorate epileptogenesis and excessive synaptic excitation in epilepsy. The **long-term objectives** of this collaborative proposal are to: (1) identify the most effective AEDs which modulate presynaptic glutamate release, and (2) determine the presynaptic mechanism of action of the new AED LEV to modulate vesicular release properties. *Our central hypothesis is that pharmacological regulation of glutamate transmitter release at presynaptic sites will be an effective, novel therapeutic strategy to treat many cases of drug-resistant epilepsy, especially epileptogenesis following traumatic brain injury.* The **long-term goals** of this collaborative project are to: (1) identify the most effective antiepileptic drugs amongst compounds that modulate presynaptic glutamate release and (2) determine the presynaptic mechanism of action of the new antiepileptic drug **levetiracetam** (LEV). ***In Year 3 of this proposal, we made meaningful progress on experiments with specific anticonvulsant drugs in the remainder of specific Aims 2 and 3 tasks that form our portion of year 03 of the collaborative project, as outlined below. We will fully complete the remaining experiments in the no-cost extension year.***

YEAR 03 Stanton Lab

Specific Aim 2: *Assess whether antiepileptic drugs acting on presynaptic sites can reduce or prevent seizure-induced long-term enhancement of vesicular release from mossy fiber boutons in MTLE.*

Working hypothesis: Epileptic rats exhibit enhanced pool size and release probability from the rapidly-recycling vesicle pool, and SV2a down-regulation contributes to this enhanced release. Chronic treatment with LEV or other presynaptic antiepileptic drugs during epileptogenesis will protect presynaptic function and normal glutamate release, reducing or preventing seizures. (October 1, 2012–September 30, 2013 = 12 months).

This aim will consist of: (a) chronic treatment with antiepileptic drugs after pilocarpine injection (b) two-photon confocal imaging of FM1-43 release from readily-releasable and total vesicle pools, and (c) two-photon imaging of vesicle release, recycling, and exchange rates of vesicle pools in pilocarpine-treated epileptic mice expressing synaptopHfluorin (SpH), a genetically-encoded fusion protein of the vesicle protein Vesicular Associated Membrane Protein (VAMP2) and pH-sensitive Enhanced Green Fluorescent Protein (EGFP).

Research Goals:

Task 1. Assess the effect of chronic treatment with antiepileptic drugs acting on presynaptic glutamate release (LEV and other drugs characterized in Specific Aims 1) investigated by two-photon imaging of vesicular release of FM1-43 from individual mossy fiber terminals in hippocampal slices from non-epileptic and epileptic rats.

- **Subtask 1c.** Prepare hippocampal slices from control and epileptic rats chronically treated with antiepileptic drugs versus vehicle (Dr. Stanton and Dr. Zhang; months, 17-24).
- **Subtask 1d.** Image presynaptic release of FM1-43 from individual mossy fiber to test whether chronic treatment protects the kinetics of transmitter release in control versus epileptic rats (Dr. Stanton and Dr. Zhang; months 17-24).
- **Subtask 1e.** Statistical analysis of the experimental data (Dr. Stanton and Dr. Zhang, Months 17-24)

Task 2. Assess the effects of chronic treatment with antiepileptic drugs (identified in Aim 1) acting on presynaptic glutamate release on presynaptic transmitter release investigated by two-photon imaging of vesicular release, recycling, and exchange rates between vesicle pools in control and epileptic SpH mice treated with antiepileptic drugs.

- **Subtask 2d.** Image presynaptic release from individual mossy fiber presynaptic terminals to test whether chronic treatment protects normal kinetics of transmitter release in epileptic SpH mice (Dr. Stanton and Dr. Zhang; months 19-24).
- **Subtask 2e.** Statistical analysis of electrophysiology data (Dr. Stanton and Dr. Zhang, months 19-24).

Aim 2, Subtasks 1.c-e. Test whether chronic treatment with antiepileptic drugs prevents presynaptic dysfunction in chronic epilepsy

In this aim we examinted the effects of acute administration of levetiracetam (LEV) on presynaptic vesicular transmitter release from excitatory Schaffer collateral terminals in hippocampal field CA1 using multiphoton laser scanning confocal imaging analysis of presynaptic release in both control and pilocarpine-induced epileptic transgenic SpH-expressing mice.

LEV reduces enhanced vesicular release from mossy fiber boutons of chronically epileptic SpH-expressing transgenic mice expressing SpH at excitatory glutamatergic terminals

Levetiracetam (Keppra®, LEV) is a new class of antiepileptic drug exhibiting selective seizure protection in chronic animal models of epilepsy. LEV binds to the synaptic vesicle protein SV2A and can modulate excitatory transmission by a mechanism depending on the inhibition of presynaptic Ca^{2+} channels. It is also known that LEV targets SV2A expression of which is reduced by epileptogenesis in animal models and epileptic patients suffering mesial temporal lobe epilepsy (MTLE). By using 2-photon laser scanning confocal microscopy, we tested whether LEV was effective in reducing enhanced vesicle release in mossy fibers from control and epileptic transgenic SpH21 mice expressing synaptopHluorin (SpH) in mossy fiber boutons. Expression changes in SV2A, SV2B and SV2C were also analyzed in the laboratory of Dr. Garrido using immunofluorescence, western blotting and real-time quantitative PCR (qPCR).

To address the hypothesis of specific aim 2, we investigated whether chronic treatment with LEV (Kepra) can reduce the abnormally enhanced presynaptic release of vesicles in the mossy fiber glutamatergic pathway . Presynaptic transmitter (vesicle) release was investigated in 4 groups of SPH transgenic mice as follows: a) control mice injected with saline vehicle for 4 weeks (control no treatment=C-NT, n=5), b) pilocarpine-treated SpH mice that developed *status epilepticus injected* with saline (*status epilepticus* no treatment=SE–NT, n=5), c) control SpH mice injected with levetiracetam (see below) (control treated=C-T, n=4), and d) pilocarpine-treated SpH mice that suffered *status epilepticus* and were treated subsequently with levetiracetam intraperitoneally (see below) (*status epilepticus* treated= SE-T, n=4). The treatment schedule for levetiracetam and saline administration consisted of repetitive injections (100 μg/kg) in alternate days during 30 days. After the end of the treatment period, animals were sacrificed for a preparation of brain slices to measure changes in presynaptic transmission and to collect mRNA samples. Similar groups of animals were sacrificed for Dr. Garrido to measure changes in expression of SV2A, SV2B, and SV2C protein. Blood samples were collected (at endpoint) to measure plasmatic levels of levetiracetam using high-pressure liquid chromatography in treated versus non-treated groups.

Results: In experiments performed in collaboration with Dr. Garrido's laboratory, four different groups of animals were analyzed to determine whether chronic treatment with levetiracetam *in vivo* may reduce presyanptic vesiclar transmitter release in the mossy fiber pathway from granule cells in hippocmapus of pilocarpine-treated epileptic SPH trasnegnic mice. Changes of SpH fluorescence were induced by a train of 600 action potentials delivered to the mossy fiber pathway using a bipolar stimulating electrode. Images of stimuli-induced SpH fluorescence changes were detected using laser scanning confocal microscopy (see above). We first compared normalized peak fluorescence changes after stimuli in control versus pilocarpine-treated (suffering status epilepticus) group of

animals that were injected with saline instead of levetiracetam for 1 month (**Figure 1A**). We detected a significant 4.4% increase in normalized peak fluorescence in status epilepticus (SE) group (F_{peak} = 119.25 ± 2.13%, n = 4, 106 boutons, 7 slices) when compared to saline-injected control group (F_{peak} = 114.18 ± 1.19 %, *n = 5, 112 boutons, 10 slices)* (**Figure A, b3**). These data is consistent with our previous findings that status epilepticus induce an abnormal increase in presynaptic vesicular release as measured by SpH fluorescence changes in transgenic mice **(Upreti et al., 2012).**

To determine if chronic treatment with levetiracetam can ameliorate or prevent such increase in presynaptic vesicular release, we treated pilocarpine-injected animals with levetirecetam (i.p, dose: 100 μg/kg) during one month immediatelly following *status epilepticus* and compared this group to control animals treated with a similar drug administration protocol. Analysis demonstrated no significant differences in of normalized peak fluorescence changes after stimulation of mossy fibers between these groups, indicating that chronic treatment with levetiracetam corrected presyanptic function abnormalities previously detected after *status epilepticus* (**Figure 1B**). (Plasma concentration of levetiracetam after treatment was assessed by high-pressure chromatography (HPLC) assays. No significant changes were detected between controls (57.1± μg/ml) versus and *status eplepticus* groups (47.9±1.5 μg/ml, Student t-test,, p>0.05)).

Conclusions: Chronic treatment with LEV after *status epilepticus* can reverse abnormally enhanced presynaptic vesicular glutamate release at mossy fibers that may be responsible for epileptogenesis and hyperexcitability in mesial temporal lobe epilepsy. Accordingly, reduction in abnormally enhanced presyanptic vesicular release is possibly the main mechanisms of action of levetiracetam. Data in experiments from Dr. Garrido's lab indicate this effect may be mediated by LEV-induced up-regulation of SV2A that protects against *status epilepticus*. Further experiments will be performed in the no-cost extension period to elucidate how LEV during status protects vesicular release, by altering release probability and/or vesicle recycling.

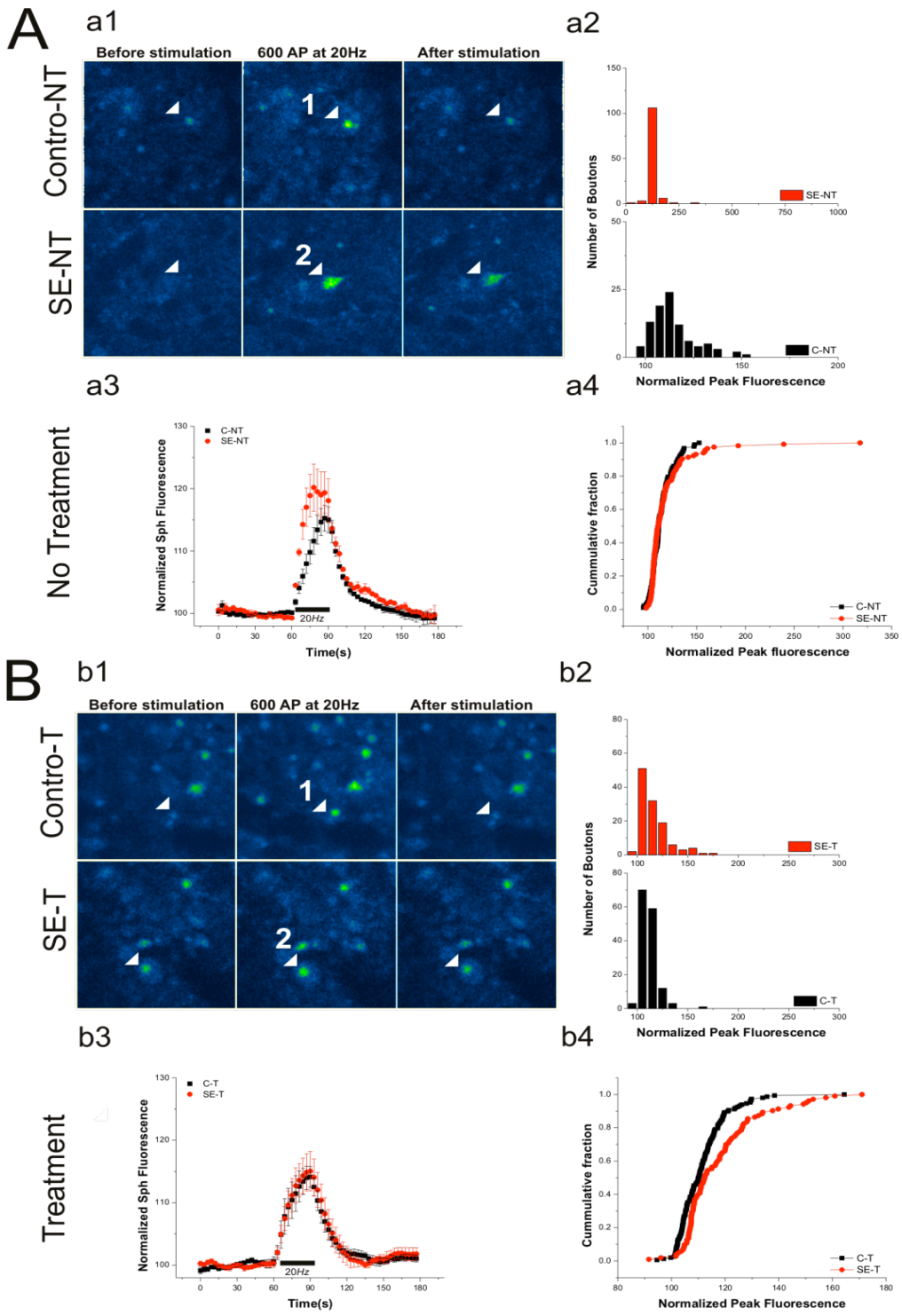

Figure 16. Effect of levetiracetam on the pilocarpine model to induced *status epilepticus* (SE) in SpH transgenic mice. A. *Stimuli-induced changes in presynaptic vesicular release at mossy fiber boutons in control and pilocarpine-treated SpH transgenic mice (no-treatment).* **a1**. Representative time-lapsed confocal images from control and post-*status epilepticus* SpH-expressing mossy fiber boutons MFBs in the proximal apical dendritic region of field CA3 in hippocampal slices of saline-treated control versus mouse one month after

suffering SE treated with saline vehicle (lower row). First column: baseline imaging, second column: imaging during 600 action potential train stimulation, last column: recover of fluorescence changes 10 sec after end of stimulation. Notice larger increase in fluorescence changes after SE (compared arrowhead 1 to 2). **a2**. Frequency distribution histogram of normalized peak SpH fluorescence for all mossy fiber boutons after stimulation in control (black) compared to *status epilepticus* (SE) group (red). Notice a change in the distribution pattern, specifically a large group of mossy fiber boutons that release more than 200% increase of baseline after *status epilepticus* while peak fluorescence changes in mossy fiber boutons from control saline-treated animals follow a normal distribution. **a3**. Normalized, evoked SpH fluorescence increases in response to a 600 pulse/20 Hz mossy fibre stimulus train, in MFBs from control (filled black circles, F_{peak} = 114.18 ± 1.19 %, *n = 5, boutons=112, 10 slices*) versus post-status epilepticus (open red circles, F_{peak} = 119.25 ± 2.13%, *n* = 4, boutons=106, 7 slices). F_{peak} was significantly increased in post-status epilepticus slices ($P < 0.05$, Student's *t*-test; all values mean ± SEM). **a4**. Cumulative histogram distribution of normalized peak fluorescence changes in control (black) versus SE group (red) showing a left shift and a significant difference towards larger fluorescence peak changes (more release) in slices from post-*status epilepticus* animals (D= 0.23, Z= 0.0305, p<0.00197, statistical comparisons using Kolmogorov-Smirnov test). **B**. *Chronic treatment with Levetiracetam (30 days period) after pilocarpine-induced status epilepticus normalized abnormally enhanced vesicular release at mossy fiber boutons*. **b1**. Time-lapsed images from representative experiments in slices from levetiracetam-treated control and epileptic SpH transgenic mice. Solid arrows indicate puncta corresponding to SpH-positive mossy fiber bouton that showed activity-dependent fluorescence changes during a 600 pulse/20 Hz stimulus train. **a2**. Frequency distribution histogram of normalized peak fluorescence for pooled mossy fiber boutons in control (black) *versus* pilocarpine-treated mice (red) chronically treated with levetiracetam after *status epilepticus*. **b3**. Representative time course of normalized, evoked SpH fluorescence increases in response to a 600 pulse/20 Hz mossy fibre stimulus train, in MFBs from control (filled black circles, F_{peak} = 115.09 ± 0.67 %, *n = 3, boutons=148, 9 slices*) versus post-*status epilepticus* (open red circles, F_{peak} = 116.25 ± 1.27%, *n* = 3, boutons=106, 6 slices). F_{peak} was not significantly changed in levetiracetam-treated post-*status epilepticus* animals ($P > 0.05$, Student's *t*-test; all values mean ± SEM). **b4**. Cumulative frequency histogram of normalized peak SpH fluorescence between the levetiracetam-treated control and SE group (red). Kolmogorov-Smirnov two-sample test indicated a significant difference between both groups (t=2.7, DF=18 p=0.014).

Task 2. Assess the effect of acute versus chronic treatment with different antiepileptic drugs (LEV versus carbamezipine) acting on presynaptic glutamate release on presynaptic transmitter release investigated by two-photon imaging of vesicular release, recycling, and exchange rates between vesicle pools in control and pilocarpine-treated epileptic SpH mice treated with antiepileptic drugs.

- **Subtask 1b.** Systemic administration of antiepileptic drugs to different mice groups, versus vehicle controls, following pilocarpine administration. We will test chronic treatment with LEV versus carbamezipine (Dr. Stanton and Dr. Zhang; months 24-36).
- **Subtask 1c.** Prepare hippocampal slices from control and epileptic SpH mice chronically treated with antiepileptic drugs (Dr. Stanton and Dr. Zhang; months, 24-36).
- **Subtask 1d.** Image presynaptic release of FM1-43 from individual mossy fiber presynaptic terminals to test whether chronic treatment protects normal kinetics of transmitter release in epileptic SpH mice (Dr. Stanton and Dr. Zhang; months 24-36).
- **Subtask 1e.** Statistical analysis of the experimental data (Dr. Stanton and Dr. Zhang, Months 30-36)

KEY RESEARCH ACCOMPLISHMENTS:

- Discovery that chronic treatment of animals with levetiracetam (LEV) is effective in inhibiting the development of abnormally enhanced presynaptic vesicular release of glutamate from mossy fiber terminals of dentate granule neurons if applied during the silent post-seizure period after pilocarpine-induced *status epilepticus.*

- This finding correlates well with the discovery by Dr. Garrido's laboratory that chronic treatment with LEV, if applied during the silent post-seizure time window, also increased protein expression of its molecular SNARE protein target SV2A in mossy fiber terminals, and reduced seizure-induced increases in SV2C (gene expression of sv2c by qrtPCR) in hippocampus after pilocarpine-induced *status epilepticus*.
- The combined data from the Garrido and Stanton laboratories indicate that LEV can be effective in counteracting pro-epileptogenic changes in transmitter release and presynaptic molecules if administered shortly after a seizure insult (status epilepticus) that would otherwise lead to chronic epilepsy.
- Commenced studies using 2-photon laser scanning microscopy will evaluate the effects of acute versus chronic repeated administration of LEV and carbamezipine on vesicle release probability compared to rates of vesicular recycling in the readily-releasable vesicle pool.

REPORTABLE OUTCOMES:

National Meetings
Data from electrophysiological and pharmacological experiments were presented in 1 scientific meeting in 2013 (1-2) and new data has been submitted for presentation at another two meetings in 2014 (3-4).

1) Inhibitory action of levetiracetam on CA1 population spikes and dentate gyrus excitatory transmission in pilocarpine-treated chronic epileptic rats. **E. G. Sanabria**, L. Pacheco, J. Zavaleta, F. Shriver, L. M. Rambo, C. Upreti, **P. K. Stanton**. Society for Neuroscience Meeting in San Diego, CA, Nov 9-13, 2013

2) Synaptic Vesicle Protein Expression in Sprague-Dawley Rats Treated with the Pilocarpine Model for Mesial Temporal Lobe Epilepsy. Mayra Velazquez, L.F. Pacheco, **E. R. Garrido-Sanabria**. 25th Anniversary Conference, HENAAC Conference, October 3 - 5, 2013, New Orleans.

3) Chronic treatment with levetiracetam upregulate SV2A and reduce abnormally augmented presynaptic vesicular release after pilocarpine-induced status epilepticus**.** Luis F. Pacheco, Vinicius Funck, Nuri Ruvalcaba, Jose M. Rodriguez, Daniela Taylor, Rubi Garcia, Jason Zavaleta, Chirag Upreti, **Patric K. Stanton**, **Emilio R. Garrido-Sanabria,** the Military Health System Research Symposium, to be held on August 18-21, 2014.

4) Treatment with levetiracetam ameliorates abnormal presynaptic vesicular release and altered presynaptic protein expression in a glutamatergic pathway after pilocarpine-induced status epilepticus**. Emilio R. Garrido-Sanabria,** Luis F. Pacheco, Vinicius Funck, Nuri Ruvalcaba, Jose M. Rodriguez, Daniela Taylor, Rubi Garcia, Jason Zavaleta, Chirag Upreti, **Patric K. Stanton**. This abstract will be submitted to the 68th Annual Meeting of the American Epilepsy Society, Dec 5-9, 2014, Seattle, Washington.

CONCLUSIONS

In year 03 and the no-cost extension year, we completed all proposed studies from the Stanton laboratory. We found that severe pilocarpine-induced seizures that result in long-term appearance of spontaneous epileptic seizures and enhanced presynaptic transmitter release upregulate the sensitivity of transmitter release to the anticonvulsant agent levetiracetam (LEV). Using two different fluorescent indicators to image, by 2-photon laser scanning microscopy, individual mossy fiber release sites in the hippocampal CA3 field, we found that vesicular glutamate release that is markedly enhanced in epileptic animals is significantly supressed by acute administration of LEV. In Aim 2, we showed that chronic administration of LEV during the silent post-seizure period when epileptogenesis occurs can prevent alterations in transmitter release.

Significance: While all but one antiepileptic drug acts by modifying postsynaptic neuronal excitability, our work indicates that extensive changes in presynaptic function are also associated with epilepsy. Increases in glutamate release, while certainly able to contribute to hyperexcitation in seizures, also have the potential to damage and even kill their postsynaptic target neurons. If we can find agents that can control presynaptic release, and do so even after development of epilepsy when release is enhanced, we would have a whole new class of treatments to help the 40% of epileptic patients who do not respond to any current therapeutics. Understanding the mechanisms by which seizures change presynaptic function is the essential first step towards this goal.

KEY RESEARCH ACCOMPLISHMENTS (from Stanton and Garrido laboratories):

Our results indicate that chronic treatment with the antiepileptic drug levetiracetam after *status epilepticus* can reduce abnormally enhanced presynaptic vesicle release of glutamatergic mossy fiber boutons in pilocarpine-treated SpH transgenic mice. In a previous study we reported a long-lasting abnormality of presynaptic structure and function in experimental epilepsy[7]. Specifically, multiphoton microscopy was used to directly measure prospective changes in vesicular recycling properties from hippocampal mossy fiber presynaptic boutons in control versus pilocarpine-treated chronic epileptic SpH21 transgenic mice expressing SpH preferentially at glutamatergic synapses. We detected significant increases in action potential-driven vesicular release at 1-2 months after pilocarpine-induced *status epilepticus*. Results from Year 3 of this proposal also indicate that levetiracetam may decrease exaggerated presynaptic vesicular release by affecting the presynaptic release machinery at excitatory pathways. Specifically, chronic treatment with levetiracetam increased deficient expression of SV2A in hippocampus (SV2A is a molecular target for levetirecetam) and reduced the abnormally increased levels of SV2C in similar pathway. Additional experiments are in progress to detect changes in another presynaptic protein mGluR2. Deciphering the mechanisms of levetiracetam-induced changes in presynaptic proteins may lead to a novel antiepileptic mechanism for this antiepileptic drug. In addition, additional studies are necessary to develop and assess the role of new antiepileptic drugs that target newly reported changes in presynaptic proteins, specifically SV2C.

These data indicate that presynaptically acting drugs such as levetiracetam reduces hyperexcitability and inhibit presynaptic transmission in mesial temporal lobe epilepsy. Preventive treatment with antiepileptic drug is a feasible strategy to reduce the development of epilepsy (specifically post-traumatic epilepsy). In our study, we investigate whether treatment with the drug levetiracetam immediately after pilocarpine-induced status epilepticus (epileptogenic insult) significantly reduced abnormally enhanced presynaptic vesicle release and reduce molecular abnormalities in presynaptic molecules (i.e. SV2A, SV2B, SV2C) in treated epileptic mice. Interestingly, we also detected that *status epilepticus* induced up-regulation of SV2C while producing down-regulation of SV2A in the mossy fiber pathways. In vivo treatment with levetiracetam partially corrected both protein and mRNA gene expression changes in SV2C while only partially restored deficient SV2A protein levels after *status epilepticus* indicating that SV2C may also play a role in the epileptogenic process. LEV is a novel antiepileptic drug that binds to presynaptic targets SV2A. Although SV2A has been identified as the main molecular target for levetiracetam[81,86,87], our data indicate that “pro-epileptic” changes in SV2C may become a novel antiepileptic therapeutic target for new pharmacological drugs in order to modify presynaptic transmitter release and reduce hyperexcitability in epilepsy.

SV2 proteins are abundant synaptic vesicle integral membrane proteins expressed in two major (*SV2A* and SV2B) and one minor isoform (SV2C) whose membrane topology resembles that of transporter proteins [88,89]. Although SV2A is the major target of the antiepileptic drug levetiracetam, its function and partner molecules are

still unknown [80,81,90,91]. Our study indicates that SV2C may play a role in the pathogenesis of epilepsy. We found that levels of SV2C transcripts increased after pilocarpine-induced *status epilepticus* consistent with previous studies in human epilepsy [77]. These authors reported that SV2C, which is weakly expressed or absent in the hippocampus of control cases, was overexpressed in 10/11 cases with classical MTS1A and mossy fibre sprouting but not in cases with other types of MTS. In our study, we demonstrated that changes in SV2C expression may start as early as 4 weeks after *status epilepticus*. Additional studies are necessary to determine the earlier time point fat which status epilepticus will induce an upregulation of SV2C. Interestingly, we also found that treatment with levetirecetam during 4 weeks after *status epilepticus* reduced the expression of SV2C significantly but still levels remained above controls. These findings indicate that SV2C expression is also dysregulated during epileptogenesis but levels can be partially restored with pharmacological treatment with antiepileptic drugs. The significance of these findings for the pathogenesis of epilepsy remains to be elucidated considering that despite a high degree of homology between SV2 isoforms SV2A is the known molecular target of levetirecetam[69,80,81,87,91]. It is known that levetiracetam failed to control convulsions/seizures in acute models of epilepsy while exerting a very potent antiepileptic effect in chronic models of epilepsy [79-81]. It is currently unknown whether seizures can induce levetirecetam-binding splice variants of SV2C. This will be a therapeutically relevant finding since upregulation of SV2C in epilepsy will allow for increased pharmacological targets for levetirecetam and consequentially improve the pharmacological action of this antiepileptic drug when compared to SV2A expression which has been found to be reduced in previous studies using animal models of epilepsy and tissue from epileptic patients [77,78]. Interestingly, in our study, we failed to demonstrate a significant down-regulation of SV2A after *status epilepticus*, neither a significant effect of levetiractam on SV2A transcript levels in animals that suffered *status epilepticus*. The role of SV2A on epilepsy has been established by 3 facts: (1) SV2A is the sole molecular target for the antiepileptic drug levetiracetam (LEV)[64,92,93], (2) SV2A knockout mice exhibit severe seizures[65,66,94], and (3) down-regulation of SV2A has been reported in epilepsy [77,78]. SV2A is consistently reduced in mossy fibers in experimental MTLE and epileptic patients. Despite these compelling findings, the exact function of SV2A remains unknown. Hence, the molecular cascades and pathways mediating the action of loevetiracetam deserve further investigation. A major problem is the lack of functional assays to probe how levetiracetam interacts with and modifies SV2A function. Moreover, the exact binding site of levetiracetam on the structure of SV2A has not been discovered yet.

4. Impact

It is important to highlight that LEV is a drug with a unique antiepileptic profile. LEV failed to block seizures in acute models of epilepsy while exhibited a potent antiepileptic effect in chronic experimental models of epilepsy as the kainate, kindling and pilocarpine models. This antiepileptic profile may be related to molecular changes that are specific for tissue undergoing epileptogenesis (i.*e.* abnormal binding sites for LEV, in addition to the already reported SV2A). This project will elucidate the presynaptic mechanisms of action of LEV and other antiepileptic drugs as a strategy to accelerate the development of novel antiepileptic drugs acting in presynapses. Understanding abnormalities of presynaptic terminals during epileptogenesis is critical to elucidate the pathogenesis of pharmacoresistant epilepsy.

LEV is a novel antiepileptic drug that binds to presynaptic targets. However, the presynaptic mechanisms are still unclear and innovative research paradigms need to be deployed to understand how this drug work in order to design similarly effective or better versions for the treatment of pharmaco-resistance epilepsy. We found that expression of LEV targts are down-regulated in epilepsy but expression of homologous protein SV2C is upregulated 10 days after status epilepticus and transcripts are upregulated during the chronic phase of the model. Sv2C my represent novel targets for LEV and similar drugs acting on presynaptic terminals to control release of glutamate. In this project will elucidate the presynaptic mechanisms of action of LEV and other antiepileptic drugs as a strategy to accelerate the development of novel antiepileptic drugs acting in presynapses. In Year 3, we assessed if treatment with LEV can restore molecular deficiencies caused by epilepsy in this animal model of mesial temporal lobe epilepsy (including down-regulation of SV2A and mGluR2. Understanding abnormalities of presynaptic terminals during epileptogenesis is critical to elucidate the pathogenesis of pharmacoresistant epilepsy.

The expression of S2V isoforms in neurochemically-distinct neuronal subtypes is also different in hippocampus. Although both SV2A and SV2C are expressed in mossy fibers, the expression of SV2A is also found in

GABAergic terminals while SV2C is predominantly expressed in glutamatergic terminals [69,88]. It is possible that levetirecetam can binds to both SV2A and spliced or upregulated SV2C. Regardless, increases in SV2C expression after status epilepticus may play a role in the pathogenesis of epilepsy as a contributing or a compensatory molecular event that needs to be elucidated.

Data in this project indicate that, in addition to the known target of levetirecetam SV2A, SV2C may play an important role in the pathogenesis of epilepsy. SV2C offers a novel target for development of new and more efficient antiepileptic drugs considering that there will be a higher density of targets (SV2C) available during the disease process while SV2A is actually down-regulated.

5. Changes/Problems

6. Products

REPORTABLE OUTCOMES:

Manuscripts

1) Manuscript published in *Brain* (2012; see Appendix), Journal Impact Factor 10.143

Upreti C, Otero R, Partida C, Skinner F, Thakker R, Pacheco LF, Zhou ZY, Maglakelidze G, Velíšková J, Velíšek L, Romanovicz D, Jones T, **Stanton PK,** Garrido-Sanabria ER (2012) Altered neurotransmitter release, vesicle recycling and presynaptic structure in the pilocarpine model of temporal lobe epilepsy. *Brain* 135 (Pt 3): 869-885.

2) A manuscript entitled will be submitted to Neuroreport in 2015. “Abnormal expression of synaptic vesicle protein 2 (SV) isoforms after pilocarpine-induced status epilepticus”. Luis F. Pacheco Otalora[1], Nuri Ruvalcaba, Jose Mario Rodriguez, Samantha Gomez, Aliya Sharif, Chirag Upreti, Patric Stanton, Emilio R. Garrido-Sanabria

NATIONAL MEETINGS (APPENDIX 2)

Abstracts

Year 1

Abnormal function and reorganization of presynaptic nanocomponents in experimental epilepsy: A multiphoton laser scanning confocal imaging and transmission electron microscopy study. Upreti C, Skinner F, Otero R, Thakker R, Rosas G, Partida C, Pacheco LF, Jones TA, Romanovicz D, Stanton PK and **Garrido-Sanabria** ER. *3rd Meeting of the American Society for Nanomedicine,* Rockville, MD, Nov 9-11, 2011.

Abnormalities in presynaptic vesicle pools of mossy fiber boutons in the pilocarpine model of mesial temporal lobe epilepsy. Upreti PK, Stanton E, **Garrido-Sanabria ER**. Poster. 779.10/Z13 *Society for Neuroscience Meeting*, Washington, Nov 16, 2011.

Abnormal functional and ultrastructural changes of synaptic vesicle pools at active zones in mossy fiber boutons in mesial temporal lobe epilepsy, (ID: 1149994), Upreti C, **Garrido-Sanabria ER**, Stanton PK, presented at the *65th America Epilepsy Society Annual Meeting*, Baltimore, December 2-6, 2011.

Abnormal Ultrastructure of Large Mossy Fiber Boutons-CA3 pyramidal Cell Synapses in Mesial Temporal Lobe Epilepsy. (ID: 1150094). **Garrido-Sanabria ER**, Otero R, Thakker R, Partida C, Skinner F, Jones T, Romanovicz D, Upreti C, Stanton PK., presented at the *65th America Epilepsy Society Annual Meeting*, Baltimore, December, 2011.

Year 2

Levetiracetam inhibits excitatory drive onto dentate gyrus granule cells: Effects of SV2A gene dosage and pilocarpine-induced epilepsy. **E. G. Sanabria,** L. F. Pacheco, L. M. Rambo, J. M. Rodriguez, C. Upreti, **P. K. Stanton**. Society for Neuroscience Meeting, New Orleans, LA, October 13 - 17, 2012 (Abstract in Appendix 1).

Inhibitory action of levetiracetam on CA1 population spikes and dentate gyrus excitatory transmission in pilocarpine-treated chronic epileptic rats. **E. G. Sanabria**, L. Pacheco, J. Zavaleta, F. Shriver, L. M. Rambo, C. Upreti, **P. K. Stanton**. Society for Neuroscience Meeting, San Diego, CA, Nov 9-13, 2013(Abstract in Appendix 2)

Year 3 and non-cost extension period

Synaptic Vesicle Protein Expression in Sprague-Dawley Rats Treated with the Pilocarpine Model for Mesial Temporal Lobe Epilepsy. Mayra Velazquez, L.F. Pacheco, **E. R. Garrido-Sanabria**. 25th Anniversary Conference, HENAAC Conference, October 3 - 5, 2013, New Orleans.

Chronic treatment with levetiracetam upregulate SV2A and reduce abnormally augmented presynaptic vesicular release after pilocarpine-induced status epilepticus**.** Luis F. Pacheco, Vinicius Funck, Nuri Ruvalcaba, Jose M. Rodriguez, Daniela Taylor, Rubi Garcia, Jason Zavaleta, Chirag Upreti, **Patric K. Stanton**, **Emilio R. Garrido-Sanabria,** the Military Health System Research Symposium, to be held on August 18-21, 2014.

Treatment with levetiracetam ameliorates abnormal presynaptic vesicular release and altered presynaptic protein expression in a glutamatergic pathway after pilocarpine-induced status epilepticus**. Emilio R. Garrido-Sanabria,** Luis F. Pacheco, Vinicius Funck, Nuri Ruvalcaba, Jose M. Rodriguez, Daniela Taylor, Rubi Garcia, Jason Zavaleta, Chirag Upreti, **Patric K. Stanton**. This abstract will be submitted to the 68th Annual Meeting of the American Epilepsy Society, Dec 5-9, 2014, Seattle, Washington.

Abnormal upregulation of SV2C after pilocarpine-induced seizures is restored after treatment with antiepileptic drug levetirecetam. Luis F. Pacheco, Vinicius Funck, Nuri Ruvalcaba, Samantha Gomez, Aliya Sharif, Jose M. Rodriguez, Daniela Taylor, Rubi Garcia, Chirag U preti, Patric K. Stanton, **Emilio R. Garrido-Sanabria,** the Military Health System Research Symposium, August, 2015.

7. Participants & Other Collaborating Organizations

Name:	*Patric K. Stanton, Ph.D.*
Project Role:	*Principal Investigator*
Researcher Identifier (e.g. ORCID ID):	*UTBID: Eg0213903*
Nearest person month worked:	*12*
Contribution to Project:	*Dr. Stanton performed work in the area of brain slice electrophysiology, two-photon laser scanning microscopic imaging, data analysis*
Funding Support:	

Name:	*Xiao-lei Zhang, M.D., Ph.D.*
Project Role:	*Research Associate*
Researcher Identifier (e.g. ORCID ID):	*UTBID LP0234778*
Nearest person month worked:	*12*
Contribution to Project:	*Dr. Zhang performed work in the area of brain slice electrophysiology, two-photon laser scanner microscopic imaging and data analysis. Development of pilocarpine model of mesial temporal lobe epilepsy.*
Funding Support:	

8. Special Reporting Requirements

Nothing to report

References

[1] Schauwecker PE. Strain differences in seizure-induced cell death following pilocarpine-induced status epilepticus. *Neurobiol Dis* 2012; **45**: 297-304.

[2] Turski WA, Cavalheiro EA, Bortolotto ZA, Mello LM, Schwarz M, Turski L. Seizures produced by pilocarpine in mice: a behavioral, electroencephalographic and morphological analysis. *Brain Res* 1984; **321**: 237-253.

[3] Muller CJ, Bankstahl M, Groticke I, Loscher W. Pilocarpine vs. lithium-pilocarpine for induction of status epilepticus in mice: development of spontaneous seizures, behavioral alterations and neuronal damage. *Eur J Pharmacol* 2009; **619**: 15-24.

[4] Burrone J, Li Z, Murthy VN. Studying vesicle cycling in presynaptic terminals using the genetically encoded probe synaptopHluorin. *Nat Protoc* 2006; **1**: 2970-2978.

[5] Li Z, Burrone J, Tyler WJ, Hartman KN, Albeanu DF, Murthy VN. Synaptic vesicle recycling studied in transgenic mice expressing synaptopHluorin. *Proc Natl Acad Sci U S A* 2005; **102**: 6131-6136.

[6] Mello LE, Cavalheiro EA, Tan AM, Kupfer WR, Pretorius JK, Babb TL *et al.* Circuit mechanisms of seizures in the pilocarpine model of chronic epilepsy: cell loss and mossy fiber sprouting. *Epilepsia* 1993; **34**: 985-995.

[7] Upreti C, Otero R, Partida C, Skinner F, Thakker R, Pacheco LF *et al.* Altered neurotransmitter release, vesicle recycling and presynaptic structure in the pilocarpine model of temporal lobe epilepsy. *Brain* 2012; **135**: 869-885.

[8] Boulland JL, Ferhat L, Tallak Solbu T, Ferrand N, Chaudhry FA, Storm-Mathisen J *et al.* Changes in vesicular transporters for gamma-aminobutyric acid and glutamate reveal vulnerability and reorganization of hippocampal neurons following pilocarpine-induced seizures. *J Comp Neurol* 2007; **503**: 466-485.

[9] Epsztein J, Represa A, Jorquera I, Ben-Ari Y, Crepel V. Recurrent mossy fibers establish aberrant kainate receptor-operated synapses on granule cells from epileptic rats. *J Neurosci* 2005; **25**: 8229-8239.

[10] Esclapez M, Hirsch JC, Ben-Ari Y, Bernard C. Newly formed excitatory pathways provide a substrate for hyperexcitability in experimental temporal lobe epilepsy. *J Comp Neurol* 1999; **408**: 449-460.

[11] Pacheco Otalora LF, Couoh J, Shigamoto R, Zarei MM, Garrido Sanabria ER. Abnormal mGluR2/3 expression in the perforant path termination zones and mossy fibers of chronically epileptic rats. *Brain Res* 2006; **1098**: 170-185.

[12] Ermolinsky B, Pacheco Otalora LF, Arshadmansab MF, Zarei MM, Garrido-Sanabria ER. Differential changes in mGlu2 and mGlu3 gene expression following pilocarpine-induced status epilepticus: a comparative real-time PCR analysis. *Brain Res* 2008; **1226**: 173-180.
[13] Garrido-Sanabria ER, Otalora LF, Arshadmansab MF, Herrera B, Francisco S, Ermolinsky BS. Impaired expression and function of group II metabotropic glutamate receptors in pilocarpine-treated chronically epileptic rats. *Brain Res* 2008; **1240**: 165-176.
[14] Winden KD, Karsten SL, Bragin A, Kudo LC, Gehman L, Ruidera J *et al.* A systems level, functional genomics analysis of chronic epilepsy. *PLoS One* 2011; **6**: e20763.
[15] Sills GJ. SV2A in epilepsy: the plot thickens. *Epilepsy Curr* 2010; **10**: 47-49.
[16] de Groot M, Toering ST, Boer K, Spliet WG, Heimans JJ, Aronica E *et al.* Expression of synaptic vesicle protein 2A in epilepsy-associated brain tumors and in the peritumoral cortex. *Neuro Oncol* 2010; **12**: 265-273.
[17] Feng G, Xiao F, Lu Y, Huang Z, Yuan J, Xiao Z *et al.* Down-regulation synaptic vesicle protein 2A in the anterior temporal neocortex of patients with intractable epilepsy. *Journal of molecular neuroscience : MN* 2009; **39**: 354-359.
[18] Kaminski RM, Gillard M, Leclercq K, Hanon E, Lorent G, Dassesse D *et al.* Proepileptic phenotype of SV2A-deficient mice is associated with reduced anticonvulsant efficacy of levetiracetam. *Epilepsia* 2009; **50**: 1729-1740.
[19] Pacheco Otalora LF, Hernandez EF, Arshadmansab MF, Francisco S, Willis M, Ermolinsky B *et al.* Down-regulation of BK channel expression in the pilocarpine model of temporal lobe epilepsy. *Brain Res* 2008; **1200**: 116-131.
[20] Carter DS, Harrison AJ, Falenski KW, Blair RE, DeLorenzo RJ. Long-term decrease in calbindin-D28K expression in the hippocampus of epileptic rats following pilocarpine-induced status epilepticus. *Epilepsy Res* 2008; **79**: 213-223.
[21] Hallermann S, Pawlu C, Jonas P, Heckmann M. A large pool of releasable vesicles in a cortical glutamatergic synapse. *Proc Natl Acad Sci U S A* 2003; **100**: 8975-8980.
[22] Blackstad TW, Brink K, Hem J, Jeune B. Distribution of hippocampal mossy fibers in the rat. An experimental study with silver impregnation methods. *J Comp Neurol* 1970; **138**: 433-449.
[23] Claiborne BJ, Amaral DG, Cowan WM. A light and electron microscopic analysis of the mossy fibers of the rat dentate gyrus. *J Comp Neurol* 1986; **246**: 435-458.
[24] Miesenbock G, De Angelis DA, Rothman JE. Visualizing secretion and synaptic transmission with pH-sensitive green fluorescent proteins. *Nature* 1998; **394**: 192-195.
[25] Bayazitov IT, Richardson RJ, Fricke RG, Zakharenko SS. Slow presynaptic and fast postsynaptic components of compound long-term potentiation. *J Neurosci* 2007; **27**: 11510-11521.
[26] Dobrunz LE, Stevens CF. Heterogeneity of release probability, facilitation, and depletion at central synapses. *Neuron* 1997; **18**: 995-1008.
[27] Murthy VN, Sejnowski TJ, Stevens CF. Heterogeneous release properties of visualized individual hippocampal synapses. *Neuron* 1997; **18**: 599-612.
[28] Matz J, Gilyan A, Kolar A, McCarvill T, Krueger SR. Rapid structural alterations of the active zone lead to sustained changes in neurotransmitter release. *Proc Natl Acad Sci U S A* 2010; **107**: 8836-8841.
[29] Schikorski T, Stevens CF. Quantitative ultrastructural analysis of hippocampal excitatory synapses. *J Neurosci* 1997; **17**: 5858-5867.
[30] Amaral DG, Dent JA. Development of the mossy fibers of the dentate gyrus: I. A light and electron microscopic study of the mossy fibers and their expansions. *J Comp Neurol* 1981; **195**: 51-86.
[31] Chicurel ME, Harris KM. Three-dimensional analysis of the structure and composition of CA3 branched dendritic spines and their synaptic relationships with mossy fiber boutons in the rat hippocampus. *J Comp Neurol* 1992; **325**: 169-182.
[32] Rollenhagen A, Satzler K, Rodriguez EP, Jonas P, Frotscher M, Lubke JH. Structural determinants of transmission at large hippocampal mossy fiber synapses. *J Neurosci* 2007; **27**: 10434-10444.
[33] Suyama S, Hikima T, Sakagami H, Ishizuka T, Yawo H. Synaptic vesicle dynamics in the mossy fiber-CA3 presynaptic terminals of mouse hippocampus. *Neurosci Res* 2007; **59**: 481-490.
[34] Patrylo PR, Dudek FE. Physiological unmasking of new glutamatergic pathways in the dentate gyrus of hippocampal slices from kainate-induced epileptic rats. *J Neurophysiol* 1998; **79**: 418-429.

[35] Dudek FE, Sutula TP. Epileptogenesis in the dentate gyrus: a critical perspective. *Prog Brain Res* 2007; **163**: 755-773.
[36] Sutula TP, Dudek FE. Unmasking recurrent excitation generated by mossy fiber sprouting in the epileptic dentate gyrus: an emergent property of a complex system. *Prog Brain Res* 2007; **163**: 541-563.
[37] Buckmaster PS, Zhang GF, Yamawaki R. Axon sprouting in a model of temporal lobe epilepsy creates a predominantly excitatory feedback circuit. *J Neurosci* 2002; **22**: 6650-6658.
[38] Pacheco Otalora LF, Skinner F, Oliveira MS, Farrell B, Arshadmansab MF, Pandari T *et al.* Chronic deficit in the expression of voltage-gated potassium channel Kv3.4 subunit in the hippocampus of pilocarpine-treated epileptic rats. *Brain research* 2011; **1368**: 308-316.
[39] Ermolinsky BS, Skinner F, Garcia I, Arshadmansab MF, Otalora LF, Zarei MM *et al.* Upregulation of STREX splice variant of the large conductance Ca2+-activated potassium (BK) channel in a rat model of mesial temporal lobe epilepsy. *Neurosci Res* 2011; **69**: 73-80.
[40] Oliveira MS, Skinner F, Arshadmansab MF, Garcia I, Mello CF, Knaus HG *et al.* Altered expression and function of small-conductance (SK) Ca(2+)-activated K+ channels in pilocarpine-treated epileptic rats. *Brain research* 2010; **1348**: 187-199.
[41] Ermolinsky B, Arshadmansab MF, Pacheco Otalora LF, Zarei MM, Garrido-Sanabria ER. Deficit of Kcnma1 mRNA expression in the dentate gyrus of epileptic rats. *Neuroreport* 2008; **19**: 1291-1294.
[42] Vogl C, Mochida S, Wolff C, Whalley BJ, Stephens GJ. The SV2A Ligand Levetiracetam Inhibits Presynaptic Ca2+ Channels Via an Intracellular Pathway. *Mol Pharmacol* 2012.
[43] Lee CY, Chen CC, Liou HH. Levetiracetam inhibits glutamate transmission through presynaptic P/Q-type calcium channels on the granule cells of the dentate gyrus. *Br J Pharmacol* 2009; **158**: 1753-1762.
[44] Fukuyama K, Tanahashi S, Nakagawa M, Yamamura S, Motomura E, Shiroyama T *et al.* Levetiracetam inhibits neurotransmitter release associated with CICR. *Neurosci Lett* 2012.
[45] Faught E. Efficacy of topiramate as adjunctive therapy in refractory partial seizures: United States trial experience. *Epilepsia* 1997; **38 Suppl 1**: S24-27.
[46] Faught E, Wilder BJ, Ramsay RE, Reife RA, Kramer LD, Pledger GW *et al.* Topiramate placebo-controlled dose-ranging trial in refractory partial epilepsy using 200-, 400-, and 600-mg daily dosages. Topiramate YD Study Group. *Neurology* 1996; **46**: 1684-1690.
[47] Gibbs JW, 3rd, Sombati S, DeLorenzo RJ, Coulter DA. Cellular actions of topiramate: blockade of kainate-evoked inward currents in cultured hippocampal neurons. *Epilepsia* 2000; **41 Suppl 1**: S10-16.
[48] Kaminski RM, Banerjee M, Rogawski MA. Topiramate selectively protects against seizures induced by ATPA, a GluR5 kainate receptor agonist. *Neuropharmacology* 2004; **46**: 1097-1104.
[49] Gryder DS, Rogawski MA. Selective antagonism of GluR5 kainate-receptor-mediated synaptic currents by topiramate in rat basolateral amygdala neurons. *J Neurosci* 2003; **23**: 7069-7074.
[50] Coulter DA, Sombati S, Delorenzo RJ. Selective effects of topiramate on sustained repetitive firing and spontaneous bursting in cultured hippocampal neurons. . *Epilepsia* 1993; **34**: S123.
[51] Rogawski MA, Porter RJ. Antiepileptic drugs: pharmacological mechanisms and clinical efficacy with consideration of promising developmental stage compounds. . *Pharmacol Rev* 1990; **42**: 223-286.
[52] Zona C, Ciotti MT, Avoli M. Topiramate attenuates voltage-gated sodium currents in rat cerebellar granule cells. *Neurosci Lett* 1997; **231**: 123-126.
[53] Wu SP, Tsai JJ, Gean PW. Frequency-dependent inhibition of neuronal activity by topiramate in rat hippocampal slices. *Br J Pharmacol* 1998; **125**: 826-832.
[54] McLean MJ, Bukhari AA, Wamil AW. Effects of topiramate on sodium-dependent action-potential firing by mouse spinal cord neurons in cell culture. *Epilepsia* 2000; **41 Suppl 1**: S21-24.
[55] Sitges M, Guarneros A, Nekrassov V. Effects of carbamazepine, phenytoin, valproic acid, oxcarbazepine, lamotrigine, topiramate and vinpocetine on the presynaptic Ca2+ channel-mediated release of [3H]glutamate: comparison with the Na+ channel-mediated release. *Neuropharmacology* 2007; **53**: 854-862.
[56] Dudek FE, Bramley JR. GluR5 Kainate Receptors and Topiramate: A New Site of Action for Antiepileptic Drugs? *Epilepsy Curr* 2004; **4**: 17.
[57] Macdonald RL, Kelly KM. Antiepileptic drug mechanisms of action. *Epilepsia* 1995; **36 Suppl 2**: S2-12.
[58] Macdonald RL, Kelly KM. Antiepileptic drug mechanisms of action. *Epilepsia* 1993; **34 Suppl 5**: S1-8.

[59] McLean MJ, Macdonald RL. Carbamazepine and 10,11-epoxycarbamazepine produce use- and voltage-dependent limitation of rapidly firing action potentials of mouse central neurons in cell culture. *J Pharmacol Exp Ther* 1986; **238**: 727-738.
[60] Meehan AL, Yang X, Yuan LL, Rothman SM. Levetiracetam has an activity-dependent effect on inhibitory transmission. *Epilepsia* 2012; **53**: 469-476.
[61] Muller CJ, Groticke I, Hoffmann K, Schughart K, Loscher W. Differences in sensitivity to the convulsant pilocarpine in substrains and sublines of C57BL/6 mice. *Genes Brain Behav* 2009; **8**: 481-492.
[62] Rush AM, Kilbride J, Rowan MJ, Anwyl R. Presynaptic group III mGluR modulation of short-term plasticity in the lateral perforant path of the dentate gyrus in vitro. *Brain Res* 2002; **952**: 38-43.
[63] Kilbride J, Rush AM, Rowan MJ, Anwyl R. Presynaptic group II mGluR inhibition of short-term depression in the medial perforant path of the dentate gyrus in vitro. *J Neurophysiol* 2001; **85**: 2509-2515.
[64] Lynch BA, Lambeng N, Nocka K, Kensel-Hammes P, Bajjalieh SM, Matagne A *et al.* The synaptic vesicle protein SV2A is the binding site for the antiepileptic drug levetiracetam. *Proc Natl Acad Sci U S A* 2004; **101**: 9861-9866.
[65] Custer KL, Austin NS, Sullivan JM, Bajjalieh SM. Synaptic vesicle protein 2 enhances release probability at quiescent synapses. *J Neurosci* 2006; **26**: 1303-1313.
[66] Crowder KM, Gunther JM, Jones TA, Hale BD, Zhang HZ, Peterson MR *et al.* Abnormal neurotransmission in mice lacking synaptic vesicle protein 2A (SV2A). *Proc Natl Acad Sci U S A* 1999; **96**: 15268-15273.
[67] Toering ST, Boer K, de Groot M, Troost D, Heimans JJ, Spliet WG *et al.* Expression patterns of synaptic vesicle protein 2A in focal cortical dysplasia and TSC-cortical tubers. *Epilepsia* 2009; **50**: 1409-1418.
[68] Crevecoeur J, Kaminski RM, Rogister B, Foerch P, Vandenplas C, Neveux M *et al.* Expression pattern of synaptic vesicle protein 2 (SV2) isoforms in patients with temporal lobe epilepsy and hippocampal sclerosis. *Neuropathol Appl Neurobiol* 2013.
[69] Bandala C, Miliar-Garcia A, Mejia-Barradas CM, Anaya-Ruiz M, Luna-Arias JP, Bazan-Mendez CI *et al.* Synaptic vesicle protein 2 (SV2) isoforms. *Asian Pac J Cancer Prev* 2012; **13**: 5063-5067.
[70] Schivell AE, Mochida S, Kensel-Hammes P, Custer KL, Bajjalieh SM. SV2A and SV2C contain a unique synaptotagmin-binding site. *Mol Cell Neurosci* 2005; **29**: 56-64.
[71] Janz R, Sudhof TC. SV2C is a synaptic vesicle protein with an unusually restricted localization: anatomy of a synaptic vesicle protein family. *Neuroscience* 1999; **94**: 1279-1290.
[72] Vogl C, Mochida S, Wolff C, Whalley BJ, Stephens GJ. The synaptic vesicle glycoprotein 2A ligand levetiracetam inhibits presynaptic Ca2+ channels through an intracellular pathway. *Mol Pharmacol* 2012; **82**: 199-208.
[73] Ozcan M, Ayar A. Modulation of action potential and calcium signaling by levetiracetam in rat sensory neurons. *J Recept Signal Transduct Res* 2012; **32**: 156-162.
[74] Marek GJ. Metabotropic glutamate 2/3 receptors as drug targets. *Curr Opin Pharmacol* 2004; **4**: 18-22.
[75] Flor PJ, Battaglia G, Nicoletti F, Gasparini F, Bruno V. Neuroprotective activity of metabotropic glutamate receptor ligands. *Adv Exp Med Biol* 2002; **513**: 197-223.
[76] Tang FR, Lee WL. Expression of the group II and III metabotropic glutamate receptors in the hippocampus of patients with mesial temporal lobe epilepsy. *J Neurocytol* 2001; **30**: 137-143.
[77] Crevecoeur J, Kaminski RM, Rogister B, Foerch P, Vandenplas C, Neveux M *et al.* Expression pattern of synaptic vesicle protein 2 (SV2) isoforms in patients with temporal lobe epilepsy and hippocampal sclerosis. *Neuropathol Appl Neurobiol* 2014; **40**: 191-204.
[78] van Vliet EA, Aronica E, Redeker S, Boer K, Gorter JA. Decreased expression of synaptic vesicle protein 2A, the binding site for levetiracetam, during epileptogenesis and chronic epilepsy. *Epilepsia* 2009; **50**: 422-433.
[79] Shetty AK. Prospects of Levetiracetam as a Neuroprotective Drug Against Status Epilepticus, Traumatic Brain Injury, and Stroke. *Front Neurol* 2013; **4**: 172.
[80] Kaminski RM, Gillard M, Klitgaard H. Targeting SV2A for Discovery of Antiepileptic Drugs. 2012.
[81] Abou-Khalil B. Levetiracetam in the treatment of epilepsy. *Neuropsychiatr Dis Treat* 2008; **4**: 507-523.
[82] Garrido-Sanabria ER, Perez-Cordova MG, Colom LV. Differential expression of voltage-gated K+ currents in medial septum/diagonal band complex neurons exhibiting distinct firing phenotypes. *Neurosci Res* 2011; **70**: 361-369.

[83] Pfaffl MW, Horgan GW, Dempfle L. Relative expression software tool (REST) for group-wise comparison and statistical analysis of relative expression results in real-time PCR. *Nucleic Acids Res* 2002; **30**: e36.
[84] Pfaffl MW. A new mathematical model for relative quantification in real-time RT-PCR. *Nucleic Acids Res* 2001; **29**: e45.
[85] Liu JX, Cao X, Liu Y, Tang FR. CCL28 in the mouse hippocampal CA1 area and the dentate gyrus during and after pilocarpine-induced status epilepticus. *Neurochem Int* 2012; **61**: 1094-1101.
[86] Frycia A, Starck JP, Jadot S, Lallemand B, Leclercq K, Lo Brutto P *et al.* Discovery of indolone acetamides as novel SV2A ligands with improved potency toward seizure suppression. *ChemMedChem* 2010; **5**: 200-205.
[87] Gillard M, Chatelain P, Fuks B. Binding characteristics of levetiracetam to synaptic vesicle protein 2A (SV2A) in human brain and in CHO cells expressing the human recombinant protein. *Eur J Pharmacol* 2006; **536**: 102-108.
[88] Bajjalieh SM, Frantz GD, Weimann JM, McConnell SK, Scheller RH. Differential expression of synaptic vesicle protein 2 (SV2) isoforms. *J Neurosci* 1994; **14**: 5223-5235.
[89] Bajjalieh SM, Peterson K, Shinghal R, Scheller RH. SV2, a brain synaptic vesicle protein homologous to bacterial transporters. *Science* 1992; **257**: 1271-1273.
[90] Krishna K, Raut AL, Gohel KH, Dave P. Levetiracetam. *J Assoc Physicians India* 2011; **59**: 656-658.
[91] Klitgaard H, Verdru P. Levetiracetam: the first SV2A ligand for the treatment of epilepsy. *Expert Opin Drug Discov* 2007; **2**: 1537-1545.
[92] Rogawski MA. Molecular targets versus models for new antiepileptic drug discovery. *Epilepsy Res* 2006; **68**: 22-28.
[93] Pitkanen A. SV2A: more than just a new target for AEDs. *Epilepsy Curr* 2005; **5**: 14-16.
[94] Janz R, Goda Y, Geppert M, Missler M, Sudhof TC. SV2A and SV2B function as redundant Ca2+ regulators in neurotransmitter release. *Neuron* 1999; **24**: 1003-1016.
[95] Acsady L, Kamondi A, Sik A, Freund T, Buzsaki G. GABAergic cells are the major postsynaptic targets of mossy fibers in the rat hippocampus. J Neurosci. 1998 May 1;18(9):3386-403.
[96] Anggono V, Smillie KJ, Graham ME, Valova VA, Cousin MA, Robinson PJ. Syndapin I is the phosphorylation-regulated dynamin I partner in synaptic vesicle endocytosis. Nat Neurosci. 2006 Jun;9(6):752-60.
[97] Bailey CP, Nicholls RE, Zhang XL, Zhou ZY, Muller W, Kandel ER, et al. Galpha(i2) inhibition of adenylate cyclase regulates presynaptic activity and unmasks cGMP-dependent long-term depression at Schaffer collateral-CA1 hippocampal synapses. Learn Mem. 2008;15(4):261-70.
[98] Boumil RM, Letts VA, Roberts MC, Lenz C, Mahaffey CL, Zhang ZW, et al. A missense mutation in a highly conserved alternate exon of dynamin-1 causes epilepsy in fitful mice. PLoS Genet. 2010 Aug;6(8).
[99] Chung C, Barylko B, Leitz J, Liu X, Kavalali ET. Acute dynamin inhibition dissects synaptic vesicle recycling pathways that drive spontaneous and evoked neurotransmission. J Neurosci. 2010 Jan 27;30(4):1363-76.
[100] Danzer SC, He X, Loepke AW, McNamara JO. Structural plasticity of dentate granule cell mossy fibers during the development of limbic epilepsy. Hippocampus. 2010 Jan;20(1):113-24.
[101] Ferguson SM, Brasnjo G, Hayashi M, Wolfel M, Collesi C, Giovedi S, et al. A selective activity-dependent requirement for dynamin 1 in synaptic vesicle endocytosis. Science. 2007 Apr 27;316(5824):570-4.
[102] Galimberti I, Gogolla N, Alberi S, Santos AF, Muller D, Caroni P. Long-term rearrangements of hippocampal mossy fiber terminal connectivity in the adult regulated by experience. Neuron. 2006 Jun 1;50(5):749-63.
[103] Gundelfinger ED, Kessels MM, Qualmann B. Temporal and spatial coordination of exocytosis and endocytosis. Nat Rev Mol Cell Biol. 2003 Feb;4(2):127-39.
[104] Macia E, Ehrlich M, Massol R, Boucrot E, Brunner C, Kirchhausen T. Dynasore, a cell-permeable inhibitor of dynamin. Dev Cell. 2006 Jun;10(6):839-50.
[105] Newton AJ, Kirchhausen T, Murthy VN. Inhibition of dynamin completely blocks compensatory synaptic vesicle endocytosis. Proc Natl Acad Sci U S A. 2006 Nov 21;103(47):17955-60.
[106] Sankaranarayanan S, Ryan TA. Real-time measurements of vesicle-SNARE recycling in synapses of the central nervous system. Nat Cell Biol. 2000 Apr;2(4):197-204.

[107] Stanton PK, Winterer J, Bailey CP, Kyrozis A, Raginov I, Laube G, et al. Long-term depression of presynaptic release from the readily releasable vesicle pool induced by NMDA receptor-dependent retrograde nitric oxide. J Neurosci. 2003 Jul 2;23(13):5936-44.
[108] Stanton PK, Winterer J, Zhang XL, Muller W. Imaging LTP of presynaptic release of FM1-43 from the rapidly recycling vesicle pool of Schaffer collateral-CA1 synapses in rat hippocampal slices. Eur J Neurosci. 2005 Nov;22(10):2451-61.
[109] Stevens CF, Williams JH. "Kiss and run" exocytosis at hippocampal synapses. Proc Natl Acad Sci U S A. 2000 Nov 7;97(23):12828-33.
[110] Winterer J, Stanton PK, Muller W. Direct monitoring of vesicular release and uptake in brain slices by multiphoton excitation of the styryl FM 1-43. Biotechniques. 2006 Mar;40(3):343-51.
[111] Zakharenko SS, Zablow L, Siegelbaum SA. Altered presynaptic vesicle release and cycling during mGluR-dependent LTD. Neuron. 2002 Sep 12;35(6):1099-110.

8. Appendices

Brain Advance Access published February 16, 2012

BRAIN
A JOURNAL OF NEUROLOGY

Altered neurotransmitter release, vesicle recycling and presynaptic structure in the pilocarpine model of temporal lobe epilepsy

Chirag Upreti,[1] Rafael Otero,[2] Carlos Partida,[2] Frank Skinner,[2] Ravi Thakker,[2] Luis F. Pacheco,[2] Zhen-yu Zhou,[1] Giorgi Maglakelidze,[1] Jana Velíšková,[1,3] Libor Velíšek,[1,4] Dwight Romanovicz,[5] Theresa Jones,[6] Patric K. Stanton[1,7] and Emilio R. Garrido-Sanabria[2]

1 Department of Cell Biology and Anatomy, New York Medical College, Valhalla, NY 10595, USA
2 Department of Biomedicine, University of Texas Brownsville, Brownsville, TX 78520, USA
3 Department of Obstetrics and Gynaecology, New York Medical College, Valhalla, NY 10595, USA
4 Department of Paediatrics, New York Medical College, Valhalla, NY 10595, USA
5 Institute for Cellular and Molecular Biology, University of Texas Austin, Austin, TX 78712, USA
6 Department of Psychology, Institute for Neuroscience, University of Texas Austin, Austin, TX 78712, USA
7 Department of Neurology, New York Medical College, Valhalla, NY 10595, USA

Correspondence to: Emilio R. Garrido-Sanabria, MD, PhD,
Epilepsy Research Laboratory,
Department of Biomedicine,
University of Texas Brownsville,
80 Fort Brown, BRHP 2117,
Brownsville,
TX 78520, USA
E-mail: emilio.garrido@utb.edu

In searching for persistent seizure-induced alterations in brain function that might be causally related to epilepsy, presynaptic transmitter release has relatively been neglected. To measure directly the long-term effects of pilocarpine-induced status epilepticus on vesicular release and recycling in hippocampal mossy fibre presynaptic boutons, we used (i) two-photon imaging of FM1-43 vesicular release in rat hippocampal slices; and (ii) transgenic mice expressing the genetically encoded pH-sensitive fluorescent reporter synaptopHluorin preferentially at glutamatergic synapses. In this study we found that, 1–2 months after pilocarpine-induced status epilepticus, there were significant increases in mossy fibre bouton size, faster rates of action potential-driven vesicular release and endocytosis. We also analysed the ultrastructure of rat mossy fibre boutons using transmission electron microscopy. Pilocarpine-induced status epilepticus led to a significant increase in the number of release sites, active zone length, postsynaptic density area and number of vesicles in the readily releasable and recycling pools, all correlated with increased release probability. Our data show that presynaptic release machinery is persistently altered in structure and function by status epilepticus, which could contribute to the development of the chronic epileptic state and may represent a potential new target for antiepileptic therapies.

Keywords: epilepsy; neurotransmitter release; hippocampus; synaptic vesicle recycling; mossy fibre terminals

Abbreviations: MFB = mossy fibre bouton; RRP = readily releasable pool; SpH = SynaptopHluorin

Received August 10, 2011. Revised October 4, 2011. Accepted November 8, 2011.

Introduction

Hippocampal mossy fibres exhibit complex structural rearrangements and abnormal synaptic function in mesial temporal lobe epilepsy (McNamara, 1994; Frotscher *et al.*, 2006; Dudek and Sutula, 2007; Danzer *et al.*, 2010). During epileptogenesis, axons of dentate gyrus granule cells sprout and establish abnormal excitatory synapses onto multiple targets, including granule cells, interneurons and CA3 pyramidal neurons (McNamara, 1994; Wenzel *et al.*, 2000; Frotscher *et al.*, 2006; Dudek and Sutula, 2007). While studies have shown alterations in postsynaptic function of excitatory and inhibitory circuits in mesial temporal lobe epilepsy (Coulter, 2000; Gorter *et al.*, 2002), far less attention has been paid to presynaptic dysfunction in the pathogenesis of epilepsy.

Large mossy fibre boutons (MFBs) have multiple release sites with substantial numbers of small and large clear synaptic vesicles containing glutamate (Chicurel and Harris, 1992; Rollenhagen *et al.*, 2007). Large synaptic vesicles are thought to mediate the monoquantal nature of 'giant' miniature excitatory postsynaptic currents onto CA3 pyramidal cells, allowing action potential invasion of presynaptic MFBs to trigger neurotransmitter release in amounts that reliably excite CA3 pyramidal neurons. During status epilepticus, excessive glutamate release from MFBs can be highly deleterious to survival of CA3 neurons and is thought to be responsible for the massive and sustained neuronal damage in the CA3 region (Zhang *et al.*, 2009).

Surprisingly little is known about the long-term effects of status epilepticus on vesicular release of transmitter from MFBs. Goussakov *et al.* (2000) found that, several weeks after kainic acid-induced status epilepticus, mossy fibre, but not associational-commissural, synapses exhibit impaired induction of long-term potentiation, markedly reduced paired-pulse facilitation and augmentation of burst induced mossy fibre-CA3 excitatory field potential (Goussakov *et al.*, 2000). These changes in activity-dependent plasticity were also associated with a significant increase in the size of the readily releasable pool (RRP) of vesicles, suggesting a persistent increase in release probability at mossy fibre–CA3 synapses (Goussakov *et al.*, 2000). Ultrastructural features and targets of abnormally sprouted MFBs in the inner molecular layer have been studied by electron microscopy in models of mesial temporal lobe epilepsy (Cavazos *et al.*, 2003; Frotscher *et al.*, 2006); indeed, redistribution of synaptic vesicles to a 'strategic position' in the vicinity of the synaptic cleft has been described after kindled seizures (Hovorka *et al.*, 1989), but these studies did not characterize the arrangement of active zones and morphological features of vesicle pools.

We used the cholinergic agonist pilocarpine to induce prolonged status epilepticus as a model of mesial temporal lobe epilepsy (Turski *et al.*, 1984; Curia *et al.*, 2008), to test the hypothesis that status epilepticus can result in long-term enhancement of vesicular release from MFBs. Assessing presynaptic release properties by patch-clamp electrophysiology in long-term epileptic animals is hampered by the CA3 pyramidal neurons being susceptible to cell death due to excitotoxicity, thus are not optimal to record from as biosensors of transmitter release. Here we utilized two different methods to directly image presynaptic vesicular release by using two-photon laser scanning microscopy of (i) the styryl dye FM1-43 (Pyle *et al.*, 1999), which selectively labels transmitter vesicles for direct visualization of destaining kinetics, in slices from control versus post-status epilepticus rats; and (ii) imaging exocytosis–endocytosis kinetics from individual MFBs in acute hippocampal slices from transgenic mice that selectively express the pH-sensitive vesicle fusion protein synaptopHluorin (SpH) (Li *et al.*, 2005). We also used transmission electron microscopy of rat hippocampus to investigate whether the post-status epilepticus period is associated with ultrastructural modifications at active zones of MFBs in the stratum lucidum correlated with functional changes in vesicular release (Dobrunz and Stevens, 1997; Murthy *et al.*, 1997; Schikorski and Stevens, 1997; Matz *et al.*, 2010).

By each of these measures, we found a persistent enhancement of vesicular release, vesicle endocytosis and ultrastructure reorganization of active zones in MFBs after status epilepticus. These changes are likely to add to observed changes in intrinsic excitability of granule cells and circuit plasticity to increase the excitatory drive from granule cells onto CA3 pyramidal neurons in MTLE.

Materials and methods

Experiments were performed in accordance with the National Institutes of Health Guidelines for the Care and Use of Laboratory Animals as approved by New York Medical College and University of Texas Brownsville Institutional Animal Care and Use Committees.

Pilocarpine-induced status epilepticus

Status epilepticus was induced by a single pilocarpine intraperitoneal injection (350 mg/kg in saline) to 30- to 35-day-old Sprague–Dawley rats (Taconic) or SpH21 mice (C57BL/6J background, kind gift from Dr Venkatesh Murthy, Harvard University) following standard procedures (Cavalheiro, 1995; Pacheco *et al.*, 2008). Animals received methylscopolamine nitrate (0.1 mg/kg in saline, subcutaneous) 30 min before pilocarpine to minimize peripheral effects of cholinergic stimulation (Turski *et al.*, 1984). Rats seized for 3 h, mice 1 h (Muller *et al.*, 2009), and motor seizures were terminated with one diazepam injection (10 mg/kg in saline, intraperitoneal). Only animals experiencing continuous status epilepticus during these periods were studied. Controls animals received methylscopolamine and saline instead of pilocarpine.

Hippocampal slice preparation and electrophysiological recordings

Rats and mice 1–2 months post-status epilepticus and age-matched controls were decapitated under deep isoflurane anaesthesia, their brains quickly removed, hemisected in ice-cold sucrose-based cutting solution (Bischofberger *et al.*, 2006) in mM: 87 NaCl, 25 $NaHCO_3$, 25 glucose, 75 sucrose, 2.5 KCl, 1.25 NaH_2PO_4, 0.5 $CaCl_2$ and 7 $MgCl_2$ (equilibrated with 95% O_2/5% CO_2), and 350–400 μm thick horizontal hippocampal slices cut with a vibratome (DSK model

DTK-1000). Slices were submerged in cutting solution at 32°C for 30 min, then transferred to a holding chamber in room temperature artificial CSF (in mM: 126 NaCl, 3 KCl, 1.25 NaH_2PO_4, 1.3 MgCl, 2.5 $CaCl_2$, 26 $NaHCO_3$, 10 glucose) saturated with 95% O_2/5% CO_2. Evoked field excitatory postsynaptic potentials were recorded in the proximal dendritic field in stratum lucidum for at least 15 min before starting an experiment.

Two-photon laser scanning microscopy

Fluorescence was visualized with a customized two-photon laser-scanning Olympus BX61WI microscope with a ×60/0.90 NA water immersion infrared objective lens and an Olympus multispectral confocal laser scan unit. The light source was a Mai-Tai^{TM} laser (Solid-State Laser Co.), tuned to 825 nm for exciting Alexa Fluor 594, and 890 nm for exciting SpH and FM1-43. Epifluorescence was detected with photomultiplier tubes of the confocal laser scan head with pinhole maximally open and emission spectral window optimized for signal over background. A 565-nm dichroic mirror (Chroma Technology) separated green and red fluorescence to eliminate transmitted or reflected excitation light. Depending on the fluorophore, HQ525/50 (SpH) or HQ605/50 (FM1-43 or Alexa Fluor 594) filters were placed in the 'green' pathways. Images were acquired with Fluoview FV300 software (Olympus America). Although there were no signs of photodamage, we used the lowest intensity needed for adequate signal-to-noise ratios. Pixel images (512 × 512) were acquired, 0.15 μm/pixel in $x-y$ axes and, in some cases, 8–10 μm steps of 0.5–1 μm in the z-axis. For imaging MFBs, glass microelectrodes with broken tips ($R < 1$ MΩ) were dipped in 1% Alexa Fluor 594 10-kDa dextran (Invitrogen) in distilled water until the tip filled by capillarity action, desiccated for 2–3 days until dye formed a crystal particle at the tip. During the experiment, dye coated tips (with sealed backends) were inserted ~50–100 μm into the dentate gyrus granule cell layer for 15–20 min, then slices were transferred to a holding chamber in artificial CSF at 32°C for 30 min, followed by room temperature for 1–1.5 h, before imaging. Using NIH ImageJ, greyscale images of Alexa Fluor 594 filled MFBs flanked by at least one axonal process were processed by automated Otsu thresholding to eliminate investigator bias (Lee *et al.*, 2011), and cross-sectional area of binary images measured. A total of 8–10 images were acquired in a z-axis stack in 0.2–0.5 μm steps for 3D reconstruction (Supplementary Video 3). For SpH fluorescence experiments, slices were perfused with 25 μM 6-cyano-7-nitroquinoxaline-2,3-dione (CNQX; Tocris) and 50 μM D-(-)-2-Amino-5-phosphonopentanoic acid (D-AP5; Tocris). A 600 stimulus 20-Hz train in the stratum lucidum evoked SpH fluorescence increases (imaged within 100 μm from stimulating electrode) in the proximal region (the first 100 μm) of CA3 apical dendrites and images were acquired every 30 s. While extracellular brain pH changes during seizures, first to alkaline and later to acidic (Xiong and Stringer, 2000), we use SpH as a pH-sensitive indicator of vesicular release in brain slices bathed in artificial CSF (containing 25 μM CNQX and 50 μM D-AP5 to prevent synaptically driven action potentials and epileptiform activity) in our recording chamber with pH maintained at or ~7.4. To calculate half-time of post-stimulus decay of SpH peak fluorescence intensity, ($t_{1/2}$) was calculated for each punctum by single exponential fits to destaining curves using the equation: $y_0 + A_1e^{(-x/t_1)}$, with t_1 the decay constant. Data were analysed with OriginPro and presented with KaleidaGraph (Synergy software).

FM1-43 loading and destaining of the readily releasable vesicle pool

FM1-43 was loaded into the RRP as previously described (Stanton *et al.*, 2003, 2005). After recording a 15 min stable baseline field excitatory postsynaptic potential (~50% of maximum amplitude), 25 μM CNQX and 50 μM D-AP5 were bath applied to prevent synaptically driven action potentials and epileptiform activity from accelerating dye release or inducing synaptic plasticity. Presynaptic boutons were loaded by 5-min bath applied 5 μM FM1-43 in normal artificial CSF, followed by hypertonic artificial CSF (800 mOsm) for 30 s to load the RRP, returned to normal artificial CSF with 5 μm FM1-43 for 1 min, then washed out with dye-free artificial CSF (Supplementary Fig. 2). Stimulus-induced destaining was evoked by a 50 stimulus 20-Hz train each 30 s, and measured after 30 min in dye-free artificial CSF plus 100 μM ADVASEP-7 to scavenge and remove extracellular FM1-43. To measure spontaneous release, after FM1-43 loading, slices were continuously bathed in 1 μM tetrodotoxin, 25 μm CNQX and 50 μM D-AP5 and extracellular [K^+] raised to 15 mM [K^+]o (*High[K+]o)* to facilitate action potential-independent release (Axmacher *et al.*, 2004). For some slices, 8–10 images were acquired in 0.5–1 μm in the z-axis at each time point, maximal intensity z-axis projections were made for this subset of the final stack. Circular regions of interest were selected around centres of bright, punctate fluorescence spots at least 2 μm in diameter within 100 μm of the CA3 pyramidal cell body layer. Activity-dependent destaining time courses were generated by correcting for bleaching, subtracting background fluorescence and normalizing each region of interest to pre-stimulus intensity as previously reported (Stanton *et al.*, 2003, 2005; Tyler *et al.*, 2006). Vertical bars show SEMs for all normalized and corrected boutons.

Tissue preparation for immunohistochemistry

Age-matched control and epileptic SpH mice (<6 months post-status epilepticus) were anaesthetized with 100 mg/kg ketamine, the brain removed and immersed for 48 h in 4% formaldehyde in 0.1 M sodium phosphate buffer (pH 7.4) plus 0.9% NaCl (phosphate-buffered saline). After a phosphate-buffered saline wash, brains were cryoprotected in 30% sucrose in phosphate-buffered saline for ~48 h at 4°C, frozen in Optimum Cutting Temperature Compound (EMS Co.) at −20°C, and 40 μm thick coronal sections sliced with a cryostat (HM500 Microm, Zeiss) and stored in 150 mM Tris plus 150 mM NaCl (Tris-buffered saline; pH 7.4) and 0.1% NaN_3. Several sections were Nissl-stained to assess seizure-mediated neuronal loss and cyto-architectonic boundaries. Free-floating sections from controls and post-status epilepticus were processed simultaneously for VGluT1 and NeuN immunofluorescence as described (Pacheco *et al.*, 2008). The extent of cell loss in the CA3 subfield was assessed at ×400 magnification by using grid morphometric techniques (Gorter *et al.*, 2003). A 240 × 240 μm box was placed over the region of interest (CA3 area) and NeuN-labelled cells in the pyramidal layer, presumed neurons, were counted by an observer masked to experimental group/condition. Counts of three sections per animal were averaged. Final neuron counts were calculated as the density of neurons per 0.1 mm^2. It should be noted that this technique provides a relative estimate and not absolute calculation of the number of neurons in a region. Statistical differences in the number of neurons per square millimetre between control and pilocarpine-treated epileptic groups were

determined by Student's *t*-test with significance set at $P < 0.05$. The cross-sectional diameter of SpH-positive VGluT1-labelled puncta in the granule cell layer and supragranular region was measured in three confocal images of dentate gyrus per animal per group using the measuring tool of Fluoview (Olympus).

Fixation and embedding for transmission electron microscopy

Tissue was prepared for transmission electron microscopy using standard methods (Miranda *et al.*, 2011). Seven post-status epilepticus and six age-matched Sprague–Dawley rats were anaesthetized with ketamine (50 mg/kg, intraperitoneal injection), transcardially perfused with saline followed by fixative (2% paraformaldehyde, 2% glutaraldehyde, 0.002% $CaCl_2$ in 0.1 M cacodylate and Hank's buffered salt solution; pH 7.3–7.4), and their brains were removed, sliced in 5-mm thick slabs, and post-fixed in fresh fixative overnight at room temperature. Serial 250-μm thick sections were cut with a vibratome in Hank's buffered salt solution (1000 Plus, Vibratome Co.), and the hippocampus and surrounding cortex dissected away. Samples were osmicated in 2% buffered osmium tetroxide, a 50:50 mixture of 4% osmium tetroxide and 4% potassium ferrocyanide in 0.2 M cacodylate buffer (EMS Co.), then contrasted in 1% aqueous uranyl acetate. Tissue was flat-embedded in 50:50 Spurr/Epon (EMS Co.) and polymerized at 60°C for 24 h before resin blocks were pseudo-randomly selected and trimmed to ~1 mm^3 trapezoids containing the CA3 pyramidal cell layer and stratum lucidum. To identify field CA3, 1–2 μm sections were stained with 0.1% cresyl violet acetate solution and viewed on a transmitted light scope. Ultrathin sections (55 ± 5 nm) were cut through stratum lucidum of CA3 with a Leica Ultracut ultramicrotome and collected on Formvar-coated copper slotted grids.

Transmission electron microscopy inspection and identification of mossy fibre boutons

Images 26 000× (FEI Tecnai) were used to identify regions of interest in field CA3 containing cross-sectioned or parallel bundles of axons and large MFBs (1–5 μm diameter) with numerous synaptic vesicles. For blind analysis of morphometry, coded images were imported into NIH ImageJ. Active zones were distinguished by the following criteria: (i) synaptic vesicles in close proximity to a presynaptic density; (ii) asymmetry between pre- and postsynaptic densities; and (iii) widening of the synaptic cleft (Rollenhagen *et al.*, 2007). Asymmetric (excitatory) non-perforated synapses with well-defined presynaptic compartments, clear synaptic clefts and postsynaptic density were analysed. Perforated synapses refer to a presumably more efficacious synapse subtype found in the CNS characterized by a discontinuous postsynaptic density (Calverley and Jones, 1987; Itarat and Jones, 1992; Adkins *et al.*, 2008). The number of perforated and non-perforated synapses was compared between groups

Active zone length was measured by a continuous line following the contour of presynaptic membrane on the synaptic cleft. Synaptic cleft width was averaged from three measures of distance between pre- and postsynaptic membranes (centre and ~20 nm from cleft ends). Postsynaptic density area was measured as the contour around electron-dense aggregates and postsynaptic membrane. The active zone length and quantification of synaptic vesicles was performed in single ultrathin sections using a modified 2D cross-sectional method as described previously (Miranda *et al.*, 2011) using NIH ImageJ.

The RRP was defined as the number of synaptic vesicles <60 nm from the presynaptic membrane, and the releasable pool of vesicles 60–200 nm from the presynaptic membrane (Rollenhagen *et al.*, 2007). Docked synaptic vesicles consisted of vesicles immediately adjacent to or fused to the active zone presynaptic membrane. Perimeter and mean area of synaptic vesicles were also measured, and number of active zones exhibiting ultrastructural signs of bulk endocytosis indicative of intense synaptic activity (Meunier *et al.*, 2010).

Differences in vesicle pool size were assessed by non-parametric Kolmogorov–Smirnov two-sample test (MiniAnalysis, Synaptosoft), and differences in means of normally distributed measurements were evaluated using two-tailed Student's *t*-test. Significance level was preset to $P < 0.05$. Correlation analysis between parameters was performed with non-parametric Spearman analysis, since most parameters were not normally distributed. Correlations were classified as weak [Spearman rho (r) value < 0.40], moderate ($0.4 < r < 0.7$) and strong ($r > 0.7$).

Results

Two-photon laser scanning microscopy imaging of large mossy fibre boutons of synaptopHluorin-expressing transgenic mice in acute hippocampal slices

SpH is a fusion protein that consists of a pH-sensitive pHluorin fused to the C-terminus luminal domain of the vesicle SNARE protein synaptobrevin (Miesenbock *et al.*, 1998). Under resting conditions, the luminal pH of the synaptic vesicle is acidic (pH ~5.5), resulting in proton dependent quenching of SpH fluorescence. When vesicle exocytosis is triggered and glutamate released, the lumen of the vesicle is exposed to the more alkaline pH of the extracellular space (pH ~7.2), resulting in a 20-fold increase in SpH fluorescence. When the vesicle membrane is retrieved by endocytosis and the vesicle reformed, it undergoes rapid reacidification by the vesicular ATPase, which returns SpH to its quenched state. The SpH21 transgenic mice line we used in this study expresses SpH preferentially at glutamatergic synapses (Li *et al.*, 2005; Burrone *et al.*, 2006; Bayazitov *et al.*, 2007). A representative two-photon laser scanning image of the CA3 region of an acute hippocampal slice from this mouse (Fig. 1A) contains bright GFP-positive boutons >2 μm in diameter, proximal to CA3 pyramidal cell bodies in the region innervated by mossy fibre axons of dentate granule cells (Blackstad *et al.*, 1970; Claiborne *et al.*, 1986). Associational-commissural CA3 synapses were significantly smaller (<1 μm in diameter) and more distal to our region of interest (rectangular box, Fig. 1A).

To independently confirm that large SpH expressing boutons were mossy fibre terminals, we used anterograde, bulk labelling of mossy fibres with Alexa Fluor 594 dextran introduced into the granule cell layer of the dentate gyrus (Fig. 1B). During a 1.5- to 2-h incubation, Alexa Fluor 594 dextran was taken up by granule cells and transported anterogradely to label mossy fibre axons and presynaptic boutons (Fig. 1C, Supplementary Fig. 1A and Supplementary Video 3). Figure 1E and F illustrate that some

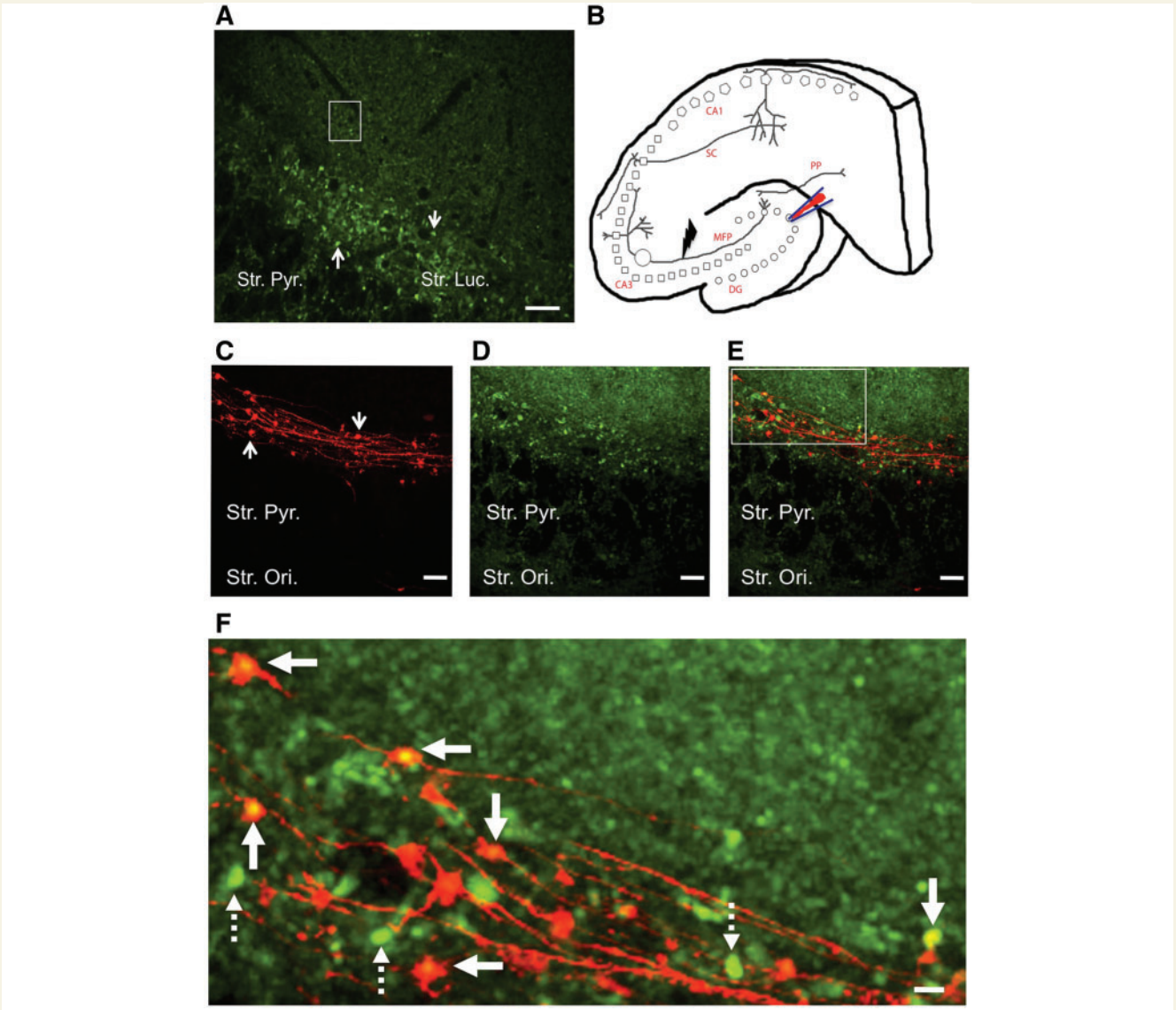

Figure 1 Visualizing MFBs in acute hippocampal slices from SpH21 transgenic mice. (**A**) Live cell two-photon laser scanning image of field CA3 of SpH-expressing glutamatergic terminals in a control hippocampal slice (post natal 60 days of age). The arrows depict representative fluorescence puncta (~4–5 μm in diameter) in the proximal (stratum lucidum, Str. Luc.) region of CA3 pyramidal cells (seen here as a ghost layer) that are likely to be giant MFBs. Distal puncta shown within the rectangular box are notably smaller in size and likely represent associational-commissural synapses in stratum radiatum. (**B**) Schematic representing hippocampal circuitry with the circle in the mossy fibre pathway (MFP) depicting the area of imaging Lightning symbol depicts the area of local stimulation and the pipette in the dentate granule cell layer (DG) showing the area of Alexa Fluor 594 dextra containing pipette insertion. Squares and pentagons depict CA3 and CA1 pyramidal cell layers, respectively. (**C**) Alexa Fluor 594 dextran filled mossy fibre axons and giant MFBs (arrows) showing characteristic *en-passant* arrangement along the axonal projections, visualized using 825 nm excitation. (**D**) Same region as (**C**) but visualized with 890-nm excitation to see SpH native fluorescence. CA3 pyramidal cell bodies can be seen as ghost cells in stratum pyramidal, and bright giant MFBs in stratum lucidum. (**E–F**) Merged images of (**C**) and (**D**) showing co-localization (**F**: arrows) between SpH and Alexa Fluor 594 dextran-labelled puncta. (**F**) Digital zoom of image from the inset box in (**E**). Note not all SpH-positive puncta co-localize with Alexa Fluor 594 puncta (broken arrows). PP = perforant path; SC = Schaffer collaterals; Str. Ori. = stratum oriens; Str. Pyr. = stratum pyramidale. Scale bars: **A** = 20 μm; **C–E** = 20 μm; and **F** = 4 μm.

(solid arrows) but not all (broken arrows) SpH and Alexa Fluor 594-positive boutons were co-labelled confirming that the large (>2 μm in diameter) SpH fluorescent puncta within the proximal 60 μm of the CA3 cell body are excitatory MFBs (Fig. 1D). Incomplete co-localization is likely because Alexa Fluor 594 labelled a subset of mossy fibre axons in stratum lucidum, along with sparse SpH expression in the excitatory terminals (Li *et al.*, 2005; Burrone *et al.*, 2006).

Pilocarpine-induced status epilepticus causes disorganization of dentate gyrus and CA3 cytoarchitecture in synaptopHluorin-expressing transgenic mice

In the hippocampal CA3 region of both control and post-status epilepticus mice (Fig. 2A), immunostaining for the presynaptic glutamate transporter VGluT1 was intense in the mossy fibre projection area in stratum lucidum, where it co-localized with native SpH fluorescence, consistent with the glutamatergic nature of presynaptic terminals expressing SpH in SpH21 mice (Li *et al.*, 2005; Burrone *et al.*, 2006). There was also ~51% reduction in CA3 stratum pyramidale of post-status epilepticus mice in the density of neurons (117.9 ± 35.4 cells/0.1 mm^2, $n = 6$, Student's *t*-test, $P < 0.01$, Fig. 2A), consistent with seizure-induced loss of CA3 pyramidal neurons following pilocarpine-induced status epilepticus reported previously (Mello *et al.*, 1993; Schauwecker, 2012).

In the dentate gyrus, we detected robust SpH fluorescence in the inner molecular layer and hilus of both control and post-status epilepticus mice (Fig. 2B), closely co-localized with VGluT1 immunofluorescence (Fig. 2B). VGluT1 puncta positive for SpH fluorescence in the inner molecular layer exhibited 39.5% larger cross-sectional diameters (Fig. 2B, 1.84 ± 0.54 µm, Student's *t*-test, $P < 0.001$) and 47.5% higher normalized mean fluorescence intensity (Fig. 2B, post-status epilepticus: VGluT1) relative to background-subtracted baseline intensity [204.8 ± 35.5 arbitrary units (a.u), $n = 29$, Student's *t*-test, $P < 0.0001$] in pilocarpine-treated post-status epilepticus mice compared with controls (Fig. 2B, control: VGluT1 138.8 ± 32.2 a.u and mean diameter of puncta: 1.31 ± 0.37 µm, $n = 29$). Interestingly, SpH puncta in granule cell somata in the control dentate gyri exhibited little immunostaining for VGluT1, whereas the granule cell layers of post-status epilepticus hippocampi showed strong co-immunolabelling for VGluT1 (Fig. 2B), suggesting either a possible upregulation of VGluT1 expression in existing terminals or neo-synaptogenesis manifested by the appearance of ectopic glutamatergic (VGluT1 positive) terminals in both inner molecular and granule cell layers during epileptogenesis, as previously reported in animal models of MTLE (Mello *et al.*, 1993; Esclapez *et al.*, 1999; Epsztein *et al.*, 2005; Pacheco *et al.*, 2006; Boulland *et al.*, 2007).

Pilocarpine-induced status epilepticus persistently increases size and vesicular release rate of mossy fibre boutons in synaptopHluorin-expressing mice

Live cell imaging of MFBs in acute hippocampal slices was done by bulk loading a group of granule cells and their axons with Alexa Fluor 594-dextran. Dye-filled excrescences (Fig. 1B) were classified as the main body of giant MFBs if they had at least a 4 µm^2 cross-sectional area (Claiborne *et al.*, 1986; Acsady *et al.*, 1998; Danzer *et al.*, 2010). The mean area of MFBs 1–2 months after pilocarpine induced-status epilepticus was significantly enhanced (~21.09%, Fig. 3C, $P = 0.008$, Mann–Whitney U-test, $n = 7$) compared with aged matched controls ($n = 7$). A frequency distribution histogram of individual MFBs from epileptic animals revealed a significant rightward shift in the curves (Fig. 3B; $P < 0.05$, Kolmogorov–Smirnov test), consistent with increased MFB volumes.

To determine whether post-status epilepticus leads to functional differences in transmitter release from excitatory MFBs, we utilized two-photon live cell imaging in slices from SpH21 mice. To trigger vesicular release from MFBs in CA3 stratum lucidum (Fig. 1B–F), granule cell axons in slices from control and post-status epilepticus animals were stimulated with a single, continuous train of 600 stimuli at 20 Hz (Fig. 1B and Supplementary Video 4A and B, respectively), a paradigm that recruits both the RRP and rapidly recycling vesicle pools (Li *et al.*, 2005). Representative time-lapse images (Fig. 4A) of control and post-status epilepticus SpH-expressing MFBs showed robust, cumulative increases in SpH fluorescence intensity during the stimulus train, followed by return of fluorescence to baseline levels ~40 s after stimulus termination. Figure 4C plots the normalized mean SpH fluorescence responses in control versus post-status epilepticus animals, which showed significantly larger stimulus-evoked rises in SpH fluorescence (2.02 ± 0.15, red circles, $n = 8$, $P < 0.05$, Student's *t*-test) compared with controls (1.47 ± 0.03, black circles, $n = 10$).

This result could be due to either a general increase in release probability of existing MFBs or appearance of a distinct sub-population of terminals with higher release probabilities. To resolve this distinction, we plotted a distribution histogram (Fig. 4D) of the normalized peak SpH fluorescence values, which is a function of the total number of vesicles released during the stimulus train. Control and post-status epilepticus distributions of peak SpH fluorescence for all individual MFBs indicate the appearance of a new sub-population of ~3-fold higher release rate MFBs in the post-status epilepticus animals. The cumulative probability distribution (Fig. 4D inset) showed a significant increase in peak SpH fluorescence attained for the post-status epilepticus MFBs compared with controls ($P < 0.001$, Kolmogorov–Smirnov test).

Taken together, these results suggest that, in the first 1–2 months post-status epilepticus, morphological changes develop in the MFB cytoarchitecture, correlated with both an increase in vesicular release rate of MFBs and appearance of a high release rate sub-population of terminals.

Pilocarpine-induced status epilepticus persistently enhances vesicular endocytosis in mossy fibre boutons of synaptopHluorin-expressing mice

To determine whether there are changes in rate of vesicle endocytosis in MFBs, we used the decay kinetics of SpH fluorescence after the end of the stimulus train. Since vesicle endocytosis is the rate-limiting step for decay in vesicle fluorescence (Sankaranarayanan and Ryan, 2000), determining the decay constant (τ) of this fluorescence gives an estimate of the rate of

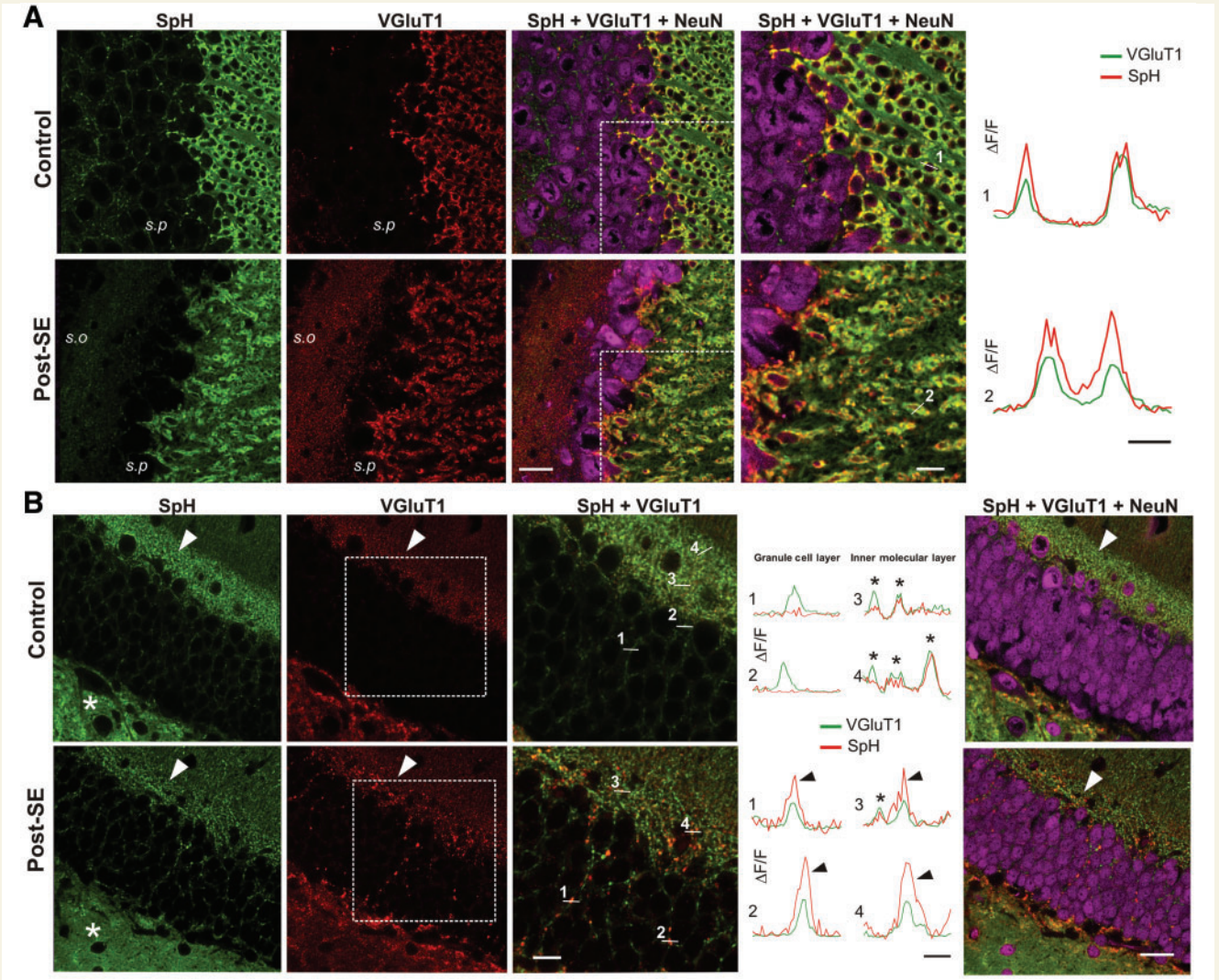

Figure 2 Confocal images of SpH, VGluT1 and NeuN expression in CA3 (**A**) and dentate granule cell (**B**) layers of control and post-status epilepticus (SE) SpH transgenic mice. (**A**) Native SpH fluorescence image (green), VGluT1 immunofluorescence image (red) and NeuN immunofluorescence image (purple) in control and post-status epilepticus mice showing co-localization of SpH with VgluT1 labelling in MFBs. A dramatic loss of cells was noticed in CA3 stratum pyramidale by NeuN staining (SpH + VGluT1 + NeuN, column 3) and SpH and VGluT1-positive terminals appear disorganized in stratum lucidum of post-status epilepticus compared with controls (SpH + VGluT1 + NeuN, column 4). Punctate SpH signals were also scattered through the pyramidal cell layer (s.p) surrounding cell somata that were stained with NeuN antibody. The column on the *right* (column 4) shows fluorescence intensity profile and co-localization along line scans (1: control and 2: post-status epilepticus) through single MFBs indicated in the respective ×2 magnification images (scale bar = 25 μm) of the rectangular boxes seen in column 3 (scale bar = 50 μm). Scale bar for line scans = 2 μm. (**B**) In the dentate granule cell layer of control and post-status epilepticus, (NeuN labelling), SpH fluorescence (green) and VGluT1 immunofluorescence (red) were intense in the hilus (asterisk) and in the inner molecular layer (arrow head). In the control (**B,** *top* row) SpH-positive puncta around putative granule cell somata were devoid of VGluT1 expression (line plots: lines 1 and 2), while SpH and VGluT1 signals co-localized in the inner molecular layer (line plots: lines 3 and 4), as shown by respective line scans of fluorescence intensity through puncta in the granule cell layer (1 and 2) versus the inner molecular layer (3 and 4). In post-status epilepticus (**B,** *bottom* row) SpH and VGluT1 co-localize in both the dentate granule cell layer (SpH + VGluT1) and inner molecular layer. NeuN immunofluorescence illustrates a lack of marked granule cell loss in post-status epilepticus dentate gyrus (SpH + VGluT1 + NeuN). Stratum oriens scale bar = 2 μm.

vesicle endocytosis. We first normalized the mean peak stimulus-evoked SpH fluorescence increases to 1.0 for control and post-status epilepticus slices, to compare directly the time courses of decay. As shown in Fig. 4E, the mean rate of decay of SpH fluorescence from peak to baseline for epileptic slices was significantly faster (red circles) compared with control slices (black circles, $P < 0.05$, Student's *t*-test), indicating an enhanced speed of endocytosis. We also fit single exponential decay functions to curves for individual MFBs to determine the decay time constants in post-status epilepticus vs. control MFBs. As shown in the Fig. 4E inset, chronic post-status epilepticus led to a significant decrease in decay time constants [red bar, $\tau = 7.23 \pm 0.32$ s versus

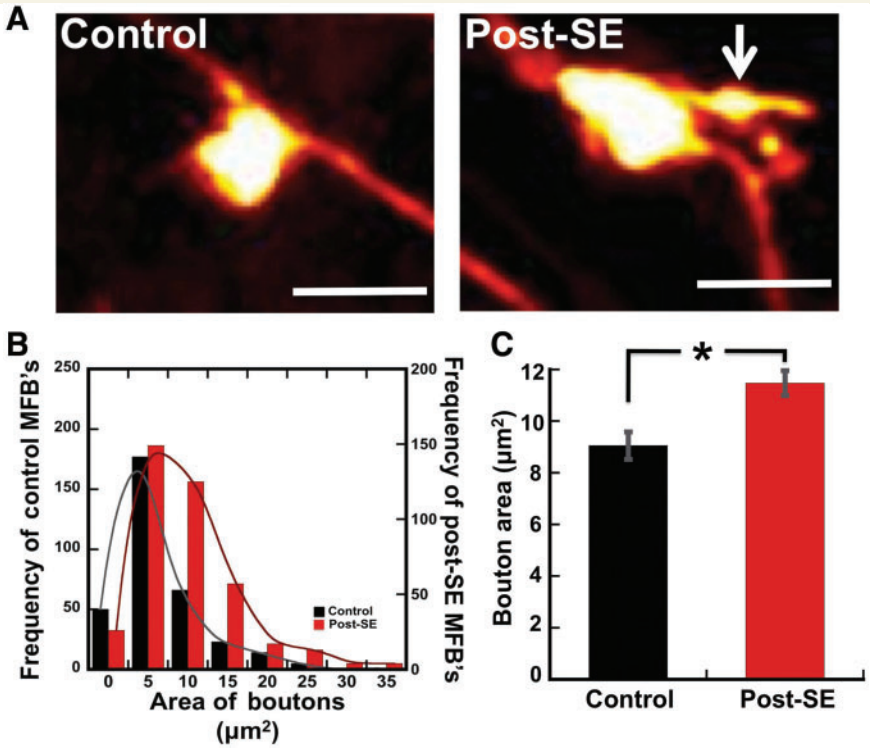

Figure 3 Pilocarpine-induced status epilepticus (SE) leads to persistent increases in dentate gyrus giant MFB area. (**A**) Live cell two-photon images of Alexa Fluor 594 dextran-loaded giant mossy fibre terminals from field CA3 of acute hippocampal slices from control and post-status epilepticus mice. The arrow shows a filopodia-like projection arising from the giant MFB. (**B**) Frequency distribution histogram of individual MFB areas from control (black columns, total of 336 boutons, $n = 7$) vs. 1–2 months post-SE mice (red columns, 394 boutons, $n = 7$). (**C**) Mean MFB area for control (black column, $9.05 \pm 0.52\ \mu m^2$) and epileptic (red column, $11.47 \pm 0.48\ \mu m^2$) mice. Data plotted as mean ± SEM, $^*P < 0.05$, Mann–Whitney U-test. Scale bar **A** = 5 μm.

control slices (black bar), $\tau = 10.4 \pm 0.77$ s, $P < 0.05$; Student's *t*-test] also consistent with acceleration in the rate of vesicle retrieval.

FM1-43 measurement of changes in vesicular release from the rat mossy fibre bouton readily releasable pool at early and late time points post-status epilepticus

As a second, independent measure of vesicular release, we estimated the time course of neurotransmitter release in slices from post-status epilepticus Sprague–Dawley rats using two-photon imaging of stimulus-evoked release of the styryl dye FM1-43 as described previously (Stanton *et al.*, 2003, 2005; Zakharenko *et al.*, 2003; Winterer *et al.*, 2006; Bailey *et al.*, 2008). We loaded FM1-43 selectively into vesicles of the RRP with a 30-s hypertonic shock (Supplementary Fig. 2) and similar to SpH fluorescence, we visualized bright puncta in the proximal region of field CA3 > 2 μm in diameter (Fig. 5A), presumed MFBs (Galimberti *et al.*, 2006). More distal puncta that took up FM1-43 were much smaller in size, consistent with associational-commissural synaptic terminals. Dye release was triggered by repetitive bursts of 50 mossy fibre stimuli at a frequency of 20 Hz, spaced 30 s apart (Fig. 5B and Supplementary Fig. 2), to allow binding and clearance by the scavenger ADVASEP-7 (100 μm) (Zakharenko *et al.*, 2003) and minimize potential movement artefacts.

Figure 5C shows that mean time courses of RRP loaded stimulus-evoked FM1-43 destaining from MFBs in slices up to 2 months post-status epilepticus was associated with a significantly enhanced release of FM1-43 (~64% from pre-stimulus baseline), when compared with age matched controls (~51% from pre-stimulus baseline, $P < 0.05$, Student's *t*-test). Interestingly, 11 months post-status epilepticus rats showed a substantial slowing in MFBs release rate in the epileptic group (~21% from pre-stimulus baseline) versus aged matched controls (~37% of baseline, $P < 0.05$, Student's *t*-test).

Action potential-independent release of FM1-43 from the mossy fibre bouton readily releasable pool is not persistently altered by pilocarpine-induced status epilepticus in rats

The above data suggest changes in stimulus evoked, but not necessarily spontaneous release rate post-status epilepticus.

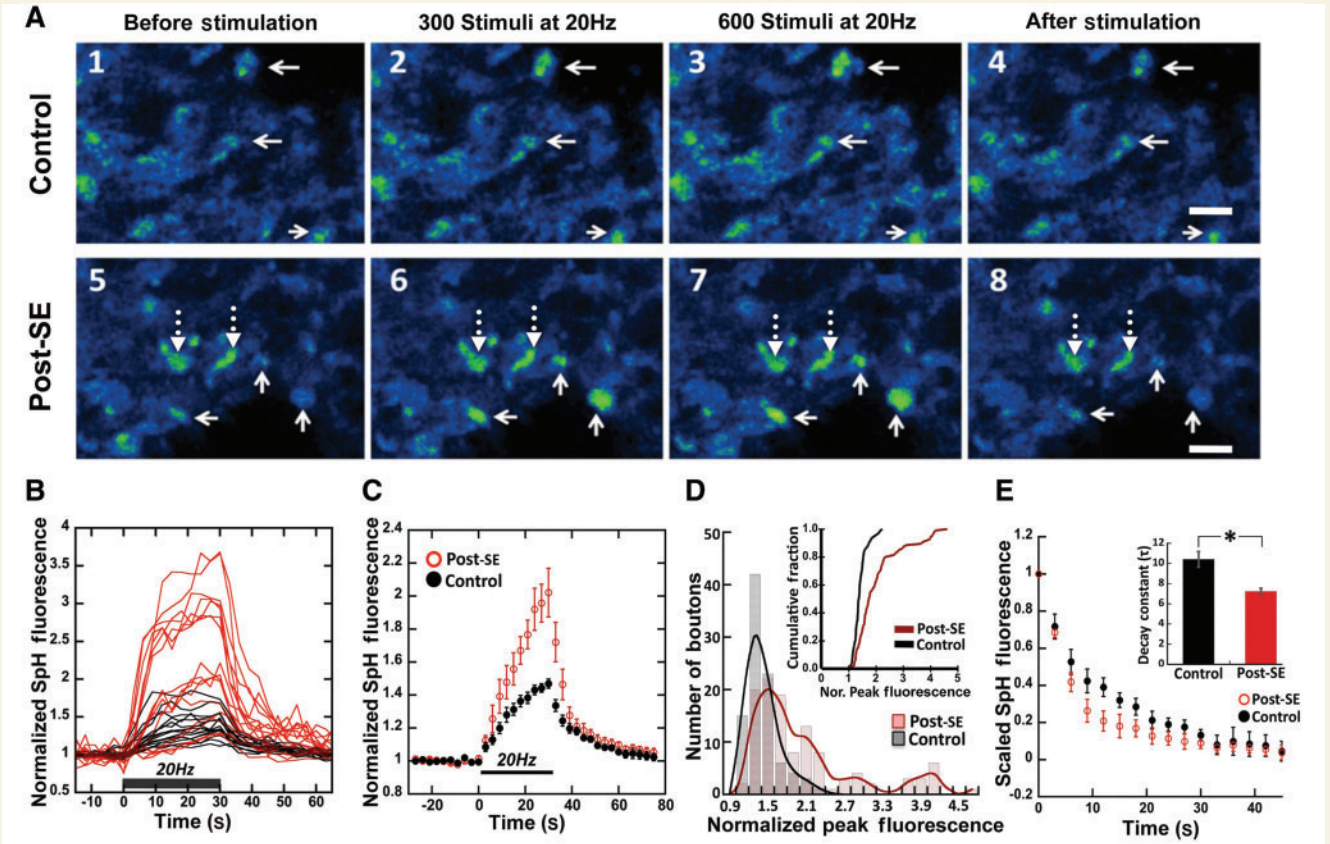

Figure 4 Pilocarpine-induced status epilepticus (SE) enhances vesicular release and endocytosis at mossy fibre terminals in CA3 stratum lucidum. (**A**) Time-lapse two-photon images from control and post-status epilepticus SpH-expressing MFBs in the proximal apical dendritic region of field CA3. Solid arrows indicate puncta that showed activity-dependent fluorescence changes during a 600 pulse/20 Hz stimulus train. The broken arrows in (**A**, *bottom* row) show there were some slowly fluorescing boutons in the epileptic slices. (**B**) Representative time course of normalized fluorescence intensity of individual boutons from a control (black traces) and a post-status epilepticus (red traces) slice in response to the 600 pulse/20 Hz mossy fibre stimulation (black bar shows duration of the train). (**C**) Normalized, evoked SpH fluorescence increases in response to a 600 pulse/20 Hz mossy fibre stimulus train, in MFBs from control (filled black circles, $F_{peak} = 1.47 \pm 0.03$, $n = 10$) versus post-status epilepticus (open red circles, $F_{peak} = 2.02 \pm 0.15$, $n = 8$) slices. F_{peak} was significantly increased in post-status epilepticus slices ($P < 0.05$, Student's *t*-test; all values mean ± SEM). (**D**) Frequency distribution histogram of normalized peak SpH fluorescence for all MFBs in post-status epilepticus ($F_{peak} = 1.76 \pm 0.04$, 100/115 puncta and 3.89 ± 0.10, 15/115 puncta) versus control slices ($F_{peak} = 1.41 \pm 0.025$, 93 puncta). Inset is a cumulative histogram of normalized peak SpH fluorescence, $P < 0.001$, Kolmogorov–Smirnov test. (**E**) Mean fluorescence values of scaled SpH fluorescence decay (data normalized to respective peak fluorescence values from (**C**) after cessation of stimulation, control (filled black circles) and post-status epilepticus (open red circles). Inset represents mean ± SEM of individual decay constants derived by a single exponential fit to the SpH fluorescence decay curve. Control (black bar), $\tau = 10.4 \pm 0.77$ s, $n = 67$ and post-status epilepticus (red bar), $\tau = 7.23 \pm 0.32$ s, $n = 133$ (*$P < 0.05$, Student's *t*-test). Scale bar: **A** = 5 μm.

To measure presynaptic spontaneous release from the RRP, we loaded FM1-43 by hypertonic shock (800 mOsm/20 s), followed by bath application of tetrodotoxin (1 μM), and extracellular [K^+] raised to 15 mM [K^+]o (*High[K+]o*) to facilitate action potential-independent release (Axmacher *et al.*, 2004). To mark the early phase of action potential-independent release, we monitored the magnitude of FM1-43 destaining within the first 4.5 min of *High[K+]o* application (Fig. 5D), which showed no significant difference between control (~15%) and post-status epilepticus (~20%) MFBs ($P > 0.20$, Student's *t*-test). To determine whether steady-state spontaneous release was altered, we examined the late phase of spontaneous release 10–25 min after application of *High[K+]o* (Fig. 5E). As in the early phase, there was no significant difference between the two groups after 25 min of *High[K+]o*, indicating action potential dependent and independent vesicular release from the RRP are differentially regulated in the post-status epilepticus state.

Status epilepticus elicits long-term ultrastructural reorganization of active zones in rat mossy fibre boutons

Previous literature has shown clear correlations between release probability and synapse morphological parameters such as sizes of the RRP (Dobrunz and Stevens, 1997) and rapidly-recycling

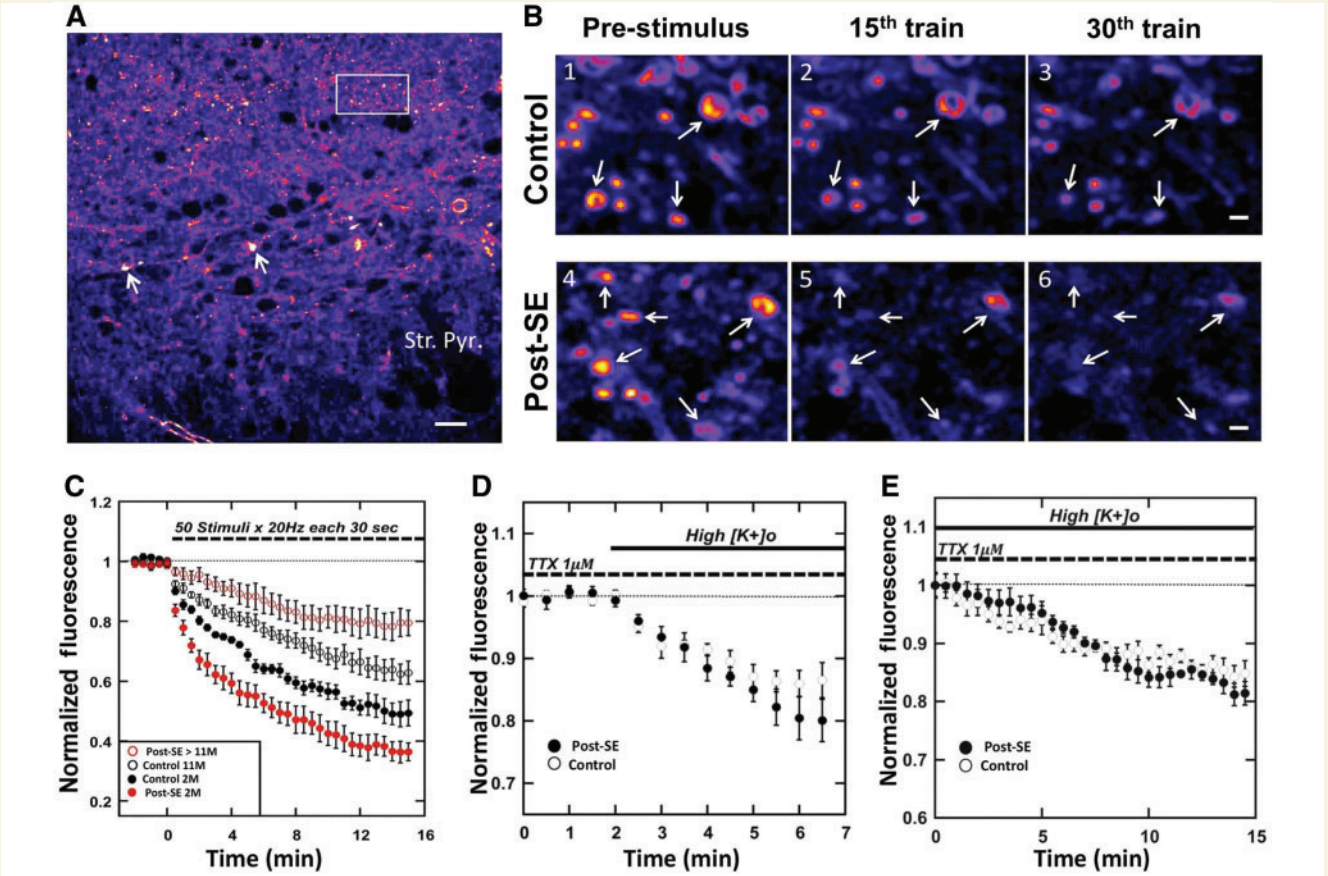

Figure 5 Pilocarpine-induced status epilepticus (SE) enhances evoked, but not action potential independent, presynaptic vesicular release of FM1-43 from the RRP in MFBs. (**A**) Two-photon image of a control field CA3 showing FM1-43 loaded RRP of MFBs. The solid arrows show staining of giant mossy fibre terminals in the proximal region of CA3 stratum lucidum. The rectangular box outlines FM1-43 staining of puncta distal to the CA3 pyramidal cell bodies and much smaller in size, likely to be associational-commissural synapses. (**B**) Representative time-lapse images of FM1-43 destaining from the RRP using repetitive mossy fibre stimulus bursts (50 stimuli/20 Hz each 30 s) to evoke release from MFBs in control and 2-month post-SE slices, respectively. [**B** (1 and 4)] Pre-stimulus baseline fluorescence, [(**B** (2 and 5)] fluorescence intensity after 15 trains, and [**B** (3 and 6)] fluorescence intensity after 30 trains of mossy fibre stimulation. Solid arrows indicate regions of interest $>2\,\mu m$ in diameter that showed robust stimulus dependent FM1-43 destaining. (**C**) Time course of FM1-43 destaining of MFBs in 1–2 months (2 M) post-SE slices (filled red circles, 0.36 ± 0.03, $n = 6$), aged-matched controls (filled black circles, 0.49 ± 0.04, $n = 5$), >11 month (11 M) post-SE slices (open red circles, 0.79 ± 0.04, $n = 5$) and aged-matched controls (open black circles, 0.62 ± 0.04, $n = 6$). All points are mean ± SEM of normalized fluorescence decay at 30th stimulus burst. $P < 0.05$, Student's *t*-test. (**D**) Time course of first 4.5 min of action potential independent FM1-43 destaining in presence of tetrodotoxin (TTX; 1 μm) and 15 mM [K+]o from the RRP in MFBs of 1–2 months post-SE slices (filled circles, $n = 4$) and aged matched control (open circles, $n = 5$) slices (all points are mean ± SEM). Decay after 4.5 min in *High[K+]o*: Control = 0.86 ± 0.028 (~14% of pre-stimulus baseline) and post-SE = 0.80 ± 0.034 (~20% of pre-stimulus baseline; $P > 0.20$, Student's *t*-test). (**E**) Late phase of spontaneous release. Time course of renormalized spontaneous FM1-43 destaining after 10–25 min in *High[K+]o*. Control normalized destaining = 0.85 ± 0.02 and post-SE destaining = 0.81 ± 0.02 ($P > 0.20$, Student's *t*-test, all points are mean ± SEM). Scale bars: **A** = 20 μm; **B** = 10 μm.

pools (Murthy *et al.*, 1997), active zone size (Schikorski and Stevens, 1997; Matz *et al.*, 2010) also known as 'release sites', postsynaptic density (Schikorski and Stevens, 1997) and presynaptic bouton size (Matz *et al.*, 2010). Since we found increased release probability post-status epilepticus as measured by both SpH (Fig. 4C) and FM1-43 destaining (Fig. 5C), we examined possible ultrastructural rearrangements in MFBs in CA3 stratum lucidum in post-status epilepticus and age-matched control Sprague–Dawley rats (Fig. 6A).

Transmission electron microscopy shows that large MFBs (2–5 μm in diameter) had multiple active zones facing postsynaptic densities, contained mitochondria of various sizes, and were filled with numerous small and large clear synaptic vesicles distributed throughout the terminal (Fig. 6A), as described previously (Amaral and Dent, 1981; Chicurel and Harris, 1992; Rollenhagen *et al.*, 2007). Asymmetric active zones were distinguished at MFBs synapses by the dense accumulation of synaptic vesicles in close proximity to the presynaptic density and characteristic widening of the synaptic cleft.

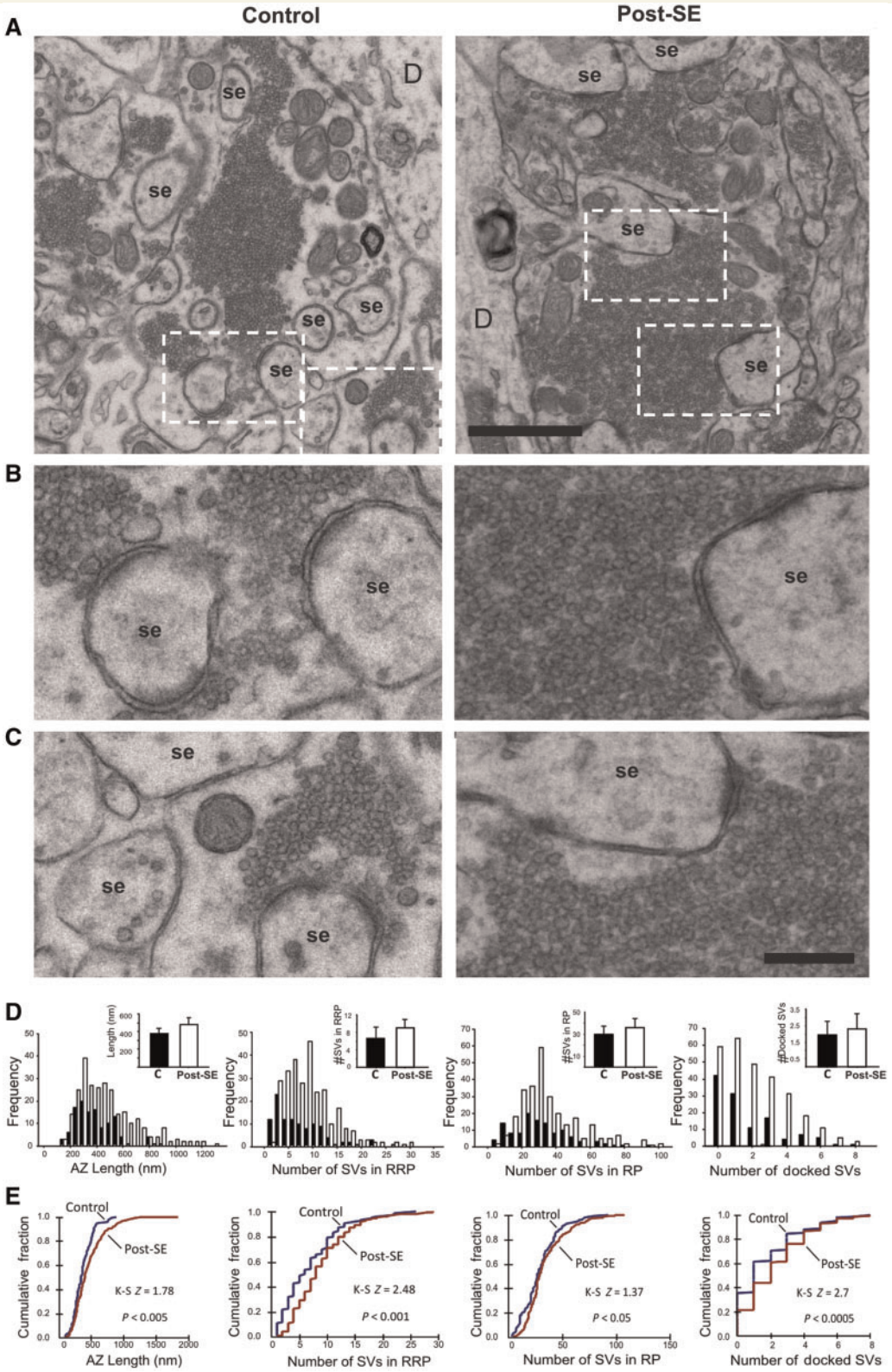

Figure 6 Transmission electron microscopy of active zones (AZ) in MFBs of control and post-status epilepticus (SE) rats. (**A**) Representative transmission electron microscopy images of control (*left*) and post-SE (*right*) MFBs illustrating active zones on synaptic excrescences (se) showing an apparent increase in synaptic vesicle density in post-SE MFBs. Boxed areas are depicted at higher magnification ($\times 4$) in images (**B** and **C**), showing arrangement of vesicles in the active zones of control and post-SE MFBs. Notice the larger density of vesicles and length of active zones in post-SE MFBs. (**D**) Frequency histograms and bar graph representation of data for active zone length, number of synaptic vesicles (SV) in RRP and releasable vesicle pool (RP), and number of docked synaptic vesicles. Notice appearance of increased number of active zones exhibiting larger lengths post-SE (>800 nm). (**E**) Cumulative histograms for these variables in control versus post-SE groups revealed significant rightward shifts toward larger sizes (Kolmogorov–Smirnov (K–S) two-sample test). Scale bars: **A** = 2 μm; **B–E** = 500 nm. D = dendrite.

Table 1 Summary of quantitative analysis of structural variables in active zones of MFBs

	Control, Mean ± SD	Post-status epilepticus, Mean ± SD	Percentage of control	K–S, *P*
Active zone ultrastructural variables				
Length of active zone (nm)	364.91 ± 44.81	485.27 ± 59.63	133.5	*<0.005*
Length of synaptic cleft (nm)	26.93 ± 3.91	29.95 ± 2.46	107.4	*0.31*
PSD area (mm^2)	12.31 ± 3.03	16.90 ± 3.31	136.9	*<0.005*
Number of SVs in RRP	7.43 ± 3.12	8.94 ± 1.78	120.3	*<0.001*
Number of SVs in the releasable pool	31.07 ± 6.05	33.44 ± 7.13	107.6	*<0.05*
Number of docked SVs per active zone	1.96 ± 0.68	2.63 ± 0.56	134.2	*<0.0005*
Docked SVs per active zone length (SV/mm)	5.48 ± 1.75	5.88 ± 0.90	108.9	*<0.05*
Percentage of docked SVs of RRP	27.92 ± 6.45	29.56 ± 3.24	105.85	*0.59*

Measurements were obtained from analysis of active zone variables in MFBs. Statistical comparisons were made using the Kolmogorov–Smirnov (K–S) two-sample test, with statistical significance set at $P < 0.05$. Values are presented as means ± SEM.
PSD = postsynaptic density; SV = synaptic vesicle.

There was a significant increase in number of active zones per MFB in post-status epilepticus rats (130 active zones in six control rats, 5.1 ± 1.36 active zones per MFB; 286 active zones in seven post-status epilepticus rats, 7.7 ± 3.05 active zones per MFB, Student's *t*-test, $P < 0.05$). The number of perforated synapses was also significantly increased in MFBs from post-status epilepticus animals (46 of 286, 16.1%) compared to controls (12 of 130, 9.2%, Student's *t*-test, $P < 0.05$). The majority of electron microscopy variables failed to follow normal distributions, necessitating use of a non-parametric Kolmogorov–Smirnov two-sample test to assess between group differences in distributions. As reported previously (Chicurel and Harris, 1992; Rollenhagen *et al.*, 2007), individual active zones varied substantially in shape and size; both large and small active zones were found in control (104–887 nm) and post-status epilepticus (105–1837 nm) hippocampus. Frequency distributions revealed the presence of a distinct group of synapses of larger length in epileptic animals that was absent in controls (Fig. 6D). A cumulative histogram indicated a significant leftward shift towards larger individual active zone lengths in MFBs post-status epilepticus (Fig. 6E), compared with controls (Table 1, Kolmogorov–Smirnov test, $P < 0.005$). There was also a significant increase in mean postsynaptic density area in the post-status epilepticus group (Table 1) compared to controls (Table 1, Kolmogorov–Smirnov test $P < 0.005$, ~37% increase). In contrast, no significant changes were detected in average synaptic cleft width between control and post-status epilepticus active zones (Table 1).

It has been previously suggested that a rapid refilling of the RRP from a larger releasable vesicle pool is a key mechanism in ensuring fidelity of mossy fibre-CA3 pyramidal cell neurotransmission (Suyama *et al.*, 2007). To determine whether ultrastructural organization of synaptic vesicle pools is altered post-status epilepticus, we measured the number of vesicles docked, within 60 nm of the active zone, 60–200 nm from an active zone, and >200 nm from an active zone, in MFBs of control versus epileptic animals. The RRP was defined as the sum of docked vesicles and those within 60 nm of the active zone, while the releasable pool was defined as vesicles 60–200 nm away from an active zone (Suyama *et al.*, 2007). Compared with controls, post-status epilepticus increased number of docked (+34.2%), RRP (+20.3%), and releasable pool (+7.6%) synaptic vesicles (Fig. 6D and Table 1). A significant difference was detected in the analysis of the cumulative distributions of these variables by Kolmogorov–Smirnov test (Fig. 6E and Table 1). Although the percentage of docked vesicles relative to RRP size was not significantly different (Table 1), the average number of docked vesicles per length of active zone was significantly higher for post-status epilepticus (+8.9%, Table 1). Additionally, the number of synaptic vesicles in each of these pools was significantly correlated with the length of individual active zones in both control (RRP: $r = 0.33$, $P < 0.001$ and releasable pool: $r = 0.41$, $P < 0.001$) and post-status epilepticus MFBs (RRP: $r = 0.57$, $P < 0.001$ and releasable pool: $r = 0.55$, $P < 0.001$, Supplementary Fig. 3).

In order to assess endocytosis, we measured the number and percent of clathrin-coated vesicles 0–200 nm from an active zone (Fig. 7A) and the area of membranous regions apparently internalized at the active zone, indicative of 'bulk endocytosis' (Fig. 7B), in MFBs of control and post-status epilepticus. There were no statistical differences in percent of synapses exhibiting one or two putative clathrin-coated vesicles at active zones between control (22.7 ± 10.1%) and post-status epilepticus (22.0 ± 7.1%, Fig. 7C) animals, or percent synapses exhibiting bulk endocytosis (control: 48.7 ± 13.1%, epileptic: 40.7 ± 15.8%). In contrast, the area of large elliptical or irregular membranous structures at the active zone was significantly higher at MFB synapses post-status epilepticus (5662 ± 385 nm^2) compared with controls (2917 ± 287 nm^2, Kolmogorov–Smirnov test, $P < 0.001$, Fig. 7D), suggesting increased rate of endocytosis.

Taken together, our electron microscopy data show pilocarpine-induced status epilepticus leads to a profound and long-lasting rearrangement of MFB transmitter release sites, resulting in significant increases in number of release sites per MFB, length of individual release sites, and RRP and releasable pool vesicle pools sizes that may underlie persistent increases in functional transmitter vesicular release rates, magnitude and recycling properties.

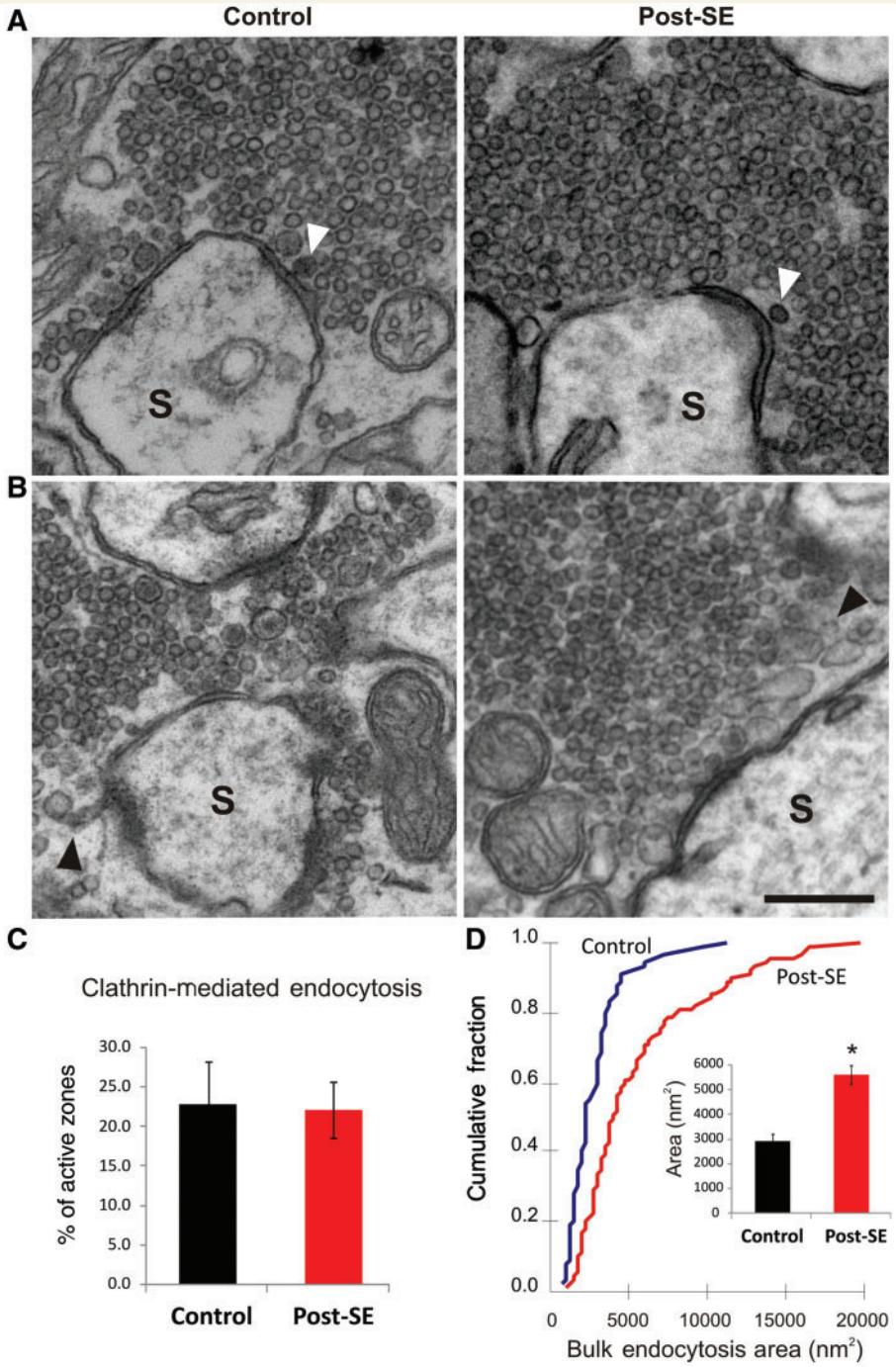

Figure 7 Representative transmission electron microscopy images of active zones in MFBs exhibiting structural signs of clathrin-mediated endocytosis and 'bulk endocytosis' in control versus epileptic rats. (**A**) Putative clathrin-coated (dark) vesicles (white arrowheads) located proximal to presynaptic membrane active zones synapsing on spines (S) of control and post-status epilepticus (SE) MFBs. (**B**) Irregular membranous structures (black arrowheads) near active zones on spines were observed in both control and post-SE MFBs. Note these structures were larger in post-SE rats. (**C**) Mean ± SEM% active zones positive for clathrin-coated vesicles, showing no difference in control versus post-SE rats ($P > 0.20$, Student's *t*-test). (**D**) Cumulative histogram plot of bulk endocytosis area showing a significant rightward shift on the size distribution towards larger values in post-SE MFBs (red) compared with controls (blue, $P < 0.001$, Kolmogorov–Smirnov test). Inset: mean area of bulk endocytosis in control (black) versus post-status epilepticus (red) rats (*$P < 0.05$, Student's *t*-test. Scale bars: **A**, **B** = 500 nm.

Discussion

We describe here a set of long-term alterations in presynaptic morphology and synaptic vesicle recycling at mossy fibre-CA3 terminals of rats and mice subjected to pilocarpine-induced status epilepticus, a model of temporal lobe epilepsy that results in spontaneous recurrent seizures within 2 months in ~97% of rats (Leite *et al.*, 1990; Cavalheiro *et al.*, 1991; Mello *et al.*, 1993; Priel *et al.*, 1996) and mice (Cavalheiro *et al.*, 1996; Muller *et al.*, 2009). In rats, the latent period ranges between 1 and 6 weeks (Curia *et al.*, 2008), with the mean latent period between 15–18 days (Leite *et al.*, 1990; Priel *et al.*, 1996), and depends on the duration of status epilepticus, where a 2-h status epilepticus corresponds to about a 7-day long latent period (Goffin *et al.*, 2007). In mice, the latent period is ~14 days (Cavalheiro *et al.*, 1996), therefore, an overwhelming majority of our animals likely developed spontaneous seizures prior to experiments. Observed presynaptic changes include increases in (i) MFB size; (ii) number of release sites per MFB; (iii) number of vesicles in the RRP and releasable pool; (iv) active zone length; (v) action potential-driven vesicular release rate measured with either FM1-43 or in SpH-expressing transgenic mice; and (vi) enhanced vesicle endocytosis. These alterations persisted for at least 1 month following a single sustained status epilepticus.

Functional enhancement in vesicular transmitter release from MFBs correlates well with previously reported structural changes (number of docked synaptic vesicles or the RRP, area of postsynaptic density, active zone length) that track vesicle release probability (Schikorski and Stevens, 1997; Matz *et al.*, 2010), suggesting that the morphological changes are probably components of the response to hyperactivation that underlie enhanced transmitter release. This agrees with a previous report that kainic acid-induced seizures lead to an increase in glutamate release from the RRP and loss of paired pulse facilitation (Goussakov *et al.*, 2000), suggesting that seizures of a variety of causes may lead to persistent increases in basal release probability.

The significant increase we observed in FM1-43 destaining post-status epilepticus and the correlated increase of vesicle pool sizes measured by transmission electron microscopy suggest an increase in both initial release probability and size of the readily releasable and rapidly recycling vesicle pools. Previous reports suggest that the size of the recycling pool is an important determinant of sustainability of release with prolonged activation (Suyama *et al.*, 2007), consistent with the increases we observed post-status epilepticus. While our transmission electron microscopy SpH and Alexa Fluor 594-dextran loading data all indicate that MFBs show increased size and larger numbers of synaptic vesicles for months after status epilepticus; the new population of terminals, with significantly larger size and faster release rate, could be from modification of existing terminals, ectopic MFBs, or both, and remains to be determined. Also, since individual MFBs contain multiple active zones (Hallermann *et al.*, 2003), we cannot tell whether increased release probability at MFBs (Figs 4D and 5C) occurs at the level of individual active zones switching to a high release state, or whether there is a uniform increase in release probability across all active zones. Additional changes such as increases in the number of active zones per bouton and size of the RRP and releasable pool in individual active zones also suggest persistent increase in glutamate release that could be a key contributor to death of CA3 pyramidal neurons characteristic of hippocampal sclerosis. Increases in the density of perforated synapses have been associated with synaptogenesis and post-lesional compensatory plasticity (Itarat and Jones, 1992; Luke *et al.*, 2004; Adkins *et al.*, 2008). Increased incidence of perforated mossy fibre synapses after status epilepticus suggest that synaptic connectivity undergoes structural remodelling favouring synapses, with potentially higher transmission efficiency during the process of epileptogenesis.

Using SpH fluorescence, we derived a decay constant of 10.4 ± 0.77 s for control boutons (Fig. 4E), similar to previous reports of an endocytic time constant of 9.0 ± 5.5 s estimated using capacitance recordings at MFBs (Hallermann *et al.*, 2003). Our observations of accelerated recovery of stimulus-evoked SpH fluorescence in slices from post-status epilepticus mice, but lack of differences between the number of clathrin-coated vesicles in electromicrographs between the post-status epilepticus and control groups, could be due to an enhanced rate of endocytosis that may or may not depend on clathrin, increased local recycling of vesicles to the RRP (Stanton *et al.*, 2003) or to the recycling pool after exocytosis (Wu and Wu, 2009), increase in bulk endocytosis (retrieval of larger membrane area, Table 1) or combinations of the above. Also, tissues used for electromicrographs were not electrically stimulated prior to fixation, and thus do not necessarily reflect activity-dependent endocytic events but, more likely, the steady-state of the presynaptic bouton ultrastructure.

The 1–2 month time point post-status epilepticus used in our experiments corresponds to the period of occurrence of spontaneous seizures in both rats (Leite *et al.*, 1990; Cavalheiro *et al.*, 1991; Priel *et al.*, 1996; Dudek and Sutula, 2007) and mice (Cavalheiro *et al.*, 1996; Muller *et al.*, 2009; Schauwecker, 2012). Interestingly, in contrast to the early increase in MFB release probability, we found that, at very long survival periods post-status epilepticus (11–12 months), rates of MFB release were markedly reduced. The reduced transmitter release from the RRP in these animals could either reflect long-term compensatory changes or dysfunction of presynaptic release machinery. Our observation that action potential independent RRP release rate in tetrodotoxin (1 μm) was not altered by pilocarpine seizures indicates that action potential dependent and independent regulation of the RRP is very different, perhaps due to potentially distinct pools of vesicles and mechanisms between evoked and spontaneous release (Fredj and Burrone, 2009; Chung *et al.*, 2010). We cannot rule out the possibility that new vesicle pools may contribute to action potential independent release of glutamate post-status epilepticus.

Our functional data demonstrating that post-status epilepticus state leads to increased vesicular release and endocytotic rates, and electron microscope data showing increased presynaptic active zone length, membrane invaginations, clathrin-coated vesicles and vesicle pool sizes, are all consistent with the conclusion that post-status epilepticus state is associated with long-term increases in transmitter release from MFBs, and perhaps other glutamatergic terminals. Since brain-derived neurotrophic factor

is highly expressed in presynaptic MFBs (Danzer and McNamara, 2004) and can elicit long-term enhancements in both transmitter release and size of the RRP (Zakharenko *et al.*, 2003; Tyler *et al.*, 2006), neurotrophins seem a likely candidate mediator of these presynaptic alterations.

Whether increase in stimulus evoked release following-status epilepticus results from alterations in Ca^{2+} influx, release of Ca^{2+} from internal stores *per se*, or whether there are downstream changes in SNARE protein sensitivity to Ca^{2+} is not known. A recent study (Pacheco *et al.*, 2008) found that pilocarpine seizures also cause downregulation of large conductance calcium-activated potassium (BK) channels in MFBs, reductions that could slow hyperpolarization and increase terminal Ca^{2+} influx. Levels of the Ca^{2+} buffer calbindin D-28K are also lowered in MFBs after pilocarpine seizures (Carter *et al.*, 2008), a change that could further increase presynaptic Ca^{2+} influx, dysregulate Ca^{2+} homeostasis and promote multivesicular release (Hallermann *et al.*, 2003).

In summary, our study is the first, to our knowledge, using the pilocarpine model of temporal lobe epilepsy in SpH-expressing transgenic mice, a new tool to investigate presynaptic alterations in epilepsy with potential application for other CNS diseases that may involve presynaptic dysfunction. Our studies indicate that the early phase of the pilocarpine model of temporal lobe epilepsy is associated with persistent structural changes in mossy fibre presynaptic terminal size, vesicle pools and active zones that are correlated with functional increases in rates of action potential-driven vesicular release and associated endocytotic recycling. The time course and mechanisms underlying these changes suggests the presynaptic terminal as a novel target for new therapeutics to treat epilepsy, especially temporal lope epilepsy.

Acknowledgements

The authors would like to thank Dr Venkatesh Murthy for providing us with the SpH21 transgenic mice line, Dr Kenichi Miyazaki for help with Alexa Fluor 594 dextran experiments, Mohini Rawat for technical assistance, Dr Pravin Sehgal and Jason Lee for discussions on Otsu thresholding and Dr Xiao-Lei Zhang and John Sullivan for additional helpful discussions.

Funding

National Institutes of Health (grants GM081109, P20 MD001091-06 and NS063950); Department of Defense (grant PR100534 to E.R.G.S.); National Institute of Neurological Diseases and Stroke (grants NS056093 to J.V., NS072966 to L.V. and NS044421 to P.K.S.); Department of Defense (grant PR100534P1 to P.K.S.).

Supplementary material

Supplementary material is available at *Brain* online.

References

Acsady L, Kamondi A, Sik A, Freund T, Buzsaki G. GABAergic cells are the major postsynaptic targets of mossy fibers in the rat hippocampus. J Neurosci 1998; 18: 3386–403.

Adkins DL, Hsu JE, Jones TA. Motor cortical stimulation promotes synaptic plasticity and behavioral improvements following sensorimotor cortex lesions. Exp Neurol 2008; 212: 14–28.

Amaral DG, Dent JA. Development of the mossy fibers of the dentate gyrus: I. A light and electron microscopic study of the mossy fibers and their expansions. J Comp Neurol 1981; 195: 51–86.

Axmacher N, Winterer J, Stanton PK, Draguhn A, Muller W. Two-photon imaging of spontaneous vesicular release in acute brain slices and its modulation by presynaptic GABAA receptors. Neuroimage 2004; 22: 1014–21.

Bailey CP, Nicholls RE, Zhang XL, Zhou ZY, Muller W, Kandel ER, et al. Galpha(i2) inhibition of adenylate cyclase regulates presynaptic activity and unmasks cGMP-dependent long-term depression at Schaffer collateral-CA1 hippocampal synapses. Learn Mem 2008; 15: 261–70.

Bayazitov IT, Richardson RJ, Fricke RG, Zakharenko SS. Slow presynaptic and fast postsynaptic components of compound long-term potentiation. J Neurosci 2007; 27: 11510–21.

Bischofberger J, Engel D, Li L, Geiger JR, Jonas P. Patch-clamp recording from mossy fiber terminals in hippocampal slices. Nat Protoc 2006; 1: 2075–81.

Blackstad TW, Brink K, Hem J, Jeune B. Distribution of hippocampal mossy fibers in the rat. An experimental study with silver impregnation methods. J Comp Neurol 1970; 138: 433–49.

Boulland JL, Ferhat L, Tallak Solbu T, Ferrand N, Chaudhry FA, Storm-Mathisen J, et al. Changes in vesicular transporters for gamma-aminobutyric acid and glutamate reveal vulnerability and reorganization of hippocampal neurons following pilocarpine-induced seizures. J Comp Neurol 2007; 503: 466–85.

Burrone J, Li Z, Murthy VN. Studying vesicle cycling in presynaptic terminals using the genetically encoded probe synaptopHluorin. Nat Protoc 2006; 1: 2970–8.

Calverley RK, Jones DG. Determination of the numerical density of perforated synapses in rat neocortex. Cell Tissue Res 1987; 248: 399–407.

Carter DS, Harrison AJ, Falenski KW, Blair RE, DeLorenzo RJ. Long-term decrease in calbindin-D28K expression in the hippocampus of epileptic rats following pilocarpine-induced status epilepticus. Epilepsy Res 2008; 79: 213–23.

Cavalheiro EA. The pilocarpine model of epilepsy. Ital J Neurol Sci 1995; 16: 33–7.

Cavalheiro EA, Leite JP, Bortolotto ZA, Turski WA, Ikonomidou C, Turski L. Long-term effects of pilocarpine in rats: structural damage of the brain triggers kindling and spontaneous recurrent seizures. Epilepsia 1991; 32: 778–82.

Cavalheiro EA, Santos NF, Priel MR. The pilocarpine model of epilepsy in mice. Epilepsia 1996; 37: 1015–9.

Cavazos JE, Zhang P, Qazi R, Sutula TP. Ultrastructural features of sprouted mossy fiber synapses in kindled and kainic acid-treated rats. J Comp Neurol 2003; 458: 272–92.

Chicurel ME, Harris KM. Three-dimensional analysis of the structure and composition of CA3 branched dendritic spines and their synaptic relationships with mossy fiber boutons in the rat hippocampus. J Comp Neurol 1992; 325: 169–82.

Chung C, Barylko B, Leitz J, Liu X, Kavalali ET. Acute dynamin inhibition dissects synaptic vesicle recycling pathways that drive spontaneous and evoked neurotransmission. J Neurosci 2010; 30: 1363–76.

Claiborne BJ, Amaral DG, Cowan WM. A light and electron microscopic analysis of the mossy fibers of the rat dentate gyrus. J Comp Neurol 1986; 246: 435–58.

Coulter DA. Mossy fiber zinc and temporal lobe epilepsy: pathological association with altered "epileptic" gamma-aminobutyric acid A receptors in dentate granule cells. Epilepsia 2000; 41 (Suppl 6): S96–9.

Curia G, Longo D, Biagini G, Jones RS, Avoli M. The pilocarpine model of temporal lobe epilepsy. J Neurosci Methods 2008; 172: 143–57.

Danzer SC, He X, Loepke AW, McNamara JO. Structural plasticity of dentate granule cell mossy fibers during the development of limbic epilepsy. Hippocampus 2010; 20: 113–24.

Danzer SC, McNamara JO. Localization of brain-derived neurotrophic factor to distinct terminals of mossy fiber axons implies regulation of both excitation and feedforward inhibition of CA3 pyramidal cells. J Neurosci 2004; 24: 11346–55.

Dobrunz LE, Stevens CF. Heterogeneity of release probability, facilitation, and depletion at central synapses. Neuron 1997; 18: 995–1008.

Dudek FE, Sutula TP. Epileptogenesis in the dentate gyrus: a critical perspective. Prog Brain Res 2007; 163: 755–73.

Epsztein J, Represa A, Jorquera I, Ben-Ari Y, Crepel V. Recurrent mossy fibers establish aberrant kainate receptor-operated synapses on granule cells from epileptic rats. J Neurosci 2005; 25: 8229–39.

Esclapez M, Hirsch JC, Ben-Ari Y, Bernard C. Newly formed excitatory pathways provide a substrate for hyperexcitability in experimental temporal lobe epilepsy. J Comp Neurol 1999; 408: 449–60.

Fredj NB, Burrone J. A resting pool of vesicles is responsible for spontaneous vesicle fusion at the synapse. Nat Neurosci 2009; 12: 751–8.

Frotscher M, Jonas P, Sloviter RS. Synapses formed by normal and abnormal hippocampal mossy fibers. Cell Tissue Res 2006; 326: 361–7.

Galimberti I, Gogolla N, Alberi S, Santos AF, Muller D, Caroni P. Long-term rearrangements of hippocampal mossy fiber terminal connectivity in the adult regulated by experience. Neuron 2006; 50: 749–63.

Goffin K, Nissinen J, Van Laere K, Pitkanen A. Cyclicity of spontaneous recurrent seizures in pilocarpine model of temporal lobe epilepsy in rat. Exp Neurol 2007; 205: 501–5.

Gorter JA, Goncalves Pereira PM, van Vliet EA, Aronica E, Lopes da Silva FH, Lucassen PJ. Neuronal cell death in a rat model for mesial temporal lobe epilepsy is induced by the initial status epilepticus and not by later repeated spontaneous seizures. Epilepsia 2003; 44: 647–58.

Gorter JA, Van Vliet EA, Proper EA, De Graan PN, Ghijsen WE, Lopes Da Silva FH, et al. Glutamate transporter alterations in the reorganizing dentate gyrus are associated with progressive seizure activity in chronic epileptic rats. J Comp Neurol 2002; 442: 365–77.

Goussakov IV, Fink K, Elger CE, Beck H. Metaplasticity of mossy fiber synaptic transmission involves altered release probability. J Neurosci 2000; 20: 3434–41.

Hallermann S, Pawlu C, Jonas P, Heckmann M. A large pool of releasable vesicles in a cortical glutamatergic synapse. Proc Natl Acad Sci USA 2003; 100: 8975–80.

Hovorka J, Langmeier M, Mares P. Are there morphological changes in presynaptic terminals of kindled rats? Neurosci Lett 1989; 107: 179–83.

Itarat W, Jones DG. Perforated synapses are present during synaptogenesis in rat neocortex. Synapse 1992; 11: 279–86.

Lee JE, Patel K, Almodovar S, Tuder RM, Flores SC, Sehgal PB. Dependence of Golgi apparatus integrity on nitric oxide in vascular cells: implications in pulmonary arterial hypertension. Am J Physiol Heart Circ Physiol 2011; 300: H1141–58.

Leite JP, Bortolotto ZA, Cavalheiro EA. Spontaneous recurrent seizures in rats: an experimental model of partial epilepsy. Neurosci Biobehav Rev 1990; 14: 511–7.

Li Z, Burrone J, Tyler WJ, Hartman KN, Albeanu DF, Murthy VN. Synaptic vesicle recycling studied in transgenic mice expressing synaptopHluorin. Proc Natl Acad Sci USA 2005; 102: 6131–6.

Luke LM, Allred RP, Jones TA. Unilateral ischemic sensorimotor cortical damage induces contralesional synaptogenesis and enhances skilled reaching with the ipsilateral forelimb in adult male rats. Synapse 2004; 54: 187–99.

Matz J, Gilyan A, Kolar A, McCarvill T, Krueger SR. Rapid structural alterations of the active zone lead to sustained changes in neurotransmitter release. Proc Natl Acad Sci USA 2010; 107: 8836–41.

McNamara JO. Cellular and molecular basis of epilepsy. J Neurosci 1994; 14: 3413–25.

Mello LE, Cavalheiro EA, Tan AM, Kupfer WR, Pretorius JK, Babb TL, et al. Circuit mechanisms of seizures in the pilocarpine model of chronic epilepsy: cell loss and mossy fiber sprouting. Epilepsia 1993; 34: 985–95.

Meunier FA, Nguyen TH, Colasante C, Luo F, Sullivan RK, Lavidis NA, et al. Sustained synaptic-vesicle recycling by bulk endocytosis contributes to the maintenance of high-rate neurotransmitter release stimulated by glycerotoxin. J Cell Sci 2010; 123 (Pt 7): 1131–40.

Miesenbock G, De Angelis DA, Rothman JE. Visualizing secretion and synaptic transmission with pH-sensitive green fluorescent proteins. Nature 1998; 394: 192–5.

Miranda R, Nudel U, Laroche S, Vaillend C. Altered presynaptic ultrastructure in excitatory hippocampal synapses of mice lacking dystrophins Dp427 or Dp71. Neurobiol Dis 2011; 43: 134–41.

Muller CJ, Bankstahl M, Groticke I, Loscher W. Pilocarpine vs. lithium-pilocarpine for induction of status epilepticus in mice: development of spontaneous seizures, behavioral alterations and neuronal damage. Eur J Pharmacol 2009; 619: 15–24.

Murthy VN, Sejnowski TJ, Stevens CF. Heterogeneous release properties of visualized individual hippocampal synapses. Neuron 1997; 18: 599–612.

Pacheco Otalora LF, Couoh J, Shigamoto R, Zarei MM, Garrido Sanabria ER. Abnormal mGluR2/3 expression in the perforant path termination zones and mossy fibers of chronically epileptic rats. Brain Res 2006; 1098: 170–85.

Pacheco Otalora LF, Hernandez EF, Arshadmansab MF, Francisco S, Willis M, Ermolinsky B, et al. Down-regulation of BK channel expression in the pilocarpine model of temporal lobe epilepsy. Brain Res 2008; 1200: 116–31.

Priel MR, dos Santos NF, Cavalheiro EA. Developmental aspects of the pilocarpine model of epilepsy. Epilepsy Res 1996; 26: 115–21.

Pyle JL, Kavalali ET, Choi S, Tsien RW. Visualization of synaptic activity in hippocampal slices with FM1-43 enabled by fluorescence quenching. Neuron 1999; 24: 803–8.

Rollenhagen A, Satzler K, Rodriguez EP, Jonas P, Frotscher M, Lubke JH. Structural determinants of transmission at large hippocampal mossy fiber synapses. J Neurosci 2007; 27: 10434–44.

Sankaranarayanan S, Ryan TA. Real-time measurements of vesicle-SNARE recycling in synapses of the central nervous system. Nat Cell Biol 2000; 2: 197–204.

Schauwecker PE. Strain differences in seizure-induced cell death following pilocarpine-induced status epilepticus. Neurobiol Dis 2012; 45: 297–304.

Schikorski T, Stevens CF. Quantitative ultrastructural analysis of hippocampal excitatory synapses. J Neurosci 1997; 17: 5858–67.

Stanton PK, Winterer J, Bailey CP, Kyrozis A, Raginov I, Laube G, et al. Long-term depression of presynaptic release from the readily releasable vesicle pool induced by NMDA receptor-dependent retrograde nitric oxide. J Neurosci 2003; 23: 5936–44.

Stanton PK, Winterer J, Zhang XL, Muller W. Imaging LTP of presynaptic release of FM1-43 from the rapidly recycling vesicle pool of Schaffer collateral-CA1 synapses in rat hippocampal slices. Eur J Neurosci 2005; 22: 2451–61.

Suyama S, Hikima T, Sakagami H, Ishizuka T, Yawo H. Synaptic vesicle dynamics in the mossy fiber-CA3 presynaptic terminals of mouse hippocampus. Neurosci Res 2007; 59: 481–90.

Turski WA, Cavalheiro EA, Bortolotto ZA, Mello LM, Schwarz M, Turski L. Seizures produced by pilocarpine in mice: a behavioral, electroencephalographic and morphological analysis. Brain Res 1984; 321: 237–53.

Tyler WJ, Zhang XL, Hartman K, Winterer J, Muller W, Stanton PK, et al. BDNF increases release probability and the size of a rapidly recycling vesicle pool within rat hippocampal excitatory synapses. J Physiol 2006; 574 (Pt 3): 787–803.

Wenzel HJ, Woolley CS, Robbins CA, Schwartzkroin PA. Kainic acid-induced mossy fiber sprouting and synapse formation in the dentate gyrus of rats. Hippocampus 2000; 10: 244–60.

Winterer J, Stanton PK, Muller W. Direct monitoring of vesicular release and uptake in brain slices by multiphoton excitation of the styryl dye FM 1-43. Biotechniques 2006; 40: 343–51.

Wu XS, Wu LG. Rapid endocytosis does not recycle vesicles within the readily releasable pool. J Neurosci 2009; 29: 11038–42.

Xiong ZQ, Stringer JL. Extracellular pH responses in CA1 and the dentate gyrus during electrical stimulation, seizure discharges, and spreading depression. J Neurophysiol 2000; 83: 3519–24.

Zakharenko SS, Patterson SL, Dragatsis I, Zeitlin SO, Siegelbaum SA, Kandel ER, et al. Presynaptic BDNF required for a presynaptic but not postsynaptic component of LTP at hippocampal CA1-CA3 synapses. Neuron 2003; 39: 975–90.

Zhang S, Khanna S, Tang FR. Patterns of hippocampal neuronal loss and axon reorganization of the dentate gyrus in the mouse pilocarpine model of temporal lobe epilepsy. J Neurosci Res 2009; 87: 1135–49.

Year 1

Abnormal function and reorganization of presynaptic nanocomponents in experimental epilepsy: A multiphoton laser scanning confocal imaging and transmission electron microscopy study. Upreti C, Skinner F, Otero R, Thakker R, Rosas G, Partida C, Pacheco LF, Jones TA, Romanovicz D, Stanton PK and **Garrido-Sanabria** ER. *3rd Meeting of the American Society for Nanomedicine,* Rockville, MD, Nov 9-11, 2011.

Mesial temporal lobe epilepsy (MTLE) is characterized by hyperexcitability of hippocampal networks leading to partial/complex seizures. It has been widely demonstrated that the mossy fiber pathway in the hippocampus undergo seizure-related structural and molecular rearrangements during epileptogenesis. Such synaptic reorganization and abnormal sprouting are thought to play a critical role in the development of recurrent excitatory circuits, hyperexcitability and ultimately seizures in MTLE. Although many studies have described abnormalities mossy fiber boutons (MFBs) and their newly formed excitatory synapses onto granule cell dendrites little is known about the functional and ultrastructural changes in the presynaptic release machinery occurring in the MFBs contacting the CA3 pyramidal cells targets. By using two-photon laser scanning confocal microscopy (2P-LSCM) and transmission electron microscopy (TEM) we assessed whether the organization of synaptic vesicle pools at MFBs synapses contacting spines in the CA3 region are disturbed during epileptogenesis. For functional imaging, SpH mice were seized by treated with pilocarpine and acute hippocampal slices were made 1-2 months after induction of status epilepticus. A 20Hz 600 stimuli train in the stratum lucidum was used to induce presynaptic responses in MFB. The stimulus train evoked, normalized peak SpH fluorescence in MFB's from epileptic slices was significantly higher than control boutons (epileptic: 2.02 ± 0.15, n=8 and control: 1.47 ± 0.03, n=10). Upon plotting a frequency distribution histogram of just the peak fluorescence attained at the end of the stimulus train the control showed a normal distribution (mean normalized fluorescence: 1.41 ± 0.025) while the epiletic boutons showed a bimodal distribution ($Mean_1$: 1.76 ± 0.04 and $Mean_2$: 3.89 ± 0.10; $p<0.05$) suggesting at least two different functional vesicle populations. Additionally, since the decay of SpH fluorescence is a function of the rate of endocytosis, single exponential decay fits to the SpH fluorescence decay after cessation of stimulation showed epileptic boutons to have a significantly faster rate of endocytosis (tau=10.4 ± 0.76sec) vs control (tau=7.2±0.32sec, $p<0.05$). This suggests that epileptic boutons are likely to replenish their recycling and readily releasable pools faster than control boutons. The significant increase in the evoked SpH fluorescence can be explained by either an increase in release probability, increase in the pool size or both. To directly estimate changes in vesicle pool size in epileptogenesis, we performed transmission electron microscopy (TEM) from six age-matched controls and seven chronically epileptic Sprague Dawley rats that were sacrificed 3-6 months after pilocarpine-induced *status epilepticus*. TEM images were acquired from the *stratum lucidum* of CA3 region to visualize the ultrastructural details of MFBs. Analysis of several presynaptic and postsynaptic morphological variables on MFB release sites were performed using NIH ImageJ. Kolgomorov-Smirnov two-sample statistics revealed that the cumulative fraction distributions of several variables were significantly different between control and epileptic MFBs including: length of the active zones (AZ), number of synaptic vesicles (SVs) in the readily releasable pool (RRP) and recycling pool (RP), number of docked SVs, density of SVs in the RRP and RP, area of the post-synaptic density (PSD), area and perimeter of SVs in the RRP and RP. The length of the active zones (AZs) was significantly 35% longer in synapses from epileptic rats, while the number of SVs in the RRP and RP at MFB active sites were significantly increased in chronically epileptic rats. Analysis of the frequency histogram indicates that a new population of active zones with large length appeared in MFBs of epileptic rats. These findings suggest seizure-related remodeling and abnormal plasticity of presynaptic and postsynaptic elements in mossy fiber-CA3 pyramidal cell synapses during the course of epileptogenesis. Increased length of AZs and larger number of SVs in the RRP and RP may lead to enhanced release of glutamate during activation of the mossy fiber pathway. We speculate that together with molecular changes, ultrastructural plasticity of the presynaptic release machinery and corresponding PSDs play a critical in the pathogenesis of MTLE.

Abnormalities in presynaptic vesicle pools of mossy fiber boutons in the pilocarpine model of mesial temporal lobe epilepsy. Upreti PK, Stanton E, **Garrido-Sanabria ER**. Poster. 779.10/Z13 *Society for Neuroscience Meeting*, Washington, Nov 16, 2011.

Mesial temporal lobe epilepsy (MTLE) is characterized by hyperexcitability of hippocampal networks leading to partial/complex seizures. It has been widely demonstrated that the mossy fiber pathway in the hippocampus undergo seizure-related structural and molecular rearrangements during epileptogenesis. Such synaptic reorganization and abnormal sprouting are thought to play a critical role in the development of recurrent excitatory circuits, hyperexcitability and ultimately seizures in MTLE. Previous studies have investigate the contribution of seizure-related changes on intrinsic properties and postsynaptic mechanisms on the pathophysiology of MTLE> Although many studies have described abnormalities mossy fiber boutons (MFBs) and their newly formed excitatory synapses onto granule cell dendrites little is known about the functional and ultrastructural changes in the presynaptic release machinery occurring in the MFBs contacting the CA3 pyramidal cells targets. By using two-photon laser scanning confocal microscopy (2P-LSCM) and transmission electron microscopy (TEM) we assessed whether the organization of synaptic vesicle pools at MFBs synapses contacting spines in the CA3 region are disturbed during epileptogenesis. For functional imaging, SpH mice were seized by treated with pilocarpine and acute hippocampal slices were made 1-2 months after induction of status epilepticus. A 20Hz 600 stimuli train in the stratum lucidum was used to induce presynaptic responses in MFB. The stimulus train evoked, normalized peak SpH fluorescence in MFB's from epileptic slices was significantly higher than control boutons (epileptic: 2.02 ± 0.15, n=8 and control: 1.47±0.03, n=10). Upon plotting a frequency distribution histogram of just the peak fluorescence attained at the end of the stimulus train the control showed a normal distribution (mean normalized fluorescence: 1.41 ± 0.025) while the epiletic boutons showed a bimodal distribution ($Mean_1$: 1.76 ± 0.04 and $Mean_2$: 3.89 ± 0.10; $p<0.05$) suggesting at least two different functional vesicle populations. Additionally, since the decay of SpH fluorescence is a function of the rate of endocytosis, single exponential decay fits to the SpH fluorescence decay after cessation of stimulation showed epileptic boutons to have a significantly faster rate of endocytosis (tau=10.4 ± 0.76sec) vs control (tau=7.2±0.32sec, $p<0.05$). This suggests that epileptic boutons are likely to replenish their recycling and readily releasable pools faster than control boutons. The significant increase in the evoked SpH fluorescence can be explained by either an increase in release probability, increase in the pool size or both. To directly estimate changes in vesicle pool size in epileptogenesis, we performed transmission electron microscopy (TEM) from six age-matched controls and seven chronically epileptic Sprague Dawley rats that were sacrificed 3-6 months after pilocarpine-induced *status epilepticus*. TEM images were acquired from the *stratum lucidum* of CA3 region to visualize the ultrastructural details of MFBs. Analysis of several presynaptic and postsynaptic morphological variables on MFB release sites were performed using NIH ImageJ. Kolgomorov-Smirnov two-sample statistics revealed that the cumulative fraction distributions of several variables were significantly different between control and epileptic MFBs including: length of the active zones (AZ), number of synaptic vesicles (SVs) in the readily releasable pool (RRP) and recycling pool (RP), number of docked SVs, density of SVs in the RRP and RP, area of the post-synaptic density (PSD), area and perimeter of SVs in the RRP and RP. The length of the active zones (AZs) was significantly 35% longer in synapses from epileptic rats (Student-T test, $P<0.05$) while the number of SVs in the RRP and RP at MFB active sites were significantly increased in chronically epileptic rats. Analysis of the frequency histogram indicates that a new population of active zones with large length appeared in MFBs of epileptic rats. These findings suggest seizure-related remodeling and abnormal plasticity of presynaptic and postsynaptic elements in mossy fiber-CA3 pyramidal cell synapses during the course of epileptogenesis. Increased length of AZs and larger number of SVs in the RRP and RP may lead to enhanced release of glutamate during activation of the mossy fiber pathway. We speculate that together with molecular changes, ultrastructural plasticity of the presynaptic release machinery and corresponding PSDs play a critical in the pathogenesis of MTLE.

Abnormal functional and ultrastructural changes of synaptic vesicle pools at active zones in mossy fiber boutons in mesial temporal lobe epilepsy, (ID: 1149994), Upreti C, **Garrido-Sanabria ER**, Stanton PK, presented at the *65th America Epilepsy Society Annual Meeting*, Baltimore, December 2-6, 2011.

Hippocampal mossy fibers exhibit complex structural rearrangements and abnormal synaptic function in mesial temporal lobe epilepsy (MTLE). During epileptogenesis, axons of dentate gyrus granule cells sprout and establish new excitatory synapses onto abnormal targets, including granule cells, interneurons, and basal dendrites of CA3 pyramidal neurons Such synaptic reorganization and abnormal sprouting are thought to play a critical role in the development of recurrent excitatory circuits, hyperexcitability and ultimately seizures in MTLE. While many studies have shown alterations in postsynaptic function of both excitatory and inhibitory circuits in MTLE, far less attention has been paid to the role of presynaptic dysfunction in the pathogenesis of epilepsy. By using two-photon laser scanning confocal microscopic imaging of presynaptic vesicular release in mice expressing a fusion protein of green fluorescent protein and the SNARE protein synaptobrevin (SynaptopHluorin, SpH), we assessed whether the organization of functional synaptic vesicle pools at dentate granule cell mossy fiber bouton (MFB) synapses contacting spines in the CA3 region is altered in chronic pilocarpine-induced epilepsy. A 20Hz/600 mossy fiber stimulus train evoked peak SpH fluorescence in MFB's from epileptic slices significantly higher than control MFB (epileptic 2.02 ± 0.15, n=8; control 1.47 ± 0.03, n=10, $P<0.05$). Control MFB peak fluorescence at the end of the stimulus train showed a normal distribution (mean normalized fluorescence = 1.41 ± 0.025), while MFB in slices from epileptic mice showed a bimodal ($\bar{x}_1$ = 1.76 ± 0.04 and $\bar{x}_2$ = 3.89 ± 0.10; $P<0.05$) suggesting two different functional vesicle pools. A single exponential decay fit to SpH fluorescence decay after cessation of stimulation showed epileptic MFB had significantly faster rates of endocytosis (τ = 7.2 ± 0.32s) compared to control MFB (τ = 10.4 ± 0.76s, $P<0.05$). Neurotransmitter release from the MFB readily-releasable vesicle pool (RRP) was estimated by destaining kinetics of the styryl dye FM1-43 selectively loaded into MFB RRP by hypertonic shock. FM1-43 destaining from the RRP was significantly faster from MFB of 1-2 month chronic epileptic animals compared to controls ($P<0.05$). In contrast, FM1-43 destaining was significantly slower in MFB of >11 chronic epileptic rat slices compared to age matched controls. These findings suggest seizure-related plasticity of presynaptic elements in mossy fiber-CA3 pyramidal cell synapses during the course of epileptogenesis leads to enhanced neurotransmitter release and vesicle recycling in an early phase of chronic epilepsy, but later exhibits reduced rates of release, perhaps due to either compensatory changes or widespread presynaptic damage. Finally, data utilizing MFB calcium imaging will be presented to separately investigate alterations in MFB calcium influx and homeostasis, versus alterations in vesicular release mechanisms downstream of calcium. Our findings indicate that persistent alterations in presynaptic vesicular exocytosis and endocytosis correlate with structural plasticity of MFB terminals at mossy fiber-CA3 synapses in chronic epilepsy, suggesting an under appreciated role in development of MTLE.

Abnormal Ultrastructure of Large Mossy Fiber Boutons-CA3 pyramidal Cell Synapses in Mesial Temporal Lobe Epilepsy. (ID: 1150094). **Garrido-Sanabria ER**, Otero R, Thakker R, Partida C, Skinner F, Jones T, Romanovicz D, Upreti C, Stanton PK., presented at the *65th America Epilepsy Society Annual Meeting*, Baltimore, December, 2011.

Medial temporal lobe epilepsy (MTLE) is characterized by defective inhibition and enhanced glutamatergic transmission, resulting in persistent hyperexcitability and neurodegeneration of neurons in hippocampal circuits. Numerous studies indicate that structural and molecular rearrangements of synaptic circuits, specifically in the hippocampal mossy fiber pathway play a critical role in epileptogenesis. However, there is limited information on the function of mossy fiber presynaptic boutons in MTLE. By using two-photon laser scanning microscopy, we investigated whether presynaptic vesicular transmitter release at mossy fiber boutons (MFBs) is altered during epileptogenesis in the pilocarpine model of MTLE. Two complementary experimental paradigms were employed. In the first experiment, the readily-releasable pool (RRP) of synaptic vesicles (SVs) at MFBs was loaded (800 mOsm ACSF + sucrose/30 sec) with the fluorescent styryl dye FM1-43 in acutely dissociated hippocampal slices from control or pilocarpine-treated chronic epileptic rats. In the second experiment, MTLE was induced by the pilocarpine model in transgenic mice expressing SynaptopHfluorin (SpH), a pH-sensitive GFP conjugated to the luminal domain of the vesicle-associated protein synaptobrevin, at glutamatergic synapses. In both experiments, SV release was triggered by repetitive electrical stimulation of the mossy fiber pathway (10-20Hz/50-300 action potentials). We observed a long-lasting potentiation of the rate of release of FM1-43 from mossy fiber presynaptic terminals that persisted in hippocampal slices for at least 2 months after pilocarpine-induced status epilepticus (SE). SpH mice subjected to pilocarpine-induced SE also exhibited significant and detectable increases in vesicular release rate, as well as detectable sprouting (synaptic rearrangement) of MF terminals into abnormal locations in stratum pyramidale and oriens of field CA3. Interestingly, these data also showed that the abnormally sprouted MF terminals behaved differently in their vesicular release properties, exhibiting slower release and faster decay of fluorescence back to baseline, suggesting reduced release and/or more rapid endocytotic vesicle recycling upon action potential-evoked release. These findings indicate the appearance of abnormal presynaptic function (enhanced SV release) associated with reorganization of the mossy fiber pathway in the hippocampus during epileptogenesis. Pharmacological agents that reduce or prevent these presynaptic changes could be effective anti-epileptic or anti-epileptogenic drugs, especially in drug-resistant epilepsies where other treatments have failed.

Year 2

Levetiracetam inhibits excitatory drive onto dentate gyrus granule cells: Effects of SV2A gene dosage and pilocarpine-induced epilepsy. **E. G. Sanabria,** L. F. Pacheco, L. M. Rambo, J. M. Rodriguez, C. Upreti, **P. K. Stanton**. Society for Neuroscience Meeting, New Orleans, LA, October 13 - 17, 2012.

Levetiracetam (Keppra®, LEV) is a new class of antiepileptic drug exhibiting selective seizure protection in chronic animal models of epilepsy. Compelling experimental evidences indicate a presynaptic action site for LEV. For instance, LEV binds to the synaptic vesicle protein SV2A and LEV can modulate excitatory transmission by a mechanism depending on the inhibition of presynaptic Ca^{2+} channels. However, it is also known that LEV targets SV2A undergo down-regulation during epileptogenesis in animal models and epileptic patients suffering mesial temporal lobe epilepsy (MTLE). In this study we evaluated the action of LEV on dentate gyrus excitatory circuits in MTLE. For this purpose, patch-clamp and field potential recordings were performed in hippocampal slices from control and epileptic rats obtained by the pilocarpine model of MTLE. In addition, the effect of LEV was was also assessed in mice with altered SV2A expression including hemizygous ($SV2A^{+/-}$) and knockout ($SV2A^{-/-}$) compared to wild-type controls and epileptic mice. By using 2-photon laser scanning confocal microscopy, we also tested whether LEV was effective in reducing enhanced vesicle release in mossy fibers from control and epileptic transgenic SpH21 mice expressing synaptopHluorin (SpH) in mossy fiber boutons. Expression changes in SV2A, SV2B and SV2C were analyzed using immunofluorescence, western blotting and real-time quantitative PCR (qPCR). Action of LEV was occluded in animals lacking SV2A expression. Our data indicate that LEV reduces excitatory (glutamatergic transmission) and activity-dependent synaptic vesicle release from readily releasable and recycling pool in chronically epileptic animals despite changes in SV2A expression and synaptic reorganization of excitatory terminals in MTLE.

Year 3 and non-cost extension period

Inhibitory action of levetiracetam on CA1 population spikes and dentate gyrus excitatory transmission in pilocarpine-treated chronic epileptic rats. **E. G. Sanabria**, L. Pacheco, J. Zavaleta, F. Shriver, L. M. Rambo, C. Upreti, **P. K. Stanton**. Society for Neuroscience Meeting, San Diego, CA, Nov 9-13, 2013.

The presynaptic target for Levetiracetam (LEV) has been identified as synaptic vesicle SV2A proteins in presynaptic terminals; however, the mechanisms of LEV's antiepileptic action remain unclear. Previous studies have shown a reduction of SV2A expression in both animal models and human suffering mesial temporal lobe epilepsy (MTLE). However, in vivo treatment with LEV appears to be still effective in those conditions in ameliorating seizures. In this study, we evaluated the in vitro effects of LEV on excitability and excitatory synaptic transmission in the pilocarpine model of mesial temporal lobe epilepsy (MTLE). In this study, we investigated the action of LEV on (a) population spikes recorded in CA1 area and (b) excitatory synaptic transmission onto dentate gyrus of control versus chronically epileptic rats obtained by the pilocarpine model of MTLE. For this purpose, we used extracellular potential recordings in acutely dissociated slices. Slices were pre-incubated in 300 microM of LEV for 3 hours prior recordings. LEV was also applied in the bath during recording sections. Field excitatory postsynaptic potentials (fEPSP) were evoked by different paradigms of repetitive stimuli of perforant path (e.g. 10@20Hz). Pre-incubation with LEV induced a 20% and 10% reduction in amplitude of CA1 population spikes in slices from control and epileptic rats respectively relative to non-treated slices. LEV induced a 37.2% and 49% significant reduction in the amplitude of the summated fEPSPs in a 20Hz train evoked by perforant path stimulations in both control and epileptic groups respectively ($df=9$, $p< 0.0001$ by paired T-test) compare to baseline. Significant changes were also detected in the first four fEPSP responses in the train with a non-significant reduction of remaining 6 fEPSPs (ANOVA repetitive Test, $p<0.01$ for both groups followed by pairwise Tukey post-hoc test). These results indicate that LEV is effective in reducing in vitro excitability and excitatory synaptic transmission in both control and epileptic groups (despite possible changes in SV2A expression). Further studies are in progress to determine presynaptic mechanisms involved in this inhibitory effect.

Synaptic Vesicle Protein Expression in Sprague-Dawley Rats Treated with the Pilocarpine Model for Mesial Temporal Lobe Epilepsy. Mayra Velazquez, L.F. Pacheco, **E. R. Garrido-Sanabria**. 25th Anniversary Conference, HENAAC Conference, October 3 - 5, 2013, New Orleans.

Epilepsy is a devastating neurological disorder that affects over three million Americans of all ages; it is as common and takes as many lives as breast cancer. On a global scale, fifty million people are affected. Of the reported cases of epilepsy, it is estimated that forty percent of these cases are mesial temporal lobe epilepsy (MTLE), a disease involving the limbic system. Epileptogenesis is the process in which the brain develops chronic epilepsy after an initiating event. This process develops during the latent period after a brain insult as *status epilepticus* (SE). During this time period, there are major molecular and physiological changes in several areas of the brain, including the hippocampus. Synaptic vesicle proteins 2 (SV2) are important hippocampal neuronal glycoproteins that are targeted when treating MTLE by a novel antiepileptic drug Levetiracetam (Keppra). Although the exact function of SV2 remains unclear, it appears that these proteins play a major role in epileptogenesis. Consequently, we decided to analyze the expression of SV2 isoforms in the hippocampus of Sprague-Dawley rats treated with the pilocarpine model for of MTLE. Calculating Evaluating the expression of SV2 isoforms in control versus epileptic animals at different times of epileptogenesis is crucial when developing drugs that bind target to these SV2 isoforms. Preliminary studies in the laboratory have yielded results that indicate a down regulation of SV2A expression in human and animal models of epilepsy. C Accordingly, we hypothesize that consequently, this has led us to believe that other SV2 isoforms, such as SV2B and SV2C, will also exhibit changes of expression in epileptic versus control animals. Additionally, our goal was is also to determine at what point in time during epileptogenesis SV2 rearrangement occurs (were the shifts in expression) encountered. To evaluate our hypothesis, we calculated the expression of SV2A, SV2B, and SV2C isoforms using immunohistochemistry, western blot, and qPCR techniques. Animals were induced into SE by administering the pilocarpine model for epilepsy (0.01% methylscopolamine, 4.0% pilocarpine, 0.1% diazepam). After the latent period from the pilocarpine treatment, which is between 5 to 15 days in Sprague-Dawley rats, animals were perfused with 4.0% paraformaldehyde and brains were extracted. For the immunohistochemistry, slices were tagged using primary antibodies with a concentration of 1:500 and secondary antibodies. Slices were then imaged using an Olympus Fluoview Confocal microscope and software. We used western blot and qPCR techniques to quantitatively measure the amount of SV2s in control versus epileptic animals at different stages of status epilepticus (24hrs, 10 days, and 1 month). Relative gene expression and immunoblot analysis of SV2A, SV2B and SV2C were performed using the comparative delta-delta CT qPCR method using TaqMan assays and western blot respectively. Our results support the hypothesis that SV2 isoforms are abnormally expressed during epileptoigenesis. Qualitative analysis of confocal images from post-latent period SE animals depicts an up-regulation of SV2C while simultaneously revealing a down regulation of SV2A and SV2B in post latent period tissue. Quantitative analysis of SV2 expression from western blot and qPCR experiments at different stages of SE revealed a decreased SV2A expression after the latent period, decreased SV2B expression at all times after SE, and increased expression of SV2C during and after the latent period. In conclusion, our results indicate a dysregulation of SV2A isoforms that may affect the effectiveness of drugs targeting these molecules. It is thereby important to consider seizure-mediated changes in pharmaceutical target expression during epileptogenesis in order to improve effectiveness and design disease-modifying antiepileptic drugs at different stages of the epilepsy. f epilepsy. From our results, it is obvious that major changes in SV2 isoform expression occurs during the latent period, when most structural and molecular changes have been known to take place without main electrographic signs of seizures. Currently, most drugs target patients at the post-latent period, when epilepsy has fully developed and major physiological changes have taken place. Congruently, it seems appropriate now to develop drugs that can target patients during the latent period to possibly halt the process of epileptogenesis in patients at risk.

Chronic treatment with levetiracetam upregulate SV2A and reduce abnormally augmented presynaptic vesicular release after pilocarpine-induced status epilepticus**.** Luis F. Pacheco, Vinicius Funck, Nuri Ruvalcaba, Jose M. Rodriguez, Daniela Taylor, Rubi Garcia, Jason Zavaleta, Chirag Upreti, **Patric K. Stanton**, **Emilio R. Garrido-Sanabria,** the Military Health System Research Symposium, August 18-21, 2014.

Epilepsy is a neurological disorder affecting 2% of the population. Levetiracetam (LEV) is a new antiepileptic drug that binds to presynaptic vesicular protein SV2A; however, the mechanism of action remains unknown. Abnormal presynaptic release of glutamate has been considered one of the seizure-induced alterations in epilepsy. Previous studies have shown abnormally enhanced vesicular release in hippocampal presynaptic boutons in epilepsy. Here, we investigate if chronic treatment with LEV will modify abnormal presynaptic release and reduction of SV2A induced by *status epilepticus*. Different groups of control and epileptic mice were treated with LEV (experimental, n=7) or saline solution (control, n=6). To induce chronic epilepsy, the pilocarpine model of temporal lobe epilepsy was developed in synaptopHluorin (SpH)-expressing transgenic mice. Protein samples were extracted and immoblottings were developed to assess expression of SV2A, SV2B, and SV2C. Imaging of electrically-evoked release was performed by confocal imaging in brain slices. Time-lapsed images were obtained from the CA3 stratum lucidum in hippocampus. For this analysis, we included 92 synaptic boutons from 7 slices in the control non-treated group, 148 boutons from 12 slices in control (treated with LEV), 115 boutons from 7 slices in epileptic (non-treated group) and 100 boutons from 6 slices in epileptic group chronically treated with LEV. As previously reported, epileptic SpH mice exhibited an increase in vesicular release when compared to control group. In contrast, LEV-treated SpH epileptic mice exhibited a reduction in release when compared to control animals treated with same. SV2A was down-regulated 22.9% in epileptic mice but after treatment with LEV SV2A expression increased 40% above controls. LEV corrected deficient SV2A and inhibited enhanced vesicular release in epileptic mice indicating that the anti-epileptic action may be mediated by changes in the vesicular release machinery.

Treatment with levetiracetam ameliorates abnormal presynaptic vesicular release and altered presynaptic protein expression in a glutamatergic pathway after pilocarpine-induced status epilepticus**. Emilio R. Garrido-Sanabria,** Luis F. Pacheco, Vinicius Funck, Nuri Ruvalcaba, Jose M. Rodriguez, Daniela Taylor, Rubi Garcia, Jason Zavaleta, Chirag Upreti, **Patric K. Stanton**. 68th Annual Meeting of the American Epilepsy Society, Dec 5-9, 2014, Seattle, Washington.

RATIONALE:
Epilepsy is a neurological disorder affecting 2% of the population. Levetiracetam (LEV) is a new antiepileptic drug that binds to presynaptic vesicular protein SV2A; however, the mechanism of action remains unknown. Abnormal presynaptic release of glutamate has been considered one of the seizure-induced alterations in epilepsy. Previous studies have shown abnormally enhanced vesicular release in hippocampal presynaptic boutons in epilepsy. Here, we investigate if chronic treatment with LEV will modify abnormal presynaptic vesicle release and synaptic vesicle proteins (SV2A, SV2B, SV2C) and transcripts expression after pilocarpine-induced status epilepticus.
METHODS:
Different groups of control and epileptic mice were treated with LEV (experimental, n=7) or saline solution (control, n=6). To induce chronic epilepsy, the pilocarpine model of temporal lobe epilepsy was developed in synaptopHluorin (SpH)-expressing transgenic mice. Protein samples were extracted and immoblottings were developed to assess expression of SV2A, SV2B, and SV2C. Gene expression was analyzed using TaqMan real time quantitative PCR assays. Imaging of electrically-evoked release was performed by confocal imaging in brain slices. Time-lapsed images were obtained from the CA3 stratum lucidum in hippocampus. For this analysis, we included 92 synaptic boutons from 7 slices in the control non-treated group, 148 boutons from 12 slices in control (treated with LEV), 115 boutons from 7 slices in epileptic (non-treated group) and 100 boutons from 6 slices in epileptic group chronically treated with LEV.
RESULTS:
As previously reported, epileptic SpH mice exhibited an increase in vesicular release when compared to control group. In contrast, LEV-treated SpH epileptic mice exhibited a reduction in release when compared to control animals treated with same. SV2A protein expression was down-regulated 22.9% in epileptic mice but after treatment with LEV SV2A expression increased 40% above controls. In contrast, sv2a transcripts were not upregulated in LEV-treated status epilepticus group.No significant changes were detected in sv2b gene expression among the groups. However, a significant change was observed for sv2c gene expression (ANOVA, $p>0.0001$, $F=11.87$) where status epilepticus induced a significant sv2c upregulation when compared to saline injected control group. Interestingly, in contrast to SV2C protein expression, chronic treatment with LEV induced a significant 33.8% and 11.7% reduction of sv2c levels in treated status epilepticus and control groups respectively when compared to saline-injected status epilepticus and control groups.
CONCLUSIONS:
Levetiracetam partially corrected abnormal SV2A and SV2C expression and inhibited abnormally enhanced vesicular release in epileptic SpH mice indicating that the anti-epileptic action and effectiveness in chronically epileptic tissue may be associated with changes in the presynaptic vesicular release machinery and its own pharmacological targets in mesial temporal lobe epilepsy.

Abnormal upregulation of SV2C after pilocarpine-induced seizures is restored after treatment with antiepileptic drug levetiracetam. Luis F. Pacheco, Vinicius Funck, Nuri Ruvalcaba, Samantha Gomez, Aliya Sharif, Jose M. Rodriguez, Daniela Taylor, Rubi Garcia, Chirag Upreti, Patric K. Stanton, **Emilio R. Garrido-Sanabria,** the Military Health System Research Symposium, August, 2015.

Background: Temporal lobe epilepsy is a devastating neurological condition. Seizures can affect the expression of numerous molecules that participate in the pathogenesis of epilepsy. In this study, we investigate whether status epilepticus affect the expression of synaptic proteins and the effect of chronic levetirecetam treatment on status *epilepticus*-induced synaptic vesicle protein abnormalities.
Methods: For this purpose, the pilocarpine model of epilepsy was developed in mice. The groups consisted of control (no *status epilepticus*) animals treated with saline (I) and animal suffering *status epilepticus* injected with saline (II), control (no *status epilepticus*) animals treated with levetirecetam for 30 days and animal suffering *status epilepticus* treated with levetirecetam for 30 days. After treatment, animals were sacrificed and proteins and mRNA was isolated for Western blotting and TaqMan-based real-time PCR assays to detect relative changes in protein and transcript expression of synaptic vesicle protein subtypes SV2A, SV2B, SV2C and vesicular Glutamate transporter type 1 among the different groups.
Results: No significant changes were found for the expression of SV2A and SV2B among groups, however,*status epilepticus* induced a significant ($p<0.01$) up regulation of 122.24% in the expression of SV2C compared to saline-injected controls. Treatment with levetiracetam 100 ul/g resulted in a decrease in the expression of SV2C in both control and *status epilepticus*-suffering mice. Expression of SV2C was significantly reduced 88.34% compared to saline-treated *status epilepticus* group.
Conclusion: SV2A is the binding site of levetiracetam and has been proposed as the molecular target in the mechanism of action of this antiepileptic drug. While the mechanism of action of levetirecetam has been associated with SV2A, our results indicate that another synaptic vesicle protein SV2C that is specifically expressed in glutamatergic terminals may be involved in the pathogenesis of epilepsy and the antiepileptic action of levetieracetam. Status epilepticus upregulate the expression of SV2C while chronic treatment with levetirecetam restore levels of this target indicating that this may be an antiepileptic mechanisms of action of this drug that will reduce presynaptic release of neurotransmitters like glutamate and hippocampal hyperexcitability in epilepsy.